# Big Temporally-Detailed Graph Data Analytics

**A THESIS**
**SUBMITTED TO THE FACULTY OF THE GRADUATE SCHOOL**
**OF THE UNIVERSITY OF MINNESOTA**
**BY**

**Venkata Maruti Viswanath Gunturi**

**IN PARTIAL FULFILLMENT OF THE REQUIREMENTS**
**FOR THE DEGREE OF**
**DOCTOR OF PHILOSOPHY**

**Prof. Shashi Shekhar**

**June, 2015**

# Acknowledgements

There are many people who have earned my gratitude for their contribution to my time in graduate school. First, I would like to thank my adviser, Prof. Shashi Shekhar, for his mentorship, support and guidance through my PhD. I am sincerely grateful for all the learning opportunities he gave me which not only helped me develop my skills as a research scholar, but also to be a good team player and a mentor. I thank all the professors who have guided me over the years in my research and course work, some of whom also served on my thesis committee: Prof. Vipin Kumar, Prof. Ravi Janardan, Prof. William Northop, Prof. Arindam Banerjee and Prof. Henry Liu.

I extend my gratitude to my collaborators Prof Kathleen Carley and Kenneth Joseph at the Carnegie Mellon University for their open mindedness and patience in exploring the applications of my work in the domain of social network analysis. I would also like to thank Andrew Kotz for patiently exploring the next directions of my work. I also deeply appreciate the feedback given by Kim Koffolt towards improving the presentation of ideas in my papers.

And last (but not the least), I would like to extend my special thanks to Prof. Shekhar's spatial computing research group and my friends at UMN. Their peer feedback helped me uncover several aspects of my research and their warmhearted nature made my stay at UMN a true delight. As I prepare to move forward in life, I must say that I have many sweet memories of this place which will last a lifetime.

## Abstract

Increasingly, temporally-detailed graphs are of a size, variety, and update rate that exceed the capability of current computing technologies. Such datasets can be called Big Temporally-Detailed Graph (Big-TDG) Data. Examples include temporally-detailed (TD) roadmaps which provide typical travel speeds experienced on every road segment for thousands of departure-times in a typical week. Likewise, we have temporally-detailed (TD) social networks which contain a temporal trace of social interactions among the individuals in the network over a time window. Big-TDG data has transformative potential. For instance, a 2011 McKinsey Global Institute report estimates that location-aware data could save consumers hundreds of billions of dollars annually by 2020 by helping vehicles avoid traffic congestion via next-generation routing services such as eco-routing.

However, Big-TDG data presents big challenges for the current computer science state of the art. First, Big-TDG data violates the cost function decomposability assumption of current conceptual models for representing and querying temporally-detailed graphs. Second, the voluminous nature of Big-TDG data can violate the stationary-ranking-of-candidate-solutions assumption of dynamic programming based techniques such Dijsktra's shortest path algorithm. This thesis proposes novel approaches to address these challenges.

To address the first challenge, this thesis proposes a novel conceptual model called, "Lagrangian Xgraphs", which models non-decomposability through a series of overlapping (in space and time) relations, each representing a single atomic unit which retains the required semantics. An initial study shows that Lagrangian Xgraphs are more convenient for representing diverse temporally-detailed graph datasets and comparing candidate travel itineraries. For the second challenge, this thesis proposes a novel divide-and-conquer technique called "critical-time-point (CTP) based approach," which efficiently divides the given time-interval (over which over non-stationary ranking is observed) into disjoint sub-intervals over which dynamic programming based techniques can be applied. Theoretical and experimental analysis show that CTP based approaches outperform the current state of the art.

# Contents

# List of Tables

# List of Figures

# Chapter 1

# Introduction

Increasing proliferation of technology and internet has given us an unprecedented opportunity to observe and collect data on network phenomena at a fine temporal scale. Examples include, study of variation in traffic congestion and route preferences on urban transportation network made possible through GPS enabled mobile phones, in-car navigation devices, location based services (e.g. Waze) and loop detectors major road segments. Similarly, the study of evolving social roles of individuals in social networks has been made possible due to the ever-increasing adoption of mobile and online social networking platforms.

However, increasingly, the data collection platforms in the domains of transportation and social networks generate network datasets which are of a volume, variety and update rate that exceed the capabilities of current graph data analytics. This thesis refers to these datasets as *Big Temporally-Detailed Graph (Big-TDG) Data*. Examples of Big-TDG data include *temporally-detailed (TD) roadmaps* which provide typical travel speeds experienced on every road segment for thousands of departure-times in a typical week. Likewise, by assembling time-stamped social events from several types of social interactions such as emails, phone calls, post-comment interactions and co-location pairs, we can construct *temporally-detailed (TD) social network* which would contain a temporal trace of social interactions among the individuals in the network over a time window. TD social networks can help in answering time-aware questions (e.g., “How did the betweenness centrality of an individual vary over the past year?”) on the underlying social systems.

Big Temporally-Detailed Graph Data has transformative potential. For instance, in the domain of transportation networks, a recent McKinsey Global Institute report [4] estimates that personal location data could save consumers hundreds of billions of dollars annually by 2020 by helping vehicles avoid traffic congestion via next-generation routing services such as eco-routing [5, 6]. Where todays route finding services are based on shortest historical average travel time or distance, eco-routing may leverage various forms of Big-TDG Data to allow commuters to compare alternative routes by typical travel-speed, fuel consumption or greenhouse gas emissions for a precise departure-time(s) of interest. Preliminary evidence of this value proposition is the experience of UPS, which saved three million gallons of fuel annually [7] by using routes that avoided left turns (see Figure 1.1(a)). Such savings can be multiplied many times over when eco-routing services become available for consumers and other fleet owners (e.g., public transportation). It may also significantly reduce US consumption of petroleum, the dominant source of energy for transportation (see Figure 1.1(b)). But, a number hurdles must be overcome before we can exploit Big-TDG data.

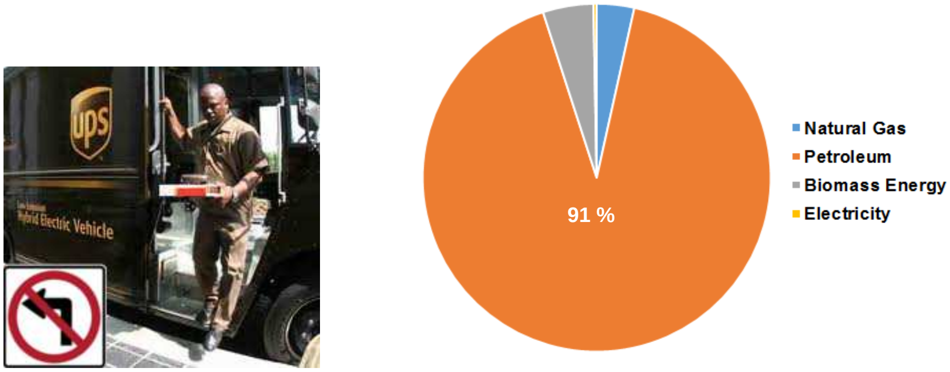

(a) UPS avoids left-turns to save fuel [7].

(b) Petroleum is dominant energy source for US Transportation (2014 data) [8].

Figure 1.1: Eco-routing supports sustainability (Best in color).

## 1.1 Challenges of Big-TDG Data

Big-TDG Data presents two main challenges: First, Big-TDG Data captures several properties of n-ary relations which cannot be completely decomposed into properties of binary relations without losing their semantic meaning. Thus, it violates the assumptions of current conceptual models for representing and querying temporally-detailed graphs, which assume that properties recorded in the data are completely decomposable.

Secondly, the voluminous nature of Big-TDG Data can violate the stationary-ranking-of-candidate-solutions assumption of dynamic programming (DP) based techniques. In other words, both TD roadmaps and TD social networks show a non-stationary ranking of alternate candidate paths across time points. This makes it non-trivial to generalize the current *single-time-point only* DP literature on shortest paths and betweenness centrality for computing optimal solutions across time-points while retaining both correctness and computational efficiency.

| | Current Literature | New Contributions | Chapter in Thesis |
|---|---|---|---|
| Conceptual | Time aggregated graphs [9--14] and Time expanded graphs [13,15] | Lagrangian Xgraphs | Chapter 2 and Section 3.1 in Chapter 3 |
| | Frame of reference: Eulerian | Frame of reference: Lagrangian | |
| Logical | | | |
| Physical | Algorithms for single start time Shortest path [15--28] on a TD roadmap | Algorithms for all start-time shortest paths on a TD roadmap | Chapter 3 and Chapter 4 |
| | Algorithms for a single time-point betweenness centrality [13, 14, 29, 30]) on a TD social network | Betweenness centrality over a time-interval in a TD social network | Chapter 5 |

Table 1.1: Current literature and novelty of this thesis.

## 1.2 Limitations of current related work

Table 1.1 summaries the current literature in the area of temporal-detailed graph data analytics. This literature can be divided into contributions at the Conceptual, Logical and Physical levels of a data analytics system (rows in Table 1.1). At the conceptual level, the goal is to design a representative model of the data which balances the trade-offs between expressive power and support for computationally scalable algorithms. An expressive model is able to capture a number of concepts in the data. For instance, the current approaches in this area (second row in Table 1.1), Time aggregated graphs (TAG) [9–14] and Time expanded graphs (TEG) [13,15], are able to model the concepts of connectivity and temporal variance of edge costs (e.g., variation in travel-time on a road segment across rush and non-rush hours). Connectivity is modeled using binary edges which connect two nodes which were considered as immediate neighbors. Each edge is associated with a list of attributes (e.g, travel-time and distance in the case of roadmaps and social interactions in the case of social networks). Temporal variation in these attributes is modeled either by a time series of values or a systematic replication of node connectivity information across multiple time points (more details in Section 3.1 of Chapter 3 and Section 5.1 of Chapter 5). Amongst TAG and TEG, TAG has been shown to be more conducive for computationally scalable algorithms [16] due to its brevity. However, both TAG and TEG are limited for Big-TDG data as they assume complete decomposability of properties of n-ary relations (e.g., delay observed across a series of coordinated traffic signals). More details are presented in Chapter 2.

At the physical level of data analytics, the goal is to design query algorithms and storage models for temporally-detailed graph data. The current literature on storage models includes temporally-detailed graph partitioning techniques such as [31]. Likewise, the literature on query algorithms for temporally-detailed graphs includes flow, minimum spanning tree and shortest path algorithms [32]. My thesis focuses only on shortest path algorithms. Research to date in this area [15–28] has mostly considered only single start-times. However, Big-TDG allows us to compute a shortest path (and centrality metrics) for thousands of time points in a given time interval. A naive approach to harness this potential could use algorithms developed for single start-times to repeatedly compute the shortest path (and centrality metrics such as betweenness and closeness) for each desired time point. However, such an approach would incur redundant re-computation across time points sharing a common solution, thereby limiting its scalability for analysis on long time intervals (more details in Chapter 3, 4 and 5). Note that due to non-stationary ranking of candidates in a TD roadmap (or in a TD social network), we cannot use just one instance of a Dynamic Programming (DP) based technique to compute optimal solutions across all time points. Thus to enure correctness, the naive approach resorts to a repeated instantiation of a DP based technique [15–28].

## 1.3 Summary of Contributions

To address the first challenge, this thesis proposes a novel representation model called *Lagrangian Xgraphs* [33] (Chapter 2). Lagrangian Xgraphs addresses the non-decomposability challenge by modeling the non-decomposable properties of n-ary relations in Big-TDG Data as a series of overlapping (in space and time) relations, each representing a single atomic unit which retains the required semantics. To address the second challenge, this thesis proposes a novel divide-and-conquer strategy called *critical-time-point (CTP) based approaches* [34, 35]. A CTP based approach addresses the challenge of non-stationary-ranking-of-candidates by dividing the given time-interval over which one desires to compute the shortest path (or betweenness centrality) into a set of disjoint sub-intervals over which ranking is stationary (while ensuring both correctness and computational efficiency). One can now use a single instance of DP based technique to compute the shortest path (or betweenness centrality) inside this sub-interval (more details in Chapter 3, 4 and 5).

## 1.4 Thesis Organization

The rest of the thesis is organized as follows. Chapter 2 describes the proposed conceptual model of Lagrangian Xgraphs which addresses the challenge of non-decomposable nature of certain properties of n-ary relations captured in Big-TDG data. Chapter 3 proposes the concept of critical-time-points to address the non-stationary ranking challenge in TD roadmaps and develops a forward-only search algorithm based on this concept for the all start-time shortest path problem. Chapter 4 proposes a bi-directional search algorithm for a critical-time-point based solution to the all start-time shortest path problem. In Chapter 5, the notion of critical-time-points (referred to as epoch points in this chapter) is used to develop an algorithm to compute betweenness centrality in TD social networks. Finally, in Chapter 6, a summary of the results is presented followed by a brief discussion on potential future research directions.

# Chapter 2

# Lagrangian Xgraphs

Increasingly a variety of spatial-temporal datasets representing diverse properties of a transportation network over space and time (STN datasets) are becoming available. Examples include temporally detailed (TD) roadmaps [5] that provide travel-time for every road-segment at 5 minute granularity, traffic signal timings and coordination [36], map-matched GPS tracks annotated with engine measurement data (e.g., fuel consumption) [5, 28], etc. Given a collection of such STN datasets and a set of use-case queries, the aim is to build a unified logical data-model across these datasets which can express a variety of travel related concepts explicitly while supporting efficient algorithms for given use-cases. The objective here is to explore the trade-off between expressiveness and computational efficiency. Such a unified logical data-model would enable richer results by allowing query algorithms to access and compare information from multiple datasets simultaneously.

**Value of STN datasets:** Collectively, STN datasets capture a wide assortment of travel-related information, e.g., historic traffic congestion patterns, "fuel efficiency index" of different road segments, emerging commuter driving preferences, etc. Such information is not only important for routing related use-cases, e.g., comparison of alternative itineraries and navigation, but also valuable for several urban planning use-cases such as traffic management and analysis of transportation network. According to a 2011 McKinsey Global Institute report, annual savings of about $600 billion could be achieved by 2020 in terms of fuel and time saved [4] by helping vehicles avoid congestion and reduce idling at red lights or left turns. Preliminary evidence on the potential of STN

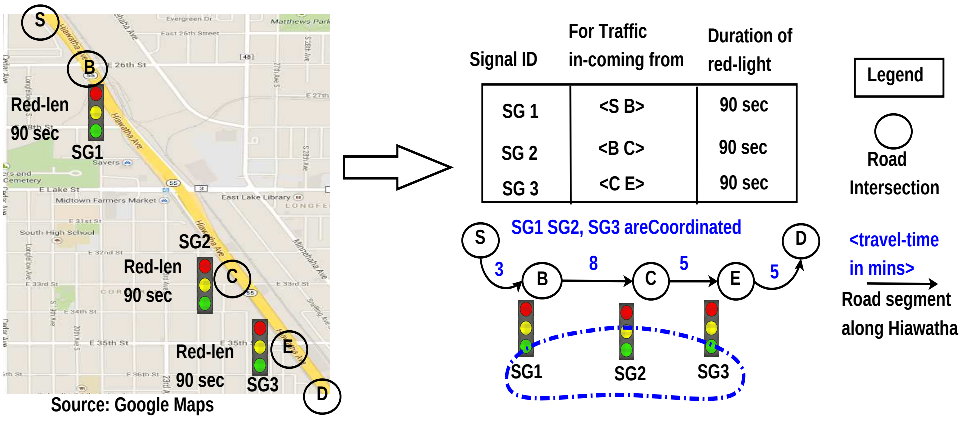

| Signal ID | For Traffic in-coming from | Duration of red-light |
|---|---|---|
| SG 1 | <S B> | 90 sec |
| SG 2 | <B C> | 90 sec |
| SG 3 | <C E> | 90 sec |

Source: Google Maps

Figure 2.1: Coordinated traffic signals [1] (best is color).

datasets include the experience of UPS which saves millions of gallons of fuel by simply avoiding left turns and associated engine-idling when selecting routes [7]. Similarly, other pilot studies with TD roadmaps [27] and congestion information derived from GPS traces [28] showed that indeed, travelers can save up to 30% in travel time compared with approaches that assume a static network. Thus, it is conceivable that immense savings in fuel-cost and green-house gas emissions are possible if other consumers avoided hot spots of idling, low fuel-efficiency, and congestion, potentially leading towards 'eco-routing' [5].

**Challenges:** Modeling a collection of STN datasets is challenging due to the conflicting requirements of expressive power and computational efficiency. In addition, the growing diversity of STN datasets requires modeling a variety of concepts accurately. For instance, it should be convenient to express all the properties of a n-ary relation in the model. A route with a sequence of coordinated traffic signals is a sample n-ary relation. Properties measured over n-ary relations cannot always be decomposed into properties over binary relations. Consider the following scenario of signal coordination on a portion of Hiawatha Ave in Minneapolis (shown in Figure 2.1). Here, the traffic signals SG1, SG2 and SG3 control the incoming traffic from segments S-B, B-C, and C-E (and going towards D) respectively. Now, the red-light durations and phase gap among traffic signals SG1, SG2 and SG3 are set such that a typical traveler starting at S and going towards D (within certain speed-limits) would typically *wait only at*

*SG1*, before being smoothly transferred through intersections C and E *with no waiting at SG2 or SG3*. In other words, in this journey initial waiting at SG1 renders SG2 and SG3 wait free. If the effects of immediate spatial neighborhood are referred to as local-interactions, e.g. waiting at SG1 delaying entry into segment B-C, then we this would be referred to as a *non-local interaction* as SG1 is not in immediate spatial neighborhood of C-E (controlled by SG2) and E-D (controlled by SG3).

Travel-time measured on a typical journey with non-local interactions (e.g. a journey from S to D in Figure 2.1) cannot be decomposed to get typical experiences on individual segments. Consider again the above sample journey from S to D in Figure 2.1. Here, the total travel-time measured on a typical journey from S to D would not include any waiting at intersections C (signal SG2) and E (signal SG2). This is, however, *not true* as a traveler starting intersection C (or E) would typically wait for some time SG2 (or SG3). We refer to this kind of behavior, where properties (e.g. travel-time) measured over larger instances (e.g. a route) loose their semantic meaning on decomposition, as *holism*. For our previous example, we say that the total travel-time measured over the route S-B-C-E-D was behaving like a *holistic property*.

**Limitations of Related work:** Current approaches for modeling STN datasets such as time aggregated graphs [37], time expanded graphs [15], and [10, 11] are most convenient when the property being represented can be completely decomposed into properties of binary relations. In other words, they are not suitable for representing the previously described holistic properties of n-ary relations. Consider again our previous signal coordination scenario. The related work would represent this using following two data structures: one containing travel-time on individual segments (binary relations) S-B, B-C, C-E, and E-D; the second containing the delays and the traffic controlled by signals SG1, SG2, and SG3 (also binary). However, this is not convenient as non-local interactions affecting travel-times on some journeys (e.g. S-B-C-E-D) are not expressed explicitly. Note that this representation would have been good enough if SG1, SG2 and SG3 were not coordinated.

**Our approach:** In contrast, our approach can support n-ary relations better by modeling non-local interactions on journeys more explicitly. Figure 2.2(b) illustrates the spirit of our logical data-model for the previous signal coordination scenario. The first entry in the figure corresponds to travel-time experienced on a journey containing road

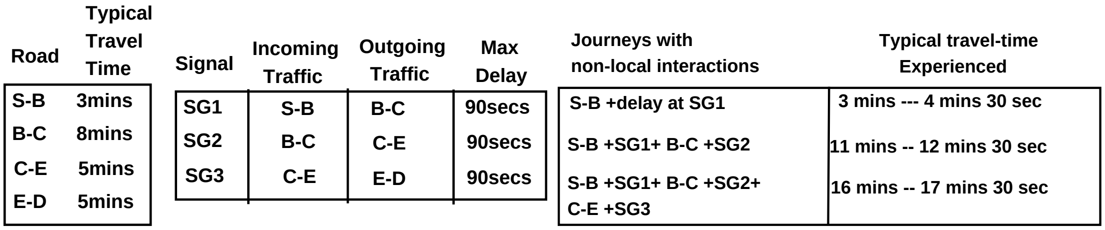

| Road | Typical Travel Time |
|---|---|
| S-B | 3mins |
| B-C | 8mins |
| C-E | 5mins |
| E-D | 5mins |

| Signal | Incoming Traffic | Outgoing Traffic | Max Delay |
|---|---|---|---|
| SG1 | S-B | B-C | 90secs |
| SG2 | B-C | C-E | 90secs |
| SG3 | C-E | E-D | 90secs |

(a) Related Work

| Journeys with non-local interactions | Typical travel-time Experienced |
|---|---|
| S-B +delay at SG1 | 3 mins --- 4 mins 30 sec |
| S-B +SG1+ B-C +SG2 | 11 mins -- 12 mins 30 sec |
| S-B +SG1+ B-C +SG2+ C-E +SG3 | 16 mins -- 17 mins 30 sec |

(b) Our approach

Figure 2.2: Related work and our approach for holistic travel-time shown in Figure 2.1.

segment S-B (3 mins) and delay at SG1 (max delay 90 secs). This would be between 3 mins and 4 mins 30 secs (no non-local interactions in this case). Next we would store travel-time experienced on the journey containing road segment S-B (3mins) , delay at SG1 (max delay 90secs), segment B-C (8mins) and delay at SG2 (max 90secs) as between 11 mins and 12 mins 30 secs. Notice that we did not consider the delay caused by SG2 due to non-local interaction from SG1. This process continues until all the possible non-local interactions are covered.

**Contributions:** This chapter makes the following contributions: (1) Elucidate valuable routing-related concepts, e.g. reference frame and type of properties, captured in STN datasets, (2) Propose a logical data-model called *Lagrangian Xgraphs* for these concepts, (3) Propose an abstract data type for Lagrangian Xgraphs, and (4) Illustrate Lagrangian Xgraphs through a sample scenario.

**Scope and Outline:** The scope of the chapter is limited to routing-related use-cases (e.g. comparison of travel itineraries and navigation) only. The rest of the chapter is organized as follows: Section 2.1 describes the STN datasets considered in this chapter. Section 2.2.1 presents the routing-related concepts captured in these datasets. Our proposed logical data-model, Lagrangian Xgraph model, and its abstract data types are described in Section 2.2.2. Lagrangian Xgraphs are illustrated in Section 2.2.3. Finally, Section 2.3 concludes this chapter.

## 2.1 Description of STN Datasets

Consider the sample transportation network shown in Figure 2.3 (on the left). Here, the arrows represent road segments and labels (in circles) represent an intersection between two road segments. Location of traffic signals are also annotated in the figure. On

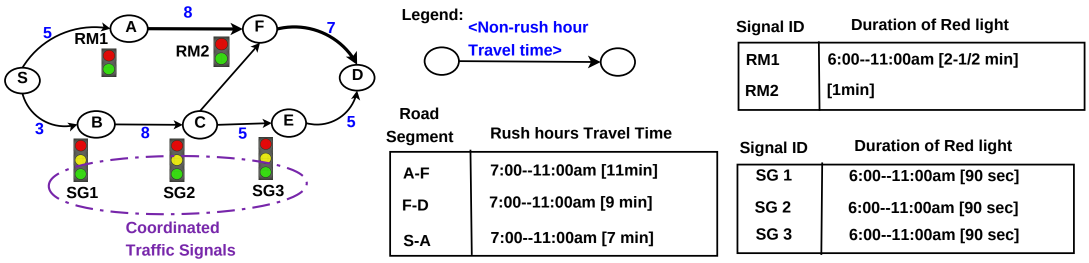

| Road Segment | Rush hours Travel Time |
|---|---|
| A-F | 7:00--11:00am [11min] |
| F-D | 7:00--11:00am [9 min] |
| S-A | 7:00--11:00am [7 min] |

| Signal ID | Duration of Red light |
|---|---|
| RM1 | 6:00--11:00am [2-1/2 min] |
| RM2 | [1min] |

| Signal ID | Duration of Red light |
|---|---|
| SG 1 | 6:00--11:00am [90 sec] |
| SG 2 | 6:00--11:00am [90 sec] |
| SG 3 | 6:00--11:00am [90 sec] |

Figure 2.3: Sample TD roadmap and traffic signal data.

this network, we consider three types of STN datasets: (a) temporally detailed (TD) roadmaps [5], (b) traffic signal data [36], and (c) annotated GPS traces [5, 28]. These datasets record either historical or evolving aspects of certain travel related phenomena on our transportation network. TD roadmaps store historical travel-time on road segments for several departure-times in typical week [5]. For simplicity, TD roadmap data is illustrated in Figure 2.3 by highlighting the morning (7:00am – 11:00am) travel-time only on segments A-F, F-D and S-A. The travel-times of other road segments in the figure are assumed to remain constant. The figure also shows the traffic signal delays during the 7:00am – 11:00am period. Additionally, traffic signals SG1, SG2 and SG3 are coordinated for a journey from S to D.

Another type of STN dataset considered in this paper are the map-matched and preprocessed [38] GPS traces. These are typically also annotated with data from engine computers to get richer datasets illustrating fuel economy of the route. We refer to them as annotated GPS traces. Each trace in this dataset is represented as a sequence of road-segments traversed in the journey along with its corresponding schedule denoting the exact time when the traversal of a particular segment began. GPS traces can potentially capture the evolving aspect of our system. For instance, if segment E-D (Figure 2.3) is congested due to an event (a non-equilibrium phenomenon), then travel-time denoted by TD roadmaps may no longer be accurate. In such a case, a traveler may prefer to follow another route (say C-F-D) which other commuters may be taking to reach D.

Figure 2.4 provides a conceptual model of the transportation network using pictogram enhanced ER diagram [39, 40]. Our model primarily contains streets, road segments and traffic signals as entity types. Additionally, we have turns, traffic signal coordination and GPS traces as weak entity types. One may observe that the attributes

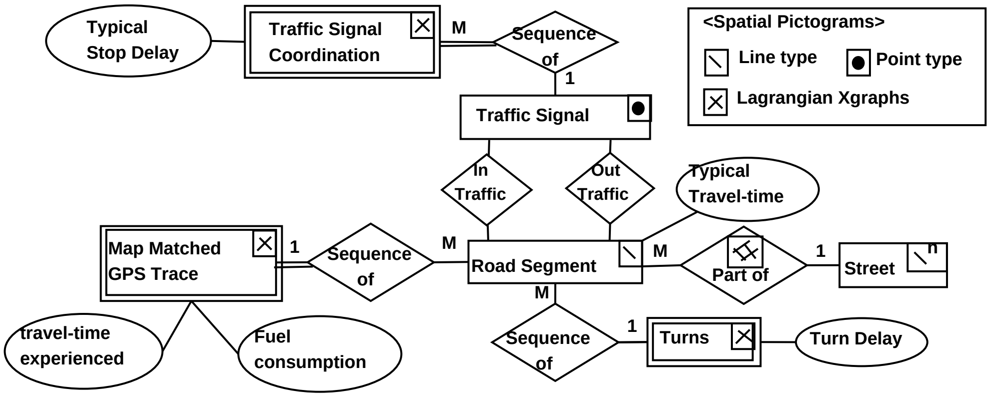

Figure 2.4: Conceptual model of a transportation network with spatial pictograms.

of these weak entity types form our previously described STN datasets. More detailed conceptual models for transportation networks (containing many more entity types and relations) have been proposed in the literature [41]. We have simplified our model in order to focus on the previously mentioned weak entity types.

Usually entities like road segments, traffic signals and streets are modeled using basic shapes like lines, points and line-strings (see spatial pictograms in Figure 2.4). These basic shapes are then queried using a logical data implemented through Open Geodata Interchange Standard (OGIS) operators. However, this approach is not suitable for use-cases that involve comparing candidate routes or itineraries (e.g. fastest path queries). As a solution, spatial [10, 11] and spatial-temporal [37] network models were developed which implement these concepts through graphs where each edge contains only two entities (a binary relation). However, as described earlier, this approach is not suitable for modeling holistic properties of n-ary relations, although they can represent decomposable properties of n-ary relations. To this end, we propose a novel logical data-model called Lagrangian Xgraphs which is capable of modeling both holistic and decomposable properties.

## 2.2 Lagrangian Xgraphs

### 2.2.1 Desired routing-related concepts to be modeled

STN datasets capture routing-related concepts along two dimensions: (i) frame of reference, (ii) nature of property recorded (see Figure 2.5).

Frame of Reference: For the first dimension, datasets are assembled with either *Eulerian* or *Lagrangian* reference frame shown upfront. In Eulerian reference frame, the phenomenon is observed through fixed locations in the system [42]. For a transportation network, this view corresponds to a stationary observer sitting on a side of a freeway (loop detectors or traffic observatory). By contrast, Lagrangian frame of reference corresponds to the perspective of an traveler driving along a particular route [42]. Data collected through annotated GPS traces is Lagrangian in nature. Both Eulerian and Lagrangian reference frames can be thought of as means to represent a set of unique space-time coordinates in the transportation network. Generally, we can consider all records in STN datasets as certain attributes associated with these space-time coordinates. For example, a data record containing the measurement 5 mins as travel-time on the road S-A at 9:00am on a Monday (TD roadmaps) of a typical week has the physical location of S-A for space and 9:00am-Monday for time coordinate respectively. Travel-time in TD-roadmaps shows Eulerian frame upfront, whereas in a annotated GPS trace it shows Lagrangian frame upfront.

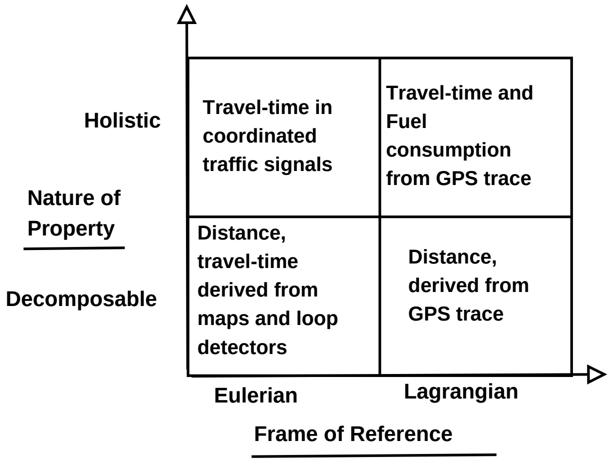

| | Eulerian | Lagrangian |
|---|---|---|
| Holistic | Travel-time in coordinated traffic signals | Travel-time and Fuel consumption from GPS trace |
| Decomposable | Distance, travel-time derived from maps and loop detectors | Distance, derived from GPS trace |

Figure 2.5: Taxonomy of concepts.

Nature of Property: Under Eulerian or Lagrangian frame of reference, the property being recorded can be either *decomposable* or *holistic*. A decomposable property when re-constructed for a larger instance (e.g. route) by joining values for smaller instances (at appropriate space-time coordinates) retains its correctness. Distance measured from a GPS trace (Lagrangian frame) or as measured through maps (Eulerian frame) is a decomposable property. Other examples include, travel-time obtained from loop detectors, signal delays (red light duration) at individual traffic signals as set by traffic managers.

Decomposable properties can be further classified as deterministic or non-deterministic. Properties which can be expressed clearly from a start-point are termed as deterministic. Travel-time as captured in TD roadmaps is deterministic as given a departure-time (in a typical week), TD roadamps will provide a unique travel-time for a road-segment. In contrast, traffic signal delays are non-deterministic unless the absolute start-time of their cycles is known. In other words, given a departure-time on a route, we cannot determine (at least in current datasets) the precise delay to be experienced at a signal.

On the other hand, holistic properties are properties when measured over a large instance cannot be broken down into corresponding values for smaller instances through space-time decomposition. This is due to presence of non-local interactions. Apart from our earlier example with coordinated traffic signals, travel-time (and fuel consumption) experienced by a commuter on a road-segment, as derived from his/her annotated GPS trace, is holistic in nature. Here, the travel-time experienced would depend on his/her initial velocity gained *before* (a non-local interaction) entering the particular road-segment under consideration. Travel-time of the commuter is deterministic as we can exactly measure its value from start of journey. By contrary, travel-time through a series of coordinated traffic signals is non-deterministic.

It is important to note that 'data-collection' reference frame may be different from 'querying' reference frame. For instance, travel-time recorded in TD roadmaps shows Eulerian frame upfront. Whereas, routing queries on the same TD roadmaps (and other STN datasets) would be more meaningful through Lagrangian frame of reference [34]. The interoperability of Eulerian and Lagrangian frame of reference allows for the 'querying' and 'data-collection' reference frames to be different. In other words, data recorded in one frame can be easily queried from (or converted to) another reference frame [42].

### 2.2.2 Proposed Logical Model

Given a collection of STN datasets measured over a time horizon $\mathcal{H}$, we formally define a Lagrangian Xgraph ($\mathcal{L}a\mathcal{X}$) as an ordered set of Xnodes ($\mathcal{X}v$), Xedges ($\mathcal{X}e$) and a time horizon parameter $\mathcal{H}$, i.e., $\mathcal{L}a\mathcal{X} = (\mathcal{X}v, \mathcal{X}e, \mathcal{H})$.

Xnodes: For any network system under consideration, Xnodes $\mathcal{X}v_i \in \mathcal{X}v$ represent the underlying entities at specific space-time coordinates.

Xedges: are used to express a 'as-traveled' or 'typical-experience-in-travel' relationship among a set of Xnodes. More formally, $\mathcal{X}e^i = \{\mathcal{X}v_s, \mathcal{X}v_1, \ldots, \mathcal{X}v_k,\ \mathcal{X}v_{d1}, \mathcal{X}v_{d2}, \ldots, \mathcal{X}v_{dj}\}$. Here, the first Xnode ($\mathcal{X}v_s$) and the last set of Xnodes ($\mathcal{X}v_{d[1 \ldots j]}$) correspond to the instance of the first and the last entities participating in the relation and are marked separately for ease.

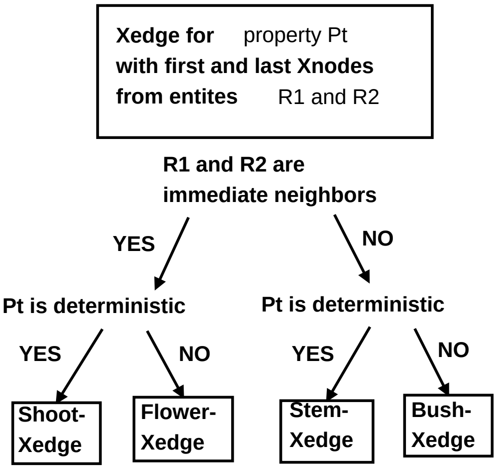

Figure 2.6: Taxonomy of Xedges.

Taxonomy of Xedges: Xedges as defined above are further categorized according to: (a) spatial relationship between the first ($\mathcal{X}v_s$) and last set of Xnodes ($\mathcal{X}v_{d[1\ j]}$) and (b) property being modeled is deterministic or non-deterministic. Figure 2.6 shows the proposed classification. Primarily, we classify an Xedge as: (i) shoot-Xedge, (ii) flower-Xedge, (iii) stem-Xedge or, (iv) bush-Xedge. The first and last Xnodes in both shoot-Xedges and flower-Xedges belong to entities which are spatially immediate neighbors.

Thus, they would be used for modeling decomposable properties. In a shoot-Xedge, each entity is present for a single time and thus, can model deterministic properties. Flower-Xedges allow one entity to be represented for multiple time coordinates and thus, can be used to model non-deterministic properties (e.g. individual signal delays).

By contrast, both stem-Xedges and bush-Xedges allow the first and last Xnode(s) to be separated physically. This physical separation allows both stem and bush-Xedges to represent holistic properties. Bush-Xedges are useful for non-deterministic properties since they allow one entity to be represented at multiple time coordinates. Stem-Xedges are employed for deterministic properties since each entity is present only for one time coordinate.

**Abstract Data Type:** Access operators for Lagrangian Xgraphs define the basic logical units of work during information retrieval for queries. Table 2.1 shows an illustrative set of access operators for Xnodes and Xedges. In the table we use ($s$,$t$) to denote the Xnode representing an entity at a particular space-time coordinates.

Access operators for Xnodes retrieve information on Xedges which are incident on a particular Xnode. For example, the operation Xnode.decom_successors (Xnode($s$,$t$), property) retrieves all the Xedges whose first Xnode is Xnode($s$,$t$) and represent a decomposable property. Similarly, get_holistc_ successors(Xnode($s$,$t$), property) returns Xedges representing a given holistic property from Xnode($s$,$t$).

Access operators for Xedges require the following parameters for retrieval: (1) the first Xnode (Xnode(s1,t) in Table 2.1); (2) the last Xnode; (3) the property. Here, the time coordinate of the last Xnode (Xnode(s2) in Table 2.1) may not always be precisely defined before hand. Based on the information retrieved, we would know the time coordinate of last Xnode(s2). Lastly, we also have an operator Xroute which can successively join Xedges to create a route as would be experienced by a person traveling on that route.

Table 2.1: Access operators for Lagrangian Xgraph.

| Category | Decomposable | Holistic |
|---|---|---|
| Xnode | Xnode.decom_successors<br>(Xnode(s,t), property) | Xnode.holistc_successors<br>(Xnode(s,t), property) |
| Xedge | Xedge.get_decom<br>(Xnode(s1,t),Xnode(s2),property) | Xedge.get_telecon<br>(Xnode(s1,t),Xnode(s2),property) |
| Xroute | Xroute.glue(an Xedge) | |

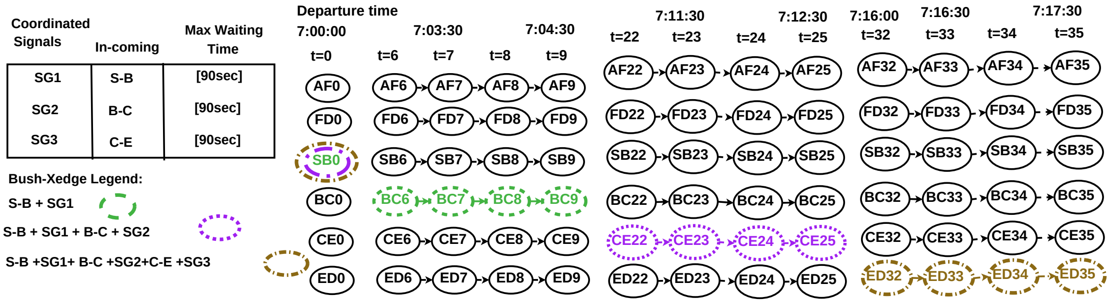
30sec temporal granularity. Some departure-times are omitted to retain clarity.

Figure 2.7: First and last Xnodes for journey through a series of coordinated signals.

### 2.2.3 Sample Lagrangian Xgraph

We now describe an instance of Lagrangian Xgraphs modeling STN datasets for routing applications. Here, Xnodes represent the road segments at multiple departure-times and Xedges express the experience of a traveler among a sequence of Xnodes. Here, each Xnode is associated with information such as: (a) start and end point of the road-segment, (b) departure-time, (c) typical travel-time on segment for the departure-time (from TD roadmaps), (d) lower bound on travel-time, and other information depending on application requirements. Due to space limitation we only illustrate Xedges for travel-time experienced in a sequence of coordinated traffic signals.

*Coordinated traffic signals:* Consider again our previous example of coordinated signals SG1, SG2 and SG3 in Figure 2.3. Here, we will represent typical experiences of journeys through these signals starting from S at 7:00:00am. Given that signal delays are non-deterministic and travel-time experienced in a sequence of coordinated traffic signals is holistic, we would use bush-Xedges. Figure 2.7 illustrates bush-Xedges for some journeys at 30secs temporal granularity. We have bush-Xedges for following journeys: (a) start at S and travel to the beginning of segment B-C (after SG1), (b) start at S and travel to the beginning of segment C-E (after SG2), (c) start at S and travel to the beginning of segment E-D (after SG3).

For case (a), the bush-Xedge would include (SB0) and (BC6, BC7, BC8 and, BC9) as Xnodes for the first ($\mathcal{X}v_s$) and last Xnodes ($\mathcal{X}v_{d[1\ j]}$). Intuitively, this Xedge means that a typical journey starting from S at 7:00am along S-B (SB0 in the Figure) can start traversing road segment B-C at times 7:03:00 (no wait at SG1, BC6 in Figure), 7:03:30

(30secs wait at SG1, BC7 in the Figure), 7:04:00 or 7:04:30 (90secs wait at SG1, BC9 in the Figure). Similarly, in case (b), we would have SB0 and (CE22, CE23, CE24, CE25) as the first and last Xnodes. Internally, this would include the Xnodes (BC6, BC7, BC8 and, BC9) (not shown in Figure to maintain clarity). Other bush-Xedges can be defined in a analogous way. Similarly, there would be other bush-Xedges representing journeys starting at beginning of B-C (after SG1).

**Discussion:** Other related work for modeling STN data includes literature on conceptual models for spatio-temporal data [43], moving objects [44, 45] and hypergraphs [46, 47]. Studies focusing on conceptual models alone [43] do not model routing-related concepts such as Lagrangian reference frame. Though, studies done on moving objects represent the Lagrangian history of an object. They are not suitable for modeling TD roadmaps and traffic signal data. Furthermore, Lagrangian Xgraphs differ from both general hypergraphs [47], which represent subsets of nodes without any reference frame and directed hypergraphs [46] which directly connect a set of sources to a set of destinations.

## 2.3 Conclusion

Modeling STN datasets is important for societal applications such as routing and navigation. It is however challenging to do so due to holistic properties increasingly being captured in these datasets. The proposed Lagrangian Xgraphs addresses this challenge at logical level by expressing the non-local interactions causing these holistic properties more explicitly. Initial study shows that the proposed Lagrangian Xgraphs can express the desired routing-related concepts in a manner which is amenable to routing frameworks.

# Chapter 3

# All-start-time Lagrangian Shortest Path Problem

Given a spatio-temporal (ST) network, a source, a destination, and a start-time interval, the All-start-time Lagrangian shortest paths problem (ALSP) determines a path set which includes the shortest path for every start time in the interval. The ALSP determines both the shortest paths and the corresponding set of time instants when the paths are optimal. For example, consider the problem of determining the shortest path between the University of Minnesota and the MSP international airport over an interval of 7:00AM through 12:00 noon. Figure 3.1(a) shows two different routes between the University and the Airport. The 35W route is preferred outside rush-hours, whereas the route via Hiawatha Avenue is preferred during rush-hours (i.e., 7:00AM - 9:00AM) (see Figure 3.1(b)). Thus, the output of the ALSP problem may be a set of two routes (one over 35W and one over Hiawatha Avenue) and their corresponding time intervals.
**Application Domain:** Determining shortest paths is a key task in many societal applications related to air travel, road travel, and other spatio-temporal networks [48]. Ideally, path finding approaches need to account for the time dependent nature of the spatial networks. Recent studies [27, 28] show that indeed, such approaches yield shortest path results that save upto 30% in travel time compared with approaches that assume static network. These savings can potentially play a crucial role in reducing delivery/commute time, fuel consumption, and greenhouse emissions.

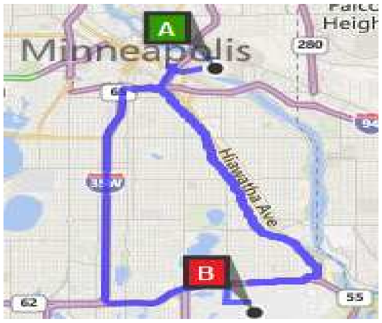

(a) Different routes between University and Airport.

| Time | Preferred Routes |
|---|---|
| 7:30am | Via Hiwatha |
| 8:30am | Via Hiwatha |
| 9:30am | via 35W |
| 10:30am | via 35W |

(b) Optimal times.

Figure 3.1: Problem illustration.

Another application of spatio-temporal networks is in the air travel. Maintaining the shortest paths across destinations is important for providing good service to passengers. The airlines typically maintain route characteristics such as average delay, flight time etc, for each route. This information creates a spatio-temporal network, allowing for queries like shortest paths for all start times etc. Figure 3.2(a) shows the Delta Airlines flight schedule between Minneapolis and Austin (Texas) for different start times [49]. It shows that total flight time varies with the start time of day.

**Challenges:** ALSP is a challenging problem for two reasons. First, the ranking of alternate paths between any particular source and destination pair in the network is not stationary. In other words, the optimal path between a source and destination for one start time may not be optimal for other start times. Second, many links in the network may violate the property of FIFO behavior. For example, in Figure 3.2(a), the travel time at 8:30AM is 6 hrs 31mins whereas, waiting 30mins would give a quicker route with 9:10AM flight. This violation of first-in-first-out (FIFO) is called non-FIFO behavior. Surface transportation networks such as road network also exhibit such behavior. For example, UPS [7, 50] minimizes the number of left turns in their delivery routes during heavy traffic conditions. This leads to faster delivery and fuel saving.

**Related work and their limitations:** The related work can be divided on the basis of FIFO vs non-FIFO networks as shown in see Figure 3.2(b). In a FIFO network, the flow arrives at the destination in the same order as it starts at the source. A* based approaches, generalized for non-stationary FIFO behavior, were proposed in [21, 51] for

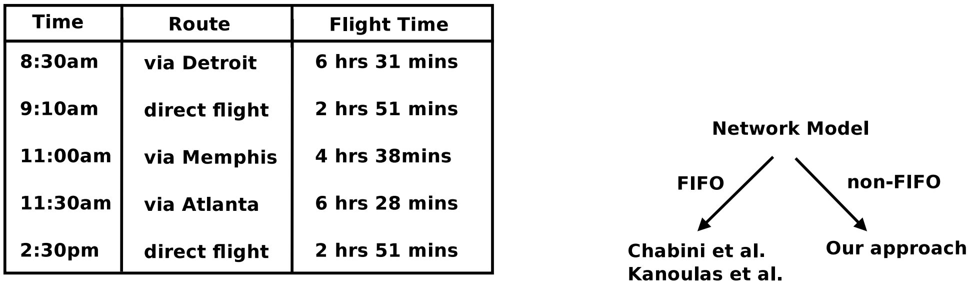

| Time | Route | Flight Time |
|---|---|---|
| 8:30am | via Detroit | 6 hrs 31 mins |
| 9:10am | direct flight | 2 hrs 51 mins |
| 11:00am | via Memphis | 4 hrs 38mins |
| 11:30am | via Atlanta | 6 hrs 28 mins |
| 2:30pm | direct flight | 2 hrs 51 mins |

(a) Minneapolis - Austin (TX) Flight schedule

(b) Related work

Figure 3.2: Application Domain and related work.

solving the shortest path problem in FIFO networks. However, transportation networks are known to exhibit non-FIFO behavior (see Figure 3.2(a)). Examples of Non-FIFO networks include multi-lane roads, car-pool lanes, airline networks etc. This paper proposes a method which is suitable for both FIFO and non-FIFO networks.

**Proposed approach:** A naive approach for solving the non-FIFO ALSP problem would involve determining the shortest path for each start time in the interval. This leads to redundant re computation of the shortest path across consecutive start times sharing a common solution. Some efficiencies can be gained using a time series generalization of a label-correcting algorithm [52]. This approach was previously used to find best start time [16], and is generalized for ALSP in Section 3.5 under the name modified-BEST. However, this approach still entails large number of redundant computations. In this paper, we propose the use of critical time points to reduce this redundancy. For instance, consider again the problem of determining the shortest path between University of Minnesota and MSP international airport over a time interval of 7:30am through 11:00am. Figure 3.1(b) shows the preferred paths at some time instants during this time interval, and Figure 3.3 shows the travel-times for all the candidate paths during this interval.

As can be seen, the Hiawatha route is faster for times in the interval [7:30am 9:30am) [1] , whereas 35W route is faster for times in the interval [9:30am 11:00am]. This shows that the shortest path changed at 9:30am. We define this time instant as *critical time point*. Critical time points can be determined by computing the earliest intersection

[1] Note: an interval (*a*,*b*) does not include the end points *a* and *b*, [*a*,*b*] includes the endpoints *a* and *b*, and [a,b) includes *a* but not *b*

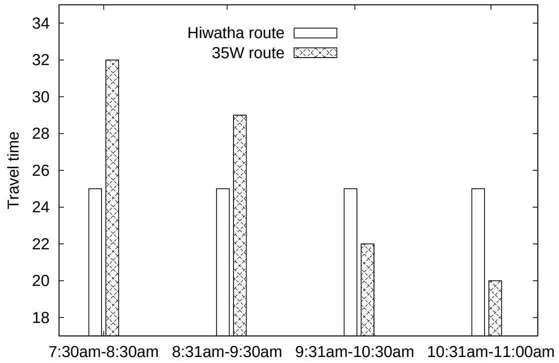

Figure 3.3: Total travel time of candidate paths.

points between the functions representing the total travel time of paths. For example, the earliest intersection point of Hiawatha route was at 9:30am (with 35W route function). Therefore, it would be redundant to recompute shortest paths for all times in interval (7:30am 9:30am) and (9:30am 11:00am] since the optimal path for times within each interval did not change. This approach is particularly useful in case when there are a fewer number of critical time points.

**Contributions:** This chapter proposes the concept of critical time points, which are the time points at which the shortest path between a source-destination pair changes. Using this idea, a novel algorithm, Critical-Time-point-based-ALSP-Solver (CTAS), is proposed for solving the ALSP problem. The correctness and completeness of the CTAS is presented. The CTAS algorithm is experimentally evaluated using real datasets. Experiment results show that the critical time point based based approach is particularly useful in cases when the number of critical times is small.

**Scope and Outline of the Chapter:** This paper models the travel time on any particular edge as a discrete time series. Turn restrictions are not considered in the ST network representation. The paper uses a Dijkstra-like framework. A*-like framework are beyond the scope of the paper. Moreover, we focus on computing the critical time points on the fly rather than precomputing them. The rest of the chapter is organized as follows. A brief description of the basic concepts and a formal problem definition is presented in Section 3.1. A description of the computational structure of the ALSP problem is presented in Section 3.2. The proposed CTAs algorithm is presented in

Section 3.3. Sectionctas-cor presents the correctness and completeness proof of the CTAS algorithm. Experimental analysis of the proposed methods is presented in Section 3.5. Finally, Section 3.6 concludes this chapter.

## 3.1 Basic Concepts and Problem Definition

**Spatio-temporal Networks:** Spatio-temporal networks may be represented in a number of ways. For example, snapshot model, as depicted in Figure 3.4, views the spatio-temporal network as snapshots of the underlying spatio network at different times. Here, each snapshot shows the edge properties at a particular time instant. For example, travel times in all the edges $((A,B)$,$(A,C)$,$(B,D)$,$(B,C))$ at time $t=0$ is represented in the top left snapshot in Figure 3.4. For the sake of simplicity, this example assumes that $(B,C)$ and $(C,B)$ have the same travel time. The same network can also be represented as a time-aggregated graph (TAG) [37] as shown in Figure 3.5(a). Here, each edge is associated with a time series which represents the total cost of the edge. For example, edge $(A,B)$ is associated with the time series [3 3 1 1 2 2 2 2]. This means that the travel time of edge $(A,B)$ at times $t=0$, $t=1$, and $t=2$ is 3, 3 and 1 respectively.

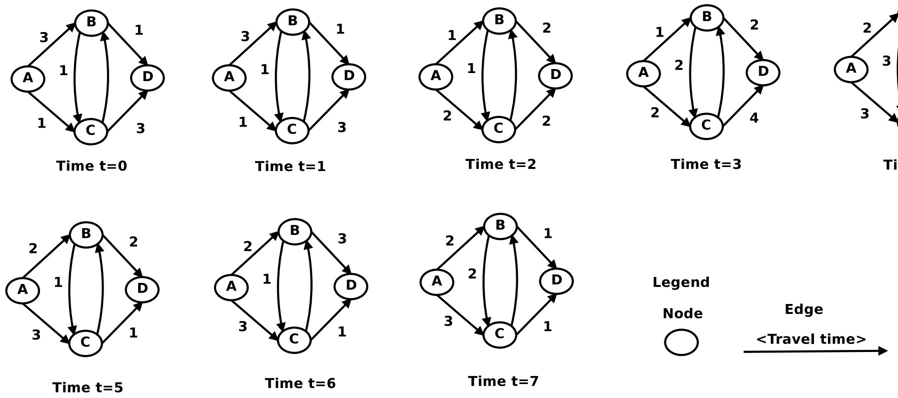

Figure 3.4: Snapshot model of spatio-temporal network.

Both TAG and snapshot representations of our sample transportation network use a *Eulerian frame of reference* for describing moving objects. In the Eulerian frame of reference, traffic is observed as it travels past specific locations in the space over a period of time [42]. It is similar to sitting on the side of a highway and watching traffic pass a fixed location.

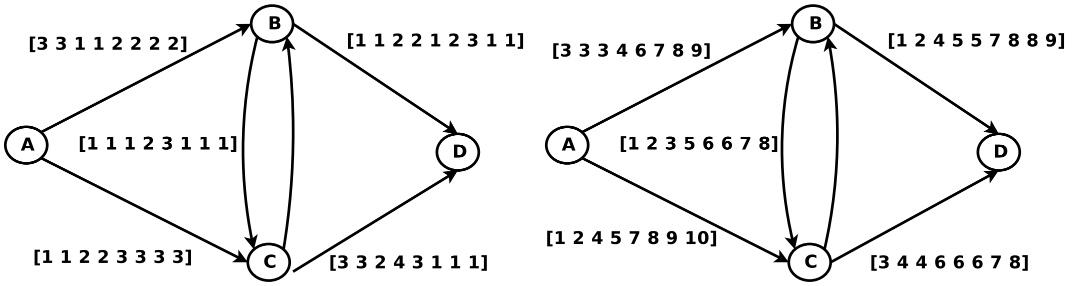

(a) Time aggregated graph.

(b) Transformed TAG.

Figure 3.5: Time aggregated graph example.

Traffic movement can also described using a *Lagrangian frame of reference*, in which the observer follows an individual moving object as it moves through space and time [42]. This can be visualized as sitting in a car and driving down a highway. The time-expanded graph (TEG) described later corresponds to this view.

Both Eulerian and Lagrangian-based views represent the same information and one view can be transformed into another view. The choice between the two depends on the problem being studied. In our problem context, it is more logical to use a Lagrangian frame of reference for finding the shortest paths because the cost of the candidate paths should be computed from the perspective of the traveler. TAG can also be used to view the network in Lagrangian frame of reference, however we use TEG for ease of communication. We now define the concept of a Lagrangian path.

**Lagrangian Path:** *A Lagrangian path $P_i$ is a spatio-temporal path experienced by the traveler between any two nodes in a network.* A Lagrangian path may be viewed as a pair of traditional path in a graph and a schedule specifying arrival time at each node. During traversal of a Lagrangian path, the weight of any particular edge $e = (x, y)$ (where $e \in P_i$) is considered at the time of arrival at node $x$. For instance, consider the path <A,C,D> for start time $t = 0$. Here, we would start at node $A$ at time $t = 0$. Therefore, the cost of edge $(A, C)$ would be considered at $t = 0$, which is 1 (see Figure 3.5(a)). Following this edge, we would reach node $C$ at time $t = 1$. Now, edge $(C, D)$ would be considered at time $t = 1$ (because it takes 1 time unit to travel on edge $(A, C)$).

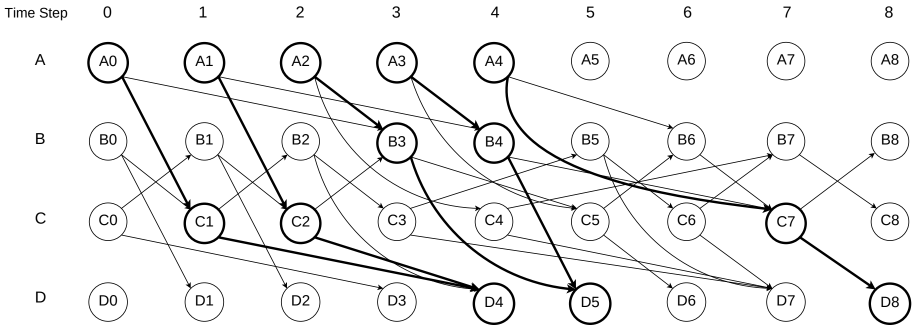

Figure 3.6: Time expanded graph example.

Conceptually, a Lagrangian path can be visualized as an explicit path in a time-expanded graph. Figure 3.6 depicts the ST network (shown in Figure 3.4) represented as a time-expanded graph [15]. Here, each node is replicated across the time instants and edges connect the nodes in a Lagrangian sense. This means that if the travel time on an edge $(A, C)$ is 1 time unit (at time $t = 0$), then there is an edge between node $A$ (at time $t = 0$) and node $C$ (at time $t = 1$). Consider the previous example of Lagrangian path <A,C,D>. This path can be represented as a simple path among nodes $A$, (at time $t = 0$, which is $A0$ in Figure 3.6), $C$ (at time $t = 1$, which is $C1$ in Figure 3.6), and $D$ (at time $t = 4$, which is $D4$ in Figure 3.6).

As discussed previously, in the case of non-FIFO networks, we may arrive at a destination earlier by waiting at intermediate nodes. For example, in Figure 3.6 if we start at node $A$ at time $t = 1$ (node $A1$), we would reach node $B$ at time $t = 4$ (node $B4$). However, if we wait at node $A$ for one time unit, then we can reach node $B$ at time $t = 3$ (node $B3$). For simplicity, Figure 3.6 does not show the wait edges across temporal copies of a physical node e.g. $A0$-$A1$, $A1$-$A2$ etc.

**Problem Definition:** We define the ALSP problem by specifying input, output, objective function and constraints. Inputs include:

(a) Spatio-temporal network $G = (V, E)$, where $V$ is the set of vertices, and $E$ is the set of edges;

(b) A source $s$ and a destination $d$ pair where $\{s, d\} \in V$;

(c) A discrete time interval $\lambda$ over which the shortest path between $s$ and $d$ is to be determined;

(d) Each edge $e \in E$ has an associated cost function, denoted as $\delta$. The cost of an edge represents the time required to travel on that edge. The cost function of an edge is represented as a time series.

*Output:* The output is a set of routes, $P_{sd}$, from $s$ to $d$ where each route $P_i \in P_{sd}$ is associated with a set of start time instants $\omega_i$, where $\omega_i$ is a subset of $\lambda$.

*Objective function:* Each path in $P_{sd}$ is a shortest commuter-experienced travel time path between $s$ and $d$ during its respective time instants.

We assume the following constraints: The length of the time horizon over which the ST network is considered is finite. The weight function $\delta$ is a discrete time series.

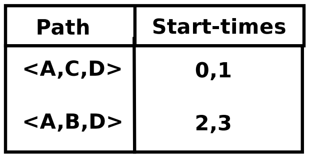

| Path | Start-times |
|---|---|
| <A,C,D> | 0,1 |
| <A,B,D> | 2,3 |

Figure 3.7: Output of ALSP problem.

**Example:** Consider the sample spatio-temporal network shown in Figure 3.5(a). An instance of the ALSP problem on this network with source $A$ destination $D$ and $\lambda = [0, 1, 2, 3]$, is shown in Figure 3.7. Here, path A-C-D is optimal for start times $t = 0$ and $t = 1$, and path A-B-D is optimal for start times $t = 2$ and $t = 3$.

## 3.2 Computational structure of the ALSP problem

The first challenge on solving the ALSP problem involves capturing the inherent non-stationarity present in the ST network. Due to this non-stationarity, traditional algorithms developed for static graphs cannot be used to solve the ALSP problem because the optimal sub-structure property no longer holds in case of ST networks [16]. On the other hand, algorithms developed for computing shortest paths for a single start time [3, 15, 16, 22, 53] are not practical because they would require redundant re-computation of shortest paths across the start times sharing a common solution.

This paper proposes a divide and conquer based approach to handle network non-stationarity. In this approach we divide the time interval over which the network exhibits non-stationarity into smaller intervals which are guaranteed to show stationary behavior

[2] . These intervals are determined by computing the critical time points, that is, the time points at which the cost functions representing the total cost of the path as a function of time intersect. Now, within these intervals, the shortest path can be easily computed using a single run of a dynamic programming (DP) based approach [16]. Recall our previous example of determining the shortest paths between the university and the airport over an interval of [7:30am 11:00am]. Here, 9:30am was the critical time point. This created two discrete sub-intervals [7:30 9:30) and [9:30 11:00]. Now, we can compute the ALSP using two runs of a DP based algorithm [16] (one on [7:30 9:30) and another on [9:30 11:00]).

Our second challenge for solving ALSP is capturing the non-FIFO behavior of the network. We do this by converting the travel information associated with an edge into earliest arrival time (at destination) information [22, 54]. This is a two step process. First, the travel time information is converted into arrival time information. Second, the arrival time information is converted into earliest arrival time information. The second step captures the possibility of arriving at an end node earlier by waiting (non-FIFO behavior). For example, in the ST network shown in Figure 3.5(a), the travel time series of edge $(A, B)$ is [3 3 1 1 2 2 2 2]. First, we convert it into arrival time series. This is done by adding the time instant index to the cost. For example, if we leave node $A$ at times $t = 0, 1, 2, 3 \ldots$, we would arrive at node $B$ at times $t = 3+0, 3+1, 1+2, 1+3, 2+4 \ldots$. Therefore, the arrival time series of $(A, B)$ is [3 4 3 4 6 7 8 9]. The second step involves comparing each value of the arrival time series to the value to its right in the arrival time series. A lower value to its right means we can arrive at the end node earlier by waiting. Consider the arrival time series of $(A, B) =$ [3 4 3 4 6 7 8 9]. Here, the arrival time for $t = 1$ is 4 (which is less than the arrival time for $t = 2$). Therefore, the earliest arrival time on edge $(A, B)$ for time $t = 1$ is 3 (by waiting for 1 time unit at node $A$). This process is repeated for each value in the time series. The earliest arrival time series of edge $(A, B)$ is [3 3 3 4 6 7 8 9]. The earliest arrival time series of the edges are precomputed. Figure 3.5(b) shows the ST network from Figure 3.5(a) after the earliest arrival time series transformation.

There are two ways to determine the stationary intervals, either by precomputing all

[2] By stationarity, we mean that ranking of the alternate paths between a particular source-destination pair does not change within the interval i.e, there is a unique shortest path

the critical time points, or by determining the critical time points at run time. The first approach was explored in [55] for a different problem. Precomputing the critical time points involves computing intersection points between cost functions of all the candidate paths. Now, in a real transportation network there can be exponential number candidate paths. Therefore, this paper follows the second approach of determining the critical time points at run-time. In this approach only a small fraction of candidate paths and their cost functions are actually considered while computation. Now, we define and describe our method of determining the critical time points.

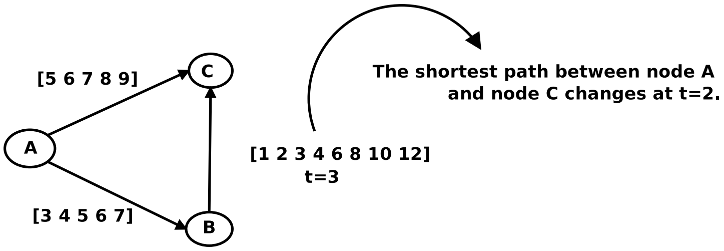

Figure 3.8: Illustrating Non-stationarity

**Critical time point:** *A start time instant when the shortest path between a source and destination may change.*

Consider an instance of the ALSP problem on the ST network shown in Figure 3.8, where the source is node $A$, the destination is $C$, and $\lambda = [0\ 1\ 2\ 3\ 4]$. Here, start time $t = 2$ is a critical time point because the shortest path between node A and C changes for start times greater that $t = 2$. Similarly, $t = 2$ is also a critical time point for the network shown in Figure 3.5(a), where the source node is $A$ and the destination node is $D$ (see Figure 3.7). Now, in order to determine these start time instants, we need to model the total cost of the path. This paper proposes using a weight function to capture the total cost of a path. This approach, which associates a weight function to a path, yields a *path-function* which represents the earliest arrival time at the end node of the path. A formal definition of the path-function is given below.

**Path Function:** *A path function represents the earliest arrival time at the end node of a path as a function of time. This is represented as a time series. A path function is determined by computing the earliest arrival times on its component edges in a Lagrangian* *fashion.*

For example, consider the path <A,B,C> in Figure 3.8. This path contains two edges, $(A, B)$ and $(B, C)$. The earliest arrival time (EAT) series of edge $(A, B)$ is [3 4 5 6 7], while the EAT of edge $(B, C)$ is [1 2 3 4 6 8 10 12]. Now, the path function of <A,B,C> for start times $[0, 4]$ is determined as follows. If we start at node $A$ at $t = 0$, the arrival time at node $B$ is 3. Now, arrival time at node $C$ through edge $(B, C)$ is considered for time $t = 3$ (Lagrangian fashion), which is 4. Thus, the value of the path function of <A,B,C> for start time $t = 0$ is 4. The value of the path-function for all the start times is computed in similar fashion. This would give the path function of <A,B,C> as [4 6 8 10 12]. This means that if we start at node $A$ at times $t = 0, 1, 2, 3, 4$ then we will arrive at end node $C$ at times $t = 4, 6, 8, 10, 12$. Similarly, the path function of path <A,C> is [5 6 7 8 9] (since it contains only one edge). By comparing the two path-functions we can see that path <A,B,C> has an earlier arrival time (at destination) for start times $t = 0$ and $t = 1$ (ties are broken arbitrarily). However, path <A,C> is shorter for start time $t \geq 2$. Thus, start time $t = 2$ becomes a critical time point. In general, the critical time points are determined by computing the intersection point (with respect to time coordinate) between path functions. In this case, the intersection point between path functions <A,C> and <A,B,C> is at time $t = 2$. Computing this point of intersection is the basis of the CTAS algorithm.

## 3.3 Critical Time-point based ALSP Solver (CTAS)

This section describes the critical time point based approach for the ALSP problem. This approach reduces the need to re-compute the shortest paths for each start time by determining the critical time points (start times) when the shortest path may change. Although Lagrangian paths are best represented by a time-expanded graph (TEG), these graphs are inefficient in terms of space requirements [16]. Therefore, this paper uses TEG model only for visualizing the ST network. For defining and implementing our algorithm we use TAG [16]. Recall that since the optimal substructure property is not guaranteed in a ST network, the given time interval is partitioned into a set of disjoint sub-intervals, where the shortest path does not change. The *Sub-interval Optimal Lagrangian Path* denotes this shortest path.

**Sub-interval optimal Lagrangian path:** *is a Lagrangian path, $P_i$, and its corresponding set of time instants $\omega_i$, where $\omega_i \in \lambda$. $P_i$ is the shortest path between a source and a destination for all the start time instants $t \in \omega_i$.*
The Lagrangian path <A,C,D> shown in Figure 3.7 is an example of sub-interval Optimal Lagrangian Path and its corresponding set $\omega = 0, 1$.

### 3.3.1 CTAS Algorithm

The algorithm starts by computing the shortest path for the first start time instant in the set $\lambda$. Since the optimal substructure property is not guaranteed in a ST network, the choice of the path to expand at each step made while computing the shortest path for a particular start time may not be valid for later time instants. Therefore, the algorithm stores all the critical time points observed while computing the shortest path for one start time in a data structure called *path-intersection table*. As discussed previously, the critical time point is determined by computing the time instants where the path functions of the candidate paths intersect. The earliest of these critical time points represents the first time instant when the current path no longer remains optimal. The algorithm re-computes the shortest paths starting from this time instant. Since the path functions represent the earliest arrival time (at end node of path) for a given start time, the intersection points represent the start times (at the source) when there is a change in relative ordering of the candidate paths.

The pseudocode for the CTAS algorithm is shown in Algorithm 1. The outer loop of ALSP ensures that a shortest path is computed for each start time instant in the set $\lambda$. The inner loop computes a single sub-interval optimal Lagrangian path. There may be several sub-interval optimal Lagrangian paths for the set $\lambda$. First, a priority queue is initialized with the source node. The inner loop determines the shortest path for start times greater than the earliest critical time points stored in the path intersection table ($t_{min}s$). For the first iteration, this would just be the first start time instant of our set $\lambda$. In each iteration, the algorithm expands along the path which has the minimum weight for time $t = t_{min}$. After a path is expanded the last node of the path is closed for start time $t = t_{min}$. For example, if a path $s - x - y$ is expanded for start time $t = t_{min}$, then node $y$ is closed for start time $t = t_{min}$. This means there cannot be any

**Algorithm 1** CTAS Algorithm

```
Determine the earliest arrival time series of each edge
Initialize the path intersection table with the first start time in $\lambda$
while a shortest path for each time $t \in \lambda$ waits to be determined do
    Select the minimum time instants among all time instants at which a shortest path might change and clear path intersection table
    Initialize a priority queue with the path functions corresponding to the source node and its neighbors
    while destination node is not expanded do
        Choose the path with the minimum weight to expand
        Determine the intersection points among the path functions in the priority queue
        Delete all the paths ending on that node from the priority queue
        Save the time coordinate of the intersection point in the path intersection table
        Determine the path functions resulting from expansion of the chosen path
        Push the newly determined path functions into the priority queue
    end while
end while
```

other shorter path from node $s$ to node $y$ for the start time $t = t_{min}$.

Before expanding a path, the algorithm computes the intersecting points among the path functions available in the priority queue. The earliest intersection point (considering intersection points in the increasing order of their time coordinate) involving the path with minimum weight is the time instant when the stationary ordering among the candidate paths change. After that the path is expanded and path functions to all its neighbors are computed and added to the priority queue. The inner loop terminates when it tries to expand a source-destination path. In the next iteration of the outer loop, the shortest path computation starts from the earliest of the optimal route change times in path intersection table. Now, the path determined in the previous iteration is closed for all the start times earlier than earliest of the critical time point (and greater than $t_{min}$ of previous iteration). In a worst case scenario, the value of the earliest critical time point could be the next time start time instant in the set $\lambda$ (one more than previous $t_{min}$). In such a case, the inner loop would have determined the shortest path only for a single start time instant. The algorithm terminates when the earliest of the path-order change times is greater than the latest start time instant in the set $\lambda$.

**Execution Trace:** Figure 3.9 gives an execution trace of the CTAS algorithm on the ST network shown in Figure 3.5(b). The first iteration of the outer loop starts with initializing the priority queue with the source node. The inner loop builds a shortest path starting from the earliest critical time point. For the first iteration, this would be time $t = 0$ (the first start time instant in $\lambda$). First, the source node is expanded for time $t = 0$. Path functions for its immediate neighbors (path <A,B> and <A,C>) are computed and added them to the priority queue. In this case, the path functions just happen to be their edge weight functions.

In the first iteration of the inner loop, the algorithm chooses the path whose path function has minimum weight at the start time instant chosen in step 4 of the algorithm. This would be $t = 0$ for the first case. At this point the algorithm has two choices, path function <A,C> and <A,B>(see Figure 3.9). The algorithm chooses <A,C> because it has lowest cost for $t = 0$. This path is expanded and path functions for its neighbors, <A,C,D> and <A,C,B>, are computed and added to the priority queue. Again the choice of path <A,C> may not be valid in later times, therefore, the algorithm closes the node C only for the start time $t = 0$. The algorithm stores the intersection point between the path <A,B> and <A,C> (which is at $t = 2$) in the path intersection table.

The next iteration expands path <A,C,B>. There is no intersection between the path functions of <A,C,D> and <A,C,B> (in our interval $\lambda$). Again, node B is closed only for $t = 0$. At this point, all the paths which end in node $B$ are deleted from the priority queue. Now, the priority queue contains two paths, <A,C,D> and <A,C,B,D>. This time the algorithm tries to expand along path <A,C,D> because it has least cost. Again the intersection point between the path functions is computed. Here, paths <A,C,D> and <A,C,B,D> do not intersect [3] . This time a complete source to destination path was expanded. This is the terminating condition of the inner loop. This completes one iteration of the outer loop. Next iteration of the outer loop builds the shortest path starting at the earliest of the critical time points stored in the previous iteration. This happens to be $t = 2$ for our example. The next iteration of the inner loop starts for start time $t = 2$. At this point the path intersection table is cleared. We see that the algorithm did not compute the shortest path for start time $t = 1$. Figure 3.6 also showed that the shortest path did not change start time $t = 1$ (shortest paths between node $A$ and node $D$ for start-times $t = 0, 1, 2, 3$ are shown in bold). The fact that the next iteration of the CTAS algorithm starts with $t = 2$ shows that it saves

[3] Note that here path <A,C,B,D> may also be expanded

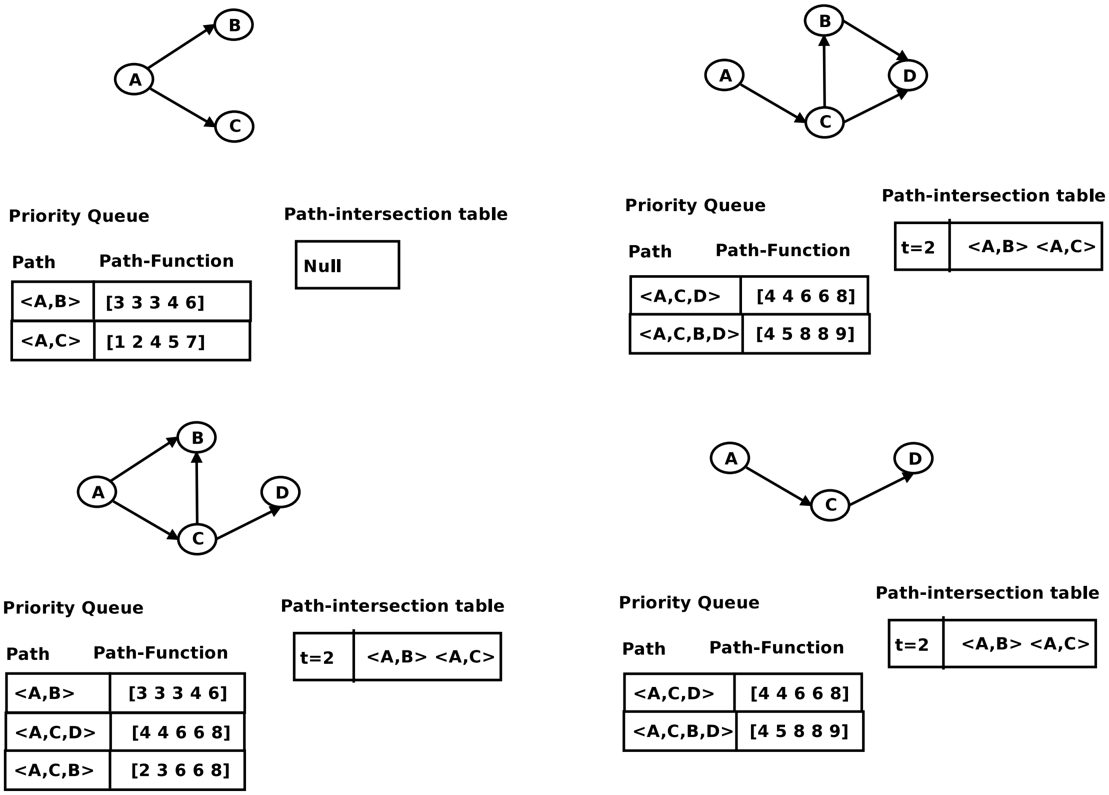

Priority Queue

| Path | Path-Function |
|---|---|
| <A,B> | [3 3 3 4 6] |
| <A,C> | [1 2 4 5 7] |

Path-intersection table

| Null |
|---|

Priority Queue

| Path | Path-Function |
|---|---|
| <A,C,D> | [4 4 6 6 8] |
| <A,C,B,D> | [4 5 8 8 9] |

Path-intersection table

| | |
|---|---|
| t=2 | <A,B> <A,C> |

Priority Queue

| Path | Path-Function |
|---|---|
| <A,B> | [3 3 3 4 6] |
| <A,C,D> | [4 4 6 6 8] |
| <A,C,B> | [2 3 6 6 8] |

Path-intersection table

| | |
|---|---|
| t=2 | <A,B> <A,C> |

Priority Queue

| Path | Path-Function |
|---|---|
| <A,C,D> | [4 4 6 6 8] |
| <A,C,B,D> | [4 5 8 8 9] |

Path-intersection table

| | |
|---|---|
| t=2 | <A,B> <A,C> |

Figure 3.9: Execution trace of CTAS algorithm.

computation. The algorithm terminates when shortest paths of all time instants in the set $\lambda$ have been determined. Figure 3.7 shows the final result of the algorithm.

## 3.4 Correctness and Completeness CTAS algorithm

The CTAS algorithm divides a given departure-time interval into a set of disjoint sub-intervals. Within these intervals, the shortest path does not change. The correctness of the CTAS algorithm requires the path returned for a particular sub-interval to be optimal and the completeness of the algorithm guarantees that none of the critical time points are missed. The correctness of the CTAS can be easily argued on the basis greedy nature of the algorithm. Lemma 7 shows that the CTAS algorithm does not miss any critical time point. Using Lemma 7, Theorem 4 proves the completeness of the CTAS algorithm.

**Lemma 1.** *The CTAS algorithm recomputes the shortest path for all those departure times $t_i \in \lambda$, where the shortest path for previous departure time $t_{i-1}$ can be different from the shortest path for departure time $t_i$.*

*Proof.* Consider the sample network shown in Figure 5.13, where a shortest path has to be determined between node $s$ and $d$ for discrete time interval $\lambda = [1, 2 \ldots T]$. First, the source node is expanded for the time instant $t = 1$. As a result, path functions for all the neighbors <s,2>, <s,1>, <s,$x_i$> are added to the priority queue. With loss of generality assume that path <s,1> is chosen in the next iteration of the inner loop. Also assume that the earliest intersection point between path functions <s,$x_i$ > and <s,1> is at $t = \alpha$ between <s,1> and <s,2>. Now, the queue contain paths <s,1,d>, <s,2>, <s,$x_i$>. Here we have two cases. First, path <s,1,d> has lower cost for start time $t = 1$. Second, path <s,2> has lower cost for start time $t = 1$.

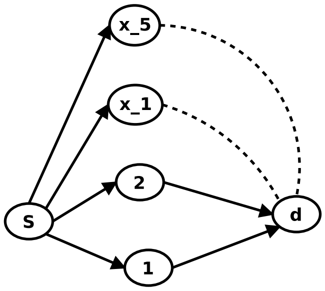

Figure 3.10: Network for Lemma 7

Considering the first case, without loss of generality assume that the earliest intersection point between the path functions <s,1,d> and <s,2> is at $t = \beta$. Note that both $t = \alpha$ and $t = \beta$ denote the departure times at the source node. Consider the case when $\beta \leq \alpha$ (Note that $\beta$ cannot be greater than $\alpha$ as all the edges have positive weights). In such a case the shortest path is recomputed for starting time $t = \beta$ and the path <s,1,d> is closed for all start times $1 \leq t < \beta$. Assume for the sake of contradiction, that there is a shortest path $P_x$ from source to destination that is different from path <s,1,d> which is optimal for departure time $t_x \in [1, \beta)$. Assume that $P_x =< s, x_1, x_2, x_3, \ldots, d >$. This means that path $< s, x_1 >$ had least for time $t = t_x$. However, by the nature of the algorithm, this path would have been expanded instead of path $< s, 1 >$ (a contradiction). Moreover, as all the travel times positive, if sub path <s,$x_1$ > was not shorter than <s,1,d> for start times earlier than $t = \beta$. Any positive weight addition to the path function (through other edges) cannot make $P_x$ shorter than <s,1,d>. Consider the second case when <s,2> had lower cost for start time $t = 1$. Now, path <s,2> would be expanded and path function <s,2,d> would be added to priority queue. Again, assume that path functions <s,1,d> and <s,2,d> intersect at time $t = \beta$. A similar argument can be given for this case as well. □

**Corollary 1.** *(Corollary to Lemma 7) Given a instance of forward search which started from node $S$ at time $t_d$ and terminated when node $D$ was closed. Now, if the earliest forecasted forward critical time point was $t_{ctp}^{min}$, then shortest path determined between $S$ and $D$ is optimal from all departure-times $t_d$ through $t_{ctp}^{min} - 1$.*

**Theorem 1.** *CTAS algorithm is complete.*

*Proof.* There may be several sub-interval optimal Lagrangian paths $P_i$ over set $\lambda$. Each $P_i$ is associated with a set of time instants $\omega_i$, where $\bigcup_{\forall i \in |P_{sd}|} \omega_i = \lambda$. The completeness proof of the CTAS algorithm is presented in two parts. First, using Lemma 7 we can conclude that the CTAS algorithm does not miss any departure time instant when the shortest path changes. Secondly, the outer loop iterates until the algorithm determines a shortest path for all the time instants in set $\lambda$. This happens when the earliest of the forecasted CTPs $t_{min}$ falls outside $\lambda$. This proves the completeness of the algorithm. □

## 3.5 Experimental evaluation

Experiments were conducted to evaluate the performance of CTAS algorithm as different parameters were varied. The experiments were carried on a real dataset containing the highway road network of Hennepin county, Minnesota, provided by NAVTEQ [56]. The dataset contained 1417 nodes and 3754 edges. The data set also contained travel times for each edge at time quanta of 15mins. Figure 3.2 shows the speed profiles for a particular highway segment in the dataset over a period of 30days. As can be seen, the speed varies with the time of day. For experimental purposes, the travel times were converted into time quanta of 1mins. This was done by replicating the data inside time interval. The experiments were conducted on an Intel Quad core Linux workstation with 2.83Ghz CPU and 4GB RAM. The performance of CTAS algorithm was compared against a modified version of the existing BEST start time algorithm proposed in [16].

**Modified-BEST (MBEST) algorithm:** The MBEST algorithm consists of two main parts. First, the shortest path between source and destination is determined for all the desired start time instants. Second, the computed shortest paths are post-processed and a set of distinct paths is returned. The MBEST algorithm uses a label correcting approach similar to that of BEST algorithm, proposed in [16] to compute the shortest paths between source and destination. The algorithm associates two lists viz, the arrival time list and ancestor list, with each node. The arrival time array, $C_v[t]$, represents the earliest arrival time at node $v$ for the start time $t$ at the source. The ancestor array, $An_v[t]$, represents the previous node in the path from source for time $t$. These lists are updated using Equation 3.1, where $\gamma_{uv}$ represents the earliest arrival time series of the edge $(u, v)$. The algorithm terminates when there are no more changes in the arrival time list of any node.

$$C_v[t] = \min\{C_v[t], \gamma_{uv}[C_u[t]]\}, uv \in E \tag{3.1}$$

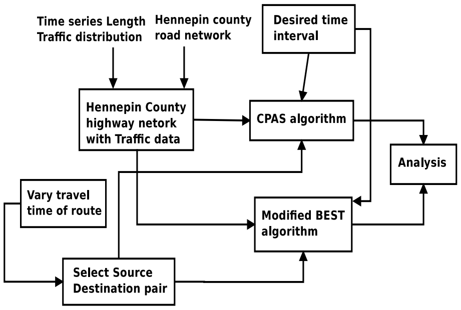
Time series Length
Traffic distribution
Hennepin county road network
Desired time interval
Hennepin County highway netork with Traffic data
CPAS algorithm
Analysis
Vary travel time of route
Modified BEST algorithm
Select Source Destination pair

Figure 3.11: Experimental setup

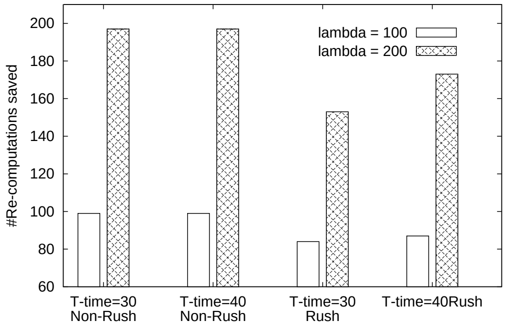

Figure 3.12: Re-computations saved

**Experimental setup:** The experimental setup is shown in Figure 3.11. The first step of the experimental evaluation involved combining the travel time information along with the spatial road network to represent the ST network as a Time-aggregated graph. A set of different queries (each with different parameters) was run on the CTAS and the MBEST algorithms. The following parameters were varied in the experiments: (a) length of the time interval over which shortest paths were desired ($|\lambda|$), (b) total travel time of the route, (c) time of day (rush hour vs non-rush hours). A speedup ratio, given by Equation 3.2, was computed for each run. The total number of re-computations avoided by CTAS was also recorded for each run. In worst case, the shortest paths may have to be re-computed for each time instant in the interval $\lambda$. The total number of re-computations saved by CTAS is the difference between $|\lambda|$ and re-computations performed.

$$speed - up\ ratio = \frac{MBEST\ runtime}{CTAS\ runtime} \tag{3.2}$$

**Number of re-computations saved in CTAS :** Figure 3.12 shows the number of re-computations saved by the CTAS algorithm. The experiments showed that more saving was gained where paths were shorter. Similarly, fewer number of re-computations were performed in case of Non-rush hours. This is because there were fewer intersections among the path-functions.

**Effect of length of start time interval ($|\lambda|$):** This experiment was performed to evaluate the effect of length of start time interval ($\lambda$) over which the shortest path was desired. Figure 3.13(a) shows the speed-up ratio for Non-rush hours and Figure 3.13(b) shows the speed-up ratio for Rush hours. The speed ratio was calculated for paths with travel time 30 and travel time 40. These travel times indicate the time required to travel on these paths during non-rush hours when there is no traffic. The experiments showed that run-time of both CTAS and MBEST increased with increase in the lambda. Runtime of MBEST increases steadily whereas CTAS increases very slowly with *lambda* for a travel time of 30. However, the run-time of CTAS increases rapidly for travel time of 40.

**Effect of total travel time of a path:** This experiment was performed to evaluate the effect of total travel time of a path on the candidate algorithms. Figure 3.14 shows the speed-up ratio as the total travel time of the path was varied. The experiments showed that the runtime of CTAS algorithm increased with a corresponding increase in the total travel time of the path, whereas the runtime of the MBEST algorithm remained the same. This is because, CTAS algorithm follows a Dijkstra's like approach and expands the paths, but MBEST is follows a label correcting approach and terminates when there

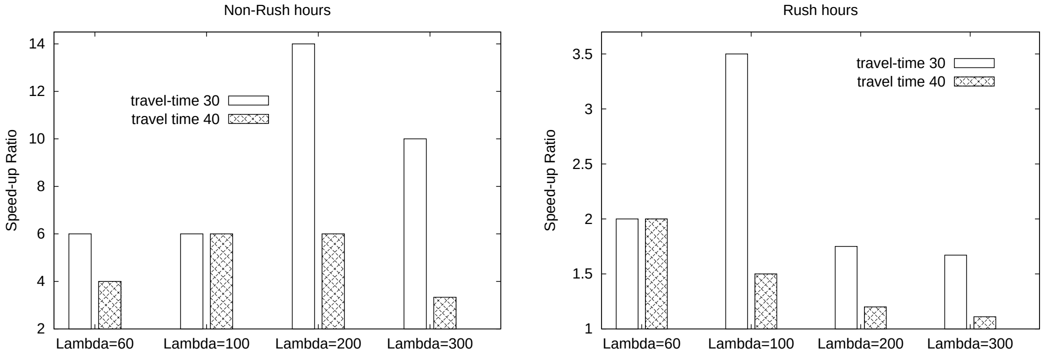

(a) (b)

Figure 3.13: Effect of Lambda on Speed-up

no more changes in the arrival time array of any node.

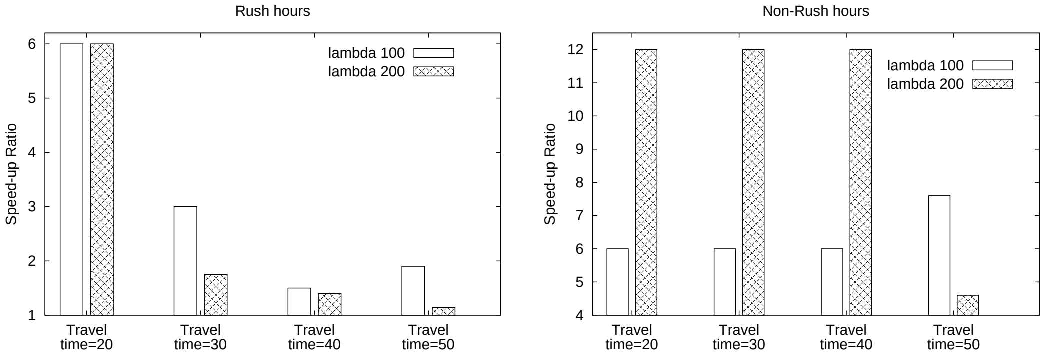

(a) (b)

Figure 3.14: Effect of travel time on Speed-up

**Effect of different start times:** Experiments showed that better speed-up was obtained for Non-rush hours than the rush hours (see Figure 3.14 and Figure 3.13). This is because there are fewer number of intersection points in case of non-Rush hours.

## 3.6 Conclusions

The All-start-time shortest Lagrangian shortest path problem (ALSP) is a key component of applications in transportation networks. ALSP is a challenging problem due to the non-stationarity of the spatio-temporal network. Traditional A* and Dijkstra's based approaches incur redundant computation across the time instants sharing a common solution. The proposed Critical Time-point based ALSP Solver (CTAS), reduces this redundant re computation by determining the time points when the ranking among the alternate paths between the source and destination change. Theoretical and experimental analysis show that this approach is more efficient than naive particularly in case of few critical time points.

# Chapter 4

# Bi-directional algorithm for the ALSP problem

Given a spatio-temporal (ST) network, a source, a destination, and a discrete departure-time interval, the All-departure-time Lagrangian shortest paths problem (ALSP) determines a path set which includes the shortest path for every departure time in the interval. The ALSP determines both the shortest paths and the corresponding set of time instants when the paths are optimal. For example, consider the problem of determining the shortest path between the University of Minnesota and the MSP international airport over the departure-time interval of 7:30am through 9:15am. Figure 4.1 (on the left) shows three different routes between the University and the Airport. The I-35W route is preferred outside rush-hours, whereas the route via Hiawatha Avenue is preferred during rush-hours (i.e., 7:30am - 8:30am). Thus, the output of the ALSP problem may be a set of these two routes and their corresponding preferred departure time intervals.
**Application Domain:** Determining shortest paths is a key task in many societal applications related to air travel, road travel, eco-routing and other spatio-temporal network applications [48, 57, 58]. Ideally, path finding approaches need to account for the time dependent nature of the spatial networks. Recent studies [27, 28] show that indeed, such approaches yield shortest path results that save up to 30% in travel time compared with approaches that assume static network. These savings can potentially play a crucial role in reducing delivery/commute time, fuel consumption, and greenhouse

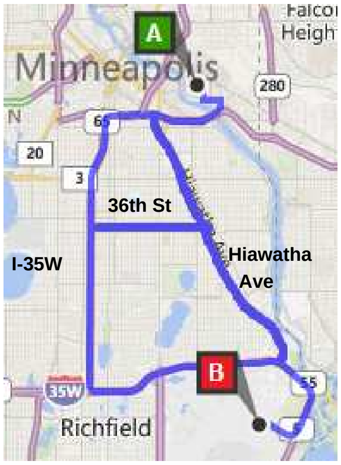

| ID | Departure Time | Preferred Route |
|---|---|---|
| 1 | 7:30am | via Hiawatha |
| 2 | 7:45am | via Hiawatha |
| 3 | 8:00am | via Hiawatha |
| 4 | 8:15am | via Hiawatha |
| 5 | 8:30am | via Hiawatha |
| 6 | 8:45am | via I35W |
| 7 | 9:00am | via I35W |
| 8 | 9:15am | via I35W |

Figure 4.1: Preferred routes between the University and Airport [2].

emissions leading to ‘eco-routing’ [5].

**Challenges:** The ALSP problem is challenging because of multiplicity of departure times. In addition, the ranking among candidate paths between any particular source and destination pair in the network is not stationary across departure times. In other words, the optimal path between a source and destination for one departure time may not be optimal for other departure times. This lack of stationarity in ST networks makes it non-trivial to use classic algorithms developed for static graphs (e.g. Dijkstra’s and A*) for solving the ALSP problem. On the other hand, it would be computationally redundant to re-compute the shortest path for each distinct departure-time when the ranking changes only few times. For example, in our previous University-Airport ALSP instance, it would be redundant to re-compute for all the departure-times in the interval of 7:30am through 9:15am when the shortest path changes only at 8:45am.

**Limitations of Related work:** Few studies have investigated ways to reduce redundant computations across consecutive departure times sharing a common solution. Figure 4.2(a) shows a classification of these approaches. These methods attempt to reduce the redundant computations by closing nodes for several departure instants during a single iteration of the algorithm. A node is said to be closed when the algorithm has found a shortest path (from the source) to that node. So, in these algorithms, an attempt is made to find the shortest path to a node for several departure-times (at the

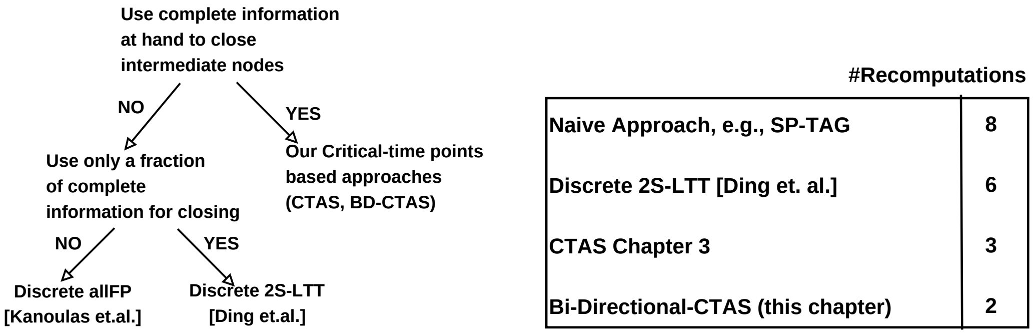

(a) Related work classification

| | #Recomputations |
|---|---|
| Naive Approach, e.g., SP-TAG | 8 |
| Discrete 2S-LTT [Ding et. al.] | 6 |
| CTAS Chapter 3 | 3 |
| Bi-Directional-CTAS (this chapter) | 2 |

(b) #re-computations on UMN-Airport ALSP instance

Figure 4.2: Comparison of Related work and our critical-time based approaches.

source) in a single iteration. Figure 4.2(b) shows the number of re-computations that would be required by different methods which close intermediate nodes on our previous University-Airport ALSP instance illustrated in Figure 4.1. A naive approach (first row in Figure), referred to as SP-TAG in this paper, computes a shortest path for each of the 8 time instants shown in Figure 4.1. Therefore, methods which reduce redundant work aim to perform less than 8 re-computations. However, they do this using only a fraction of the available information at hand. For instance, discrete version of [3] (referred to as Discrete 2S-LTT in this paper) compares the time series of arrival times at an intermediate node against a single (scalar) lowest feasible cost along other candidate paths to that node leading to 6 re-computations (second row in Figure 4.2(b)). However, this can be further improved as the shortest path changes only once (at 8:45am) in our ALSP instance.

Another discrete version of approach [51] (referred to as Discrete allFP in this paper) does not close any intermediate nodes. Consequently all paths between a source and a destination whose destination arrival time is less than the optimal arrival time for the last desired departure-time are enumerated. As there can be a huge number of candidate paths between a source and a destination, it usually results in significant computational bottlenecks. This limitation was also highlighted by other works [3, 17]. Running time ramifications of this limitation are shown in our experimental analysis.

**Proposed Approach:** In contrast, we propose to use all of the available information by comparing the entire available time series of arrival times along candidate paths at each intermediate node before destination is closed. As a result, nodes are likely to be closed for a longer range of departure times, and hence incur fewer redundant re-computations. The last two rows in Figure 4.2(b) illustrate the superior performance of our critical-time-points based approaches which use all of the available information to reduce the re-computations to just 3 or 2. Note that reducing the number of re-computations to less than 2 is not possible for our problem instance as the shortest path does change at 8:45am (see Figure 3.1). Appendix A.1 provides a detailed trace of all the above mentioned algorithms on this University-Airport ALSP instance.

We propose to operationalize the use of complete information through the our concept of *critical-time-points*. This helps in reducing the redundant computations across departure times sharing a common solution. For instance, consider again our previous University-Airport ALSP instance. As Figure 4.1 shows, the Hiawatha route is faster for times in the interval [7:30am 8:30am], whereas I-35W route is faster for times in the interval [8:45am 9:15am]. This shows that the shortest path changed at some instant between 8:30am and 8:45am. For the sake of convenience we assume it changed at 8:45am. We define this time instant as a *critical time point* (CTP), i.e., a departure time before which optimal path is guaranteed not to change. Critical time points can be determined by computing the earliest intersection points between functions representing the total travel time of paths. For example, the earliest intersection point of the Hiawatha route would be at 8:45am (with the I-35W route function).

A candidate way to compute the critical-time points for a given ALSP problem instance would be to first enumerate the costs (as a function of departure-time) of all the possible candidate paths between the source and destination and, then compute the lower envelope of these cost functions to give us the critical time points for the given problem. However, this would be computational intensive as in a real road network, there can be huge number of candidate paths. Thus, we propose to use a expand and refine search strategy (similar to Dijkstra's) to enumerate paths for determining their cost functions. As mentioned earlier, due to non-stationarity in the ST network, we would not have a clear ranking of candidates across departure-times. To this end, we propose to use the ranking for a particular departure-time (which is stationary) to conservatively forecast only the next time departure-time (forcasted critical-time point) when the ranking is expected to change (while maintaining correctness). The same procedure is repeated for this departure-time as well, and continued until all the desired departure-times in the given ALSP instance are covered.

It is important to note that due to the expand and refine nature of the search strategy, we would not be enumerating all the possible candidate paths (and their cost functions) between source and destination. In other words, we would computing critical-time points based on partial paths itself which might lead to forecasts which are irrelevant to our source-destination pair. Figure 4.3 (on the left) illustrates this conceptually. Here, the search started from $S$ (for a specific departure-time) and terminated at node $D$. The shaded region shows the area covered by the search, i.e., the enumerated candidate paths belong to this region. Now, our forecasted critical-time point might come due to an intersection between cost functions of paths $S \rightsquigarrow V$ and $S \rightsquigarrow D$. It is necessary to consider this because there might be a path through $V$ which might be optimal for the departure-time corresponding to the intersection. But at the same time it might be irrelevant as the cost on the $V \rightsquigarrow D$ portion was not considered while computing the intersection point.

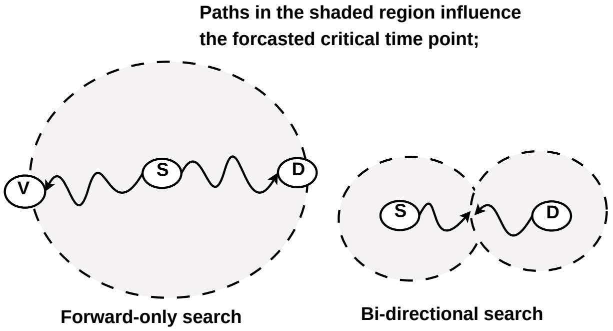
Paths in the shaded region influence
the forcasted critical time point;
V
S
D
S
D
Forward-only search
Bi-directional search

Figure 4.3: Exploration space of forward-only and bi-directional searches.

Our previous algorithm CTAS (Section 3.3 in Chapter 3) focused on this kind of search strategy which started from the source and terminated when shortest path to destination was found. But, as mentioned before, it can lead to irrelevant critical-time points due to large search space. This was specifically true when the shortest path turned out to be long. This was primarily because a larger search area was explored in these cases making it more likely to encounter an irrelevant critical-time point. In this paper, we propose to use a bi-directional search which starts at both source and destination. This allows us to do a more focused search for paths to the desired destination. Figure 4.3 (on the right) illustrates this conceptually. As the figure shows, due to the focused nature we would have much less number of irrelevant critical-time points (formal argument in Theorem 3 in Section 4.5) making it computationally more efficient even for long paths (Section 4.6).

**New Contributions in this chapter:** In our previous chapter on the ALSP problem (Chapter 3), we proposed the concept of critical time points. Using this idea, we designed a forward search only algorithm called Critical Time point based ALSP Solver (CTAS) (Section 3.3 in Chapter 3). We also provided rigorous correctness and completeness proof of our algorithm and evaluated it experimentally using real datasets. This chapter makes the following additional contributions.

- (a) We propose *temporal bi-directional* search for the ALSP problem. This technique takes advantage of lower bounded arrival times at a destination to facilitate searches from both the source and the destination. A bi-directional search allows us to pursue a more focused search.

- (b) We propose a novel termination condition called the *impromptu rendezvous* for our *temporal bi-directional* search which guarantees correctness without degrading the performance.

- (c) Based on *temporal bi-directional* search and *impromptu rendezvous* condition, we propose a new algorithm called Bi-Directional CTAS (BD-CTAS) for the ALSP problem. This approach addresses the computational bottlenecks of CTAS by reducing the number of irrelevant critical time points.

- (d) We provide correctness and completeness proof of the BD-CTAS algorithm

- (e) We also present asymptotic complexity analysis for our new BD-CTAS algorithm and previous CTAS algorithm.

- (f) We compared our approaches with related work based on asymptotic time complexity

- (g) Finally, we also evaluated our proposed methods using real and synthetic datasets.

**Scope and Outline:** This chapter models the travel time on any particular edge as a discrete time series. Continuous models for ST networks [17] are not considered here and would be explored in the future. Also, we are limiting the scope of the paper to strong fifo networks, where an earlier departure on any route strictly implies an earlier arrival at its terminal node. Turn restrictions are not considered in the ST network representation. Comparisons with single departure time algorithms, bi-directional (with reverse search done on the underlying static graph) and other forward search algorithms (e.g. Hierarchical and A*) are beyond the scope of the paper.

The rest of the paper is organized as follows. A brief description of the basic concepts and a formal problem definition is presented in Section 4.1. A description of the computational structure of the ALSP problem is presented in Section 4.2. The proposed temporal bi-directional CTAS algorithm (BD-CTAS) is presented in Section 4.3. Correctness and completeness of the proposed BD-CTAS algorithm is presented in Section 4.4. Section 4.5 presents an analytical evaluation our critical-time based approaches. Experimental evaluation of the algorithms is presented in Section 4.6. Finally, this chapter concludes in Section 4.7.

## 4.1 Basic Concepts and Problem Definition

**Spatio-temporal (ST) Networks** are spatial networks (e.g. road networks) whose properties (e.g. typical travel-time on the road segments) change with time. Typically in a ST-network, nodes represent the road intersections, whereas edges represent road segments between the intersections. A ST network can be represented in several ways as discussed in [37]. In this paper, we choose to represent it using a time-aggregated graphs (TAG) due its simplicity and less storage overhead over others [16, 37]. Figure 4.4 illustrates a sample ST network represented as a TAG [37]. Here, each edge is associated with a time series which represents the travel-time of the edge as a function of time. For example, edge $(S, B)$ is associated with the travel time series [1 1 6 6]. This means that the travel time of edge $(S, B)$ at departure times $t = 0$, $t = 1$, and $t = 2$ is 1, 1 and 6 respectively. Travel time information can also be represented in terms of arrival times. In order to get this, the travel time of the edge is added to the departure times. For instance, the arrival time series of the edge $(S, B)$ in our previous example would be: [1+0 1+1 6+2 6+3], which is, [1 2 8 9]. This means that a journey departing from node $S$ at times $t = 0$, $t = 1$, $t = 2$, and $t = 3$ would arrive at node $B$ at times 1,2,8 and 9 respectively. In this paper, we choose to use TAG with arrival time series (right side of Figure 4.4) for ease of communication.

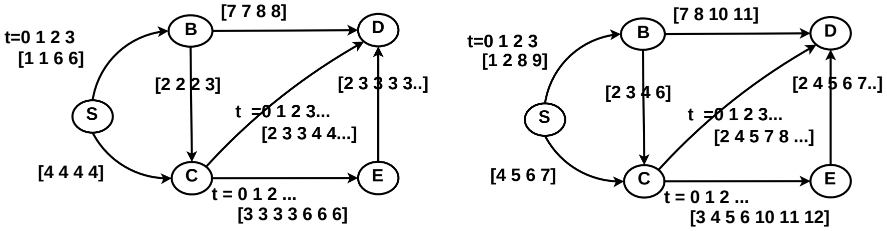

TAG with Travel time series

Transformed TAG with Arrival Time Series

Figure 4.4: ST network represented as a TAG.

**Lagrangian vs Eulerian frame of reference:** ST networks can be queried through either Lagrangian or Eulerian frame of reference. In Eulerian frame of reference, the traffic (or typical travel-time) is observed from specific locations in the space over a period of time [42]. It is similar to sitting on the side of a highway and watching traffic pass a fixed location. In contrast, the Lagrangian frame of reference corresponds to an observer driving along a particular route [42]. It is important to that the total cost of a candidate path would be different across these reference frames. For example, consider the cost of path B-C-D for a departure time $t = 0$ in Figure 4.4. In an Eulerian reference frame, this would be sum of times travel-times of edges $(B, C)$ and $(C, D)$ for $t = 0$, which is 4 time units. However, one may note that, after departing from B at $t = 0$, it takes 2 time units to travel along the edge $(B, C)$. Thus, we should consider the cost of $(C, D)$ for time $t = 2$ and not at $t = 0$ as done in the Eulerian frame of reference. This kind of view, where the cost of the edge is considered for the time when the traveler arrives at its starting point, is known as the Lagrangian frame of reference. Routing queries over ST networks would be more meaningful through Lagrangian frame of reference. This was also pointed in other literature in this area [16, 17, 34]. In this paper, paths whose cost is viewed through Lagrangian frame of reference are referred to as *Lagrangian paths.*

**Closing of a node:** A search starting at a source (or destination) for a specific departure-time *closes* a node when it has found a shortest path to the node for the departure-time under consideration. In other words, there does not exist any other Lagrangian path which starts at source at the specified departure-time and arrives earlier at the node being closed.

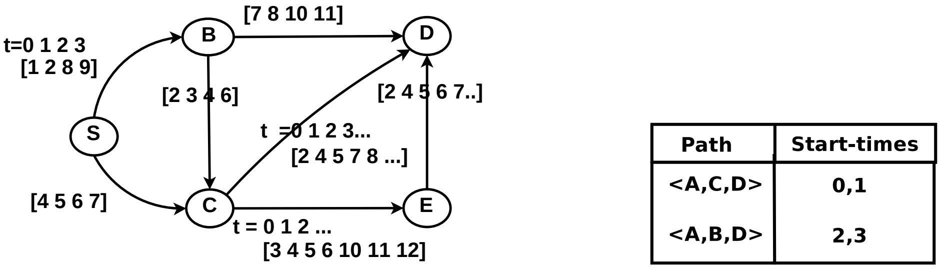

| Path | Start-times |
|---|---|
| <A,C,D> | 0,1 |
| <A,B,D> | 2,3 |

(a) Sample input ST-network

(b) Output of problem

Figure 4.5: Sample input and output of ALSP problem.

**Problem Definition:** We define the ALSP problem by specifying input, output, objective function and constraints. Inputs include:

(a) A ST network $G = (V, E)$, where $V$ is the set of vertices, and $E$ is the set of edges;

(b) A source $s$ and a destination $d$ pair where $\{s, d\} \in V$;

(c) A discrete departure time interval $\lambda = [t_{d_1} \ldots t_{d_k}]$ over which the shortest path between $s$ and $d$ is to be determined;

(d) Each edge $e \in E$ is associated with a cost function, denoted as $\delta$, representing travel-time of that edge. The cost function of an edge is represented as an arrival time series.

*Output:* The output is a set of routes, $P_{sd}$, from $s$ to $d$, where each route $P_i \in P_{sd}$ is associated with a set of departure-time instants $\omega_i$, where $\omega_i$ is a subset of $\lambda$.

*Objective function:* (1) Each path in $P_{sd}$ is a shortest commuter-experienced travel time path between $s$ and $d$ during its respective departure time instants. (2) Computational efficiency.

*Constraints:* The length of the time horizon over which the ST network is considered is finite. The cost function $\delta$ is a discrete time series.

**Example:** A sample ST network is shown in Figure 4.5(a). Figure 4.5(b) shows the output of an ALSP problem instance on this network with source $S$, destination $D$, and $\lambda = [0, 1, 2, 3]$. Here, the path S-B-C-D is optimal for departure times $t = 0$ and $t = 1$, and the path S-C-D is optimal for departure times $t = 2$ and $t = 3$.

## 4.2 Computational structure of the ALSP problem

Given (a) a source, (b) destination and (c) a departure-time, the basic computational unit in our scheme computes: (1) a shortest path between the source and destination for the given departure-time and, (2) a forecasted critical-time point, which serves as the next departure-time for re-computation. We refer to this as the *sub-interval optimal lagrangian path*, defined formally as follows:

A **Sub-interval optimal Lagrangian path** *is a pair of Lagrangian path, $P_i$, and its corresponding set of departure time instants $\omega_i$, where $\omega_i \in \lambda$. $P_i$ is a shortest path between the source and the destination for all the departure times $t \in \omega_i$.*

The Lagrangian path *S-B-C-D* and its corresponding $\omega = 0, 1$ (shown in Figure 4.5(b)) is an example of a sub-interval optimal Lagrangian path. Output of any ALSP problem instance can be considered as a set of several *sub-interval optimal lagrangian paths*. Given a sub-interval optimal Lagrangian path $P_i$ with $\omega_i = [t_{d_i}, t_{d_{i+1}}, \ldots, t_{d_{nt}}] \in \lambda$, the departure-time $t_{d_{nt+1}} \in \lambda$ forms the forecasted critical-time point at which re-computation starts.

Our proposed bi-directional search consists of a forward search and a trace search. The forward search starts exploring the candidate paths from the source (given in the ALSP problem instance) for a particular departure-time. Whereas the trace search starts from the destination (given in the ALSP problem instance) for a particular time in estimated arrival time interval at the destination (described later in Section 4.3). The proposed temporal bi-directional approach employs the forward and trace search along with the our novel impromptu rendezvous condition (described later) to determine successive sub-interval optimal lagrangian paths forming a solution to the ALSP problem instance.

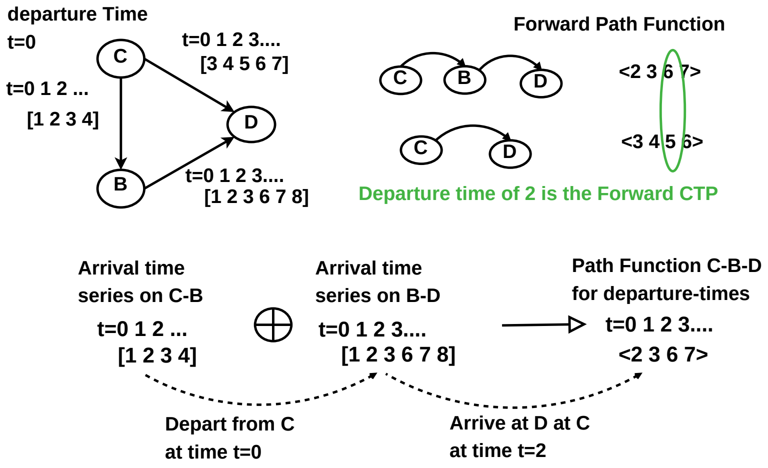

Figure 4.6: Forward critical-time points and path functions.

### 4.2.1 Forward Search Basic Concepts

The goal of the forward search is to explore candidate paths from the source node for a specific departure-time in the given departure-time interval ($\lambda$). The forward search, while exploring paths for a departure-time, maintains some information to forecast the critical time point (forward critical time point) at which the search needs to re-start the exploration.

**Forward Critical time point:** *A departure-time instant at the source (as determined by the forward search) when the shortest path between the source and a destination changes.*

In order to determine these critical time points (CTPs), we need to model the total cost of the path. This is achieved through *forward path-function*, a time-series which represents the earliest arrival time at the end node of the path for different departure-times at the source. A formal definition of a path-function is given below.

**Forward Path Function:** *A forward path function represents the arrival time at the end node of a path as a function of time (representing the departure-times at the start node). This is represented as a time series. A path function is determined by composing the arrival times on its component edges in a Lagrangian fashion.*

Figure 4.6 illustrates the construction of forward path function for the path $C$-$B$-$D$. The Figure also illustrates the forward CTPs for a search with $C$ as the source,

$D$ as the destination and $t = 0, 1, 2, 3$ as the desired departure-times. Forward CTPs are determined by computing the intersection point (with respect to time coordinate) between candidate path functions. In this case, the path functions for $C$-$B$-$D$ and $C$-$D$ intersect at time $t = 2$ making it a forward critical-time-point.

### 4.2.2 Trace Search Basic Concepts

The goal of the trace search is to compute shortest paths from other nodes to the destination such that these paths arrive (at the destination) at a particular time instant within an estimated arrival time interval ($\lambda_{rev}$). Similar to the forward search, a trace search maintains some additional information to forecast the time point (trace critical time point) when a certain shortest path to the destination changes. However, in this case, candidate paths are explored in a *reverse ST network* ($STN_{rev}$). This network is defined on the same set of nodes $V$ as the original ST network, but contains a flipped edge $(v, u)$ for each $(u, v)$ in the original network.

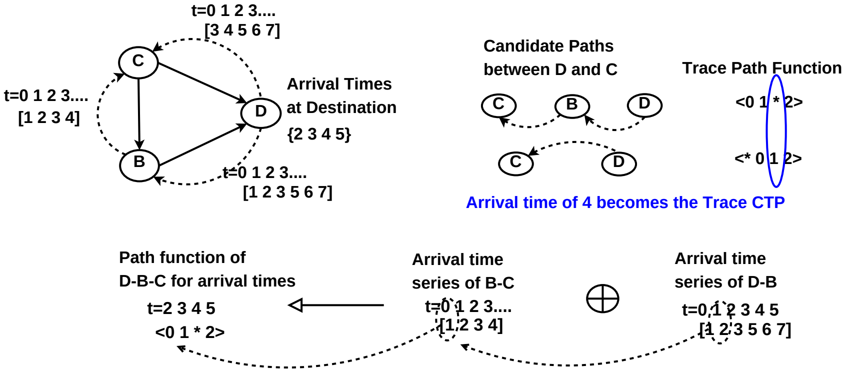

Figure 4.7: Illustration of Trace Critical-time points.

**Trace Critical-time point:** *An arrival time instant at the destination (as determined by the trace search) when the shortest path to this destination from a source changes.*

Consider an instance of the trace search on the ST network shown in Figure 4.7, where the destination is $D$, and $\lambda_{rev} = \{2\ 3\ 4\ 5\}$. This means we want to find shortest paths from all other nodes to node $D$ such that they arrive at $D$ at times $t = 2, 3, 4, 5$. The trace search is performed on a reverse ST network where each edge in the original ST network is reversed (showed as dotted edges in the Figure 4.7). The arrival times series in the original network are interpreted as an *inverse-mapping* from arrival times to departure-times. For instance, in Figure 4.7, consider the original edge (C,D) (shown in bold) and its corresponding reverse (shown using a dotted arrow). The arrival time series of the original edge was [3 4 5 6 7], which means that a departure at $t = 0$ at node $C$ would have an arrival at $D$ at $t = 3$. Since this is a trace search, we would read this time series as: *If need to arrive at $D$ at $t = 3$, what is the latest departure time at $C$?*.

Similar to forward CTPs, in order to determine trace CTPs, we model the total cost of the path using a cost function. This cost function, which we call *trace path function*, is defined formally below.

A **Trace Path Function** *represents the latest departure times at the end node as a time series. Each item in this time series represents the latest departure at the end node for the corresponding arrival time at the start node of the path.*

Similar to a forward path function, a trace path function is determined by combining the arrival times on its component edges in a Lagrangian fashion. The only difference is that, due to inverse mapping, we look backwards while composing the time series. Figure 4.7 illustrates the construction of a trace path function for the path $D$-$B$-$C$ for a trace search with destination $D$ and $\lambda_{rev}$ = [2 3 4 5]. While composing the arrival time series for the component edges, we consider only the latest departure time that incurs no waiting. Note that in some cases, the arrival times cannot be mapped backwards. For instance, in our previous example of $D$-$B$-$C$, the arrival time 4 at $D$ cannot be mapped back along edge $(D, B)$. In other words, there does not exist a departure-time at $B$ such that its corresponding arrival time (with no waiting) at $D$ is 4. Note that a departure-time of 2 at $B$ would not be considered as it would arrive at $D$ early and wait. Cases like these are represented using '*' in the trace function (and implemented as $-\infty$). Figure 4.7 also illustrates the arrival time $t = 4$ as a trace critical time point because the shortest path to $D$ from $C$ changes for arrival times greater that $t = 4$.

We now begin our discussion on our proposed temporal bi-directional search for the ALSP problem. During the discussion, we may sometimes drop the prefix "trace" or "forward" from critical-time-points and path functions when the context is clear.

## 4.3 Proposed Temporal Bi-directional Search for ALSP problem

Designing an efficient bi-directional search for the ALSP problem poses two challenges. First, unlike the forward search which explores over a given set of departure-times, appropriate "departure-times" for the trace search at the destination are not known in advance. Second, designing a suitable termination condition which gives good performance while ensuring correctness is non-trivial.

**"Departure-times" for trace search:** To address the first challenge, we compute a bound on the arrival times at the destination. These bounds are computed by executing a single start-time shortest path algorithm developed for ST networks [16] for the first and the last departure-time in $\lambda$. Given the fifo nature of our network, we can claim that arrival times for all the other departure-times in $\lambda$ would fall inside the interval defined by the arrival times corresponding to the first and last departure-times. The range defined by these arrival times at the destination form the set of "departure-times" (denoted by $\lambda_{rev}$) for the trace search. To avoid ambiguity, we use the term *trace-times* instead of "departure-times" when discussing the trace search [1] . We use the term *departure-times* in context of the forward search or the problem instance ($\lambda$). Figure 4.8 shows the upper and lower bounds defining the range $\lambda_{rev}$ for our ALSP instance in Figure 4.5.

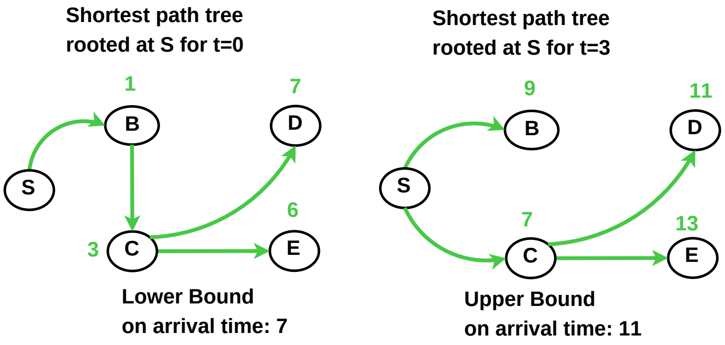

Figure 4.8: Arrival times corresponding to first and last departure-times.

***impromptu rendezvous* condition:** Our second challenge for bi-directional search

[1] trace-times refer to time points in $\lambda_{rev}$, while departure-times refer to time points in $\lambda$ (in the ALSP instance)

was designing an appropriate termination which gives good performance while ensuring correctness. Current termination conditions for bi-directional searches work only when the trace search is done on the underlying static graph [17, 23–26] and thus cannot be applied in our case. The trace search in these studies is used to prune the search space for the forward search to continue efficiently until destination node is closed. In contrast, our trace search is executed on the ST network itself, thus, allowing us to avoid visiting the nodes already closed by the trace search. We now describe our novel *impromptu rendezvous* condition on our previous ST network in Figure 4.5(a).

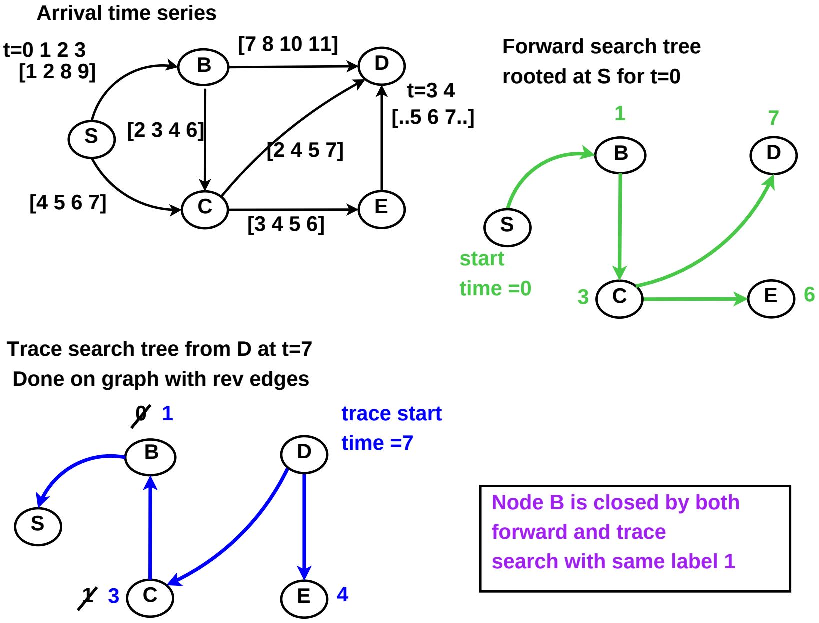

Figure 4.9: Illustration of impromptu rendezvous condition.

Consider again the ST network illustrated in Figure 4.5(a) (replicated in top left of Figure 4.9). Suppose we want to determine the shortest path between $S$ and $D$ which departs $S$ at time $t = 0$. A bi-directional search for this problem would involve a forward search from node $S$ and a trace search from node $D$. Clearly, the forward search from $S$ would start at time $t = 0$. By contrast, the choice of trace-time for the trace search is non-trivial and is discussed next with an intuitive explanation of the termination condition.

Figure 4.9 contains a forward search tree (explored until node $D$ was closed) from node $S$ for time $t = 0$ (top right). This can be considered as a instance of forward search algorithm with departure time $t = 0$ run until node $D$ was closed. The Figure also contains a trace search tree from node $D$ which starts at time $t = 7$. This can be considered as instance of trace search being executed from $D$ on reverse ST network until node $S$ was closed. The numbers written beside the nodes in the figure represent their respective distance labels when they were closed. For instance, the forward search closed the node $E$ at time 6, i.e, the shortest path to $E$ from $S$ arrives at time 6. On the other hand, the trace search closed node $E$ at time $t = 4$. This means we need to depart node $E$ at the latest by $t = 4$ in order to arrive at $D$ by $t = 7$. A comparison of these two trees shows that nodes $B$ and $C$ happen to be closed with the same label by both the forward and the trace search. In other words, both the forward (starting at $S$ at $t = 0$) and the trace search (starting at $D$ at $t = 7$) "agree" on node $B$ and $C$ along the path $S$-$B$-$C$-$D$, which happens to be the shortest path between $S$ and $D$ for the departure-time $t = 0$. This shows that when the trace-time of a trace search at the destination is correct (shortest path to $D$ from $S$ indeed arrives at $t = 7$), *both forward and trace searches close the nodes on the shortest path with the same labels.*

If the trace search does not start at the optimal time, there are only two other possibilities: it started *earlier* or *later* than the optimal time. A trace search starting earlier would close all the nodes at an earlier time than the forward search. In other words, there would be no "agreement" between the forward and trace search on any node. On the other hand, a trace search starting later (e.g. $t = 9$) might lead to an agreement between the two searches on a node *which does not lie* on the shortest path. This leads our proposed termination condition, called the *impromptu rendezvous*, which states: it is sufficient to terminate when both the forward and trace search close a node with the same label, provided the trace-time is *not an over-estimate* of the optimal arrival time. This is formally stated as Lemma 4 in Appendix 4.4.

### 4.3.1 BD-CTAS Algorithm

In this section we describe our proposed *temporal Bi-Directional* based *Critical-Time-point Alsp Solver* (BD-CTAS). The forward and the trace search along with the impromptu rendezvous condition form the key parts of this algorithm. In the algorithm, the forward and the trace search start from the source and the destination respectively. The priority queue for the forward search is sorted in ascending order on the values in the path functions, while the priority queue in the trace search is sorted (also in ascending order) on the difference between the trace-time at the destination and the values in the trace function. This kind of ordering in the trace search ensures that the closest node (to the destination) is closed first, an essential requirement for correctness as discussed later.

The impromptu rendezvous condition is only used as a *sufficiency* condition for terminating the algorithm. It is possible for the algorithm to run without meeting this condition. This happens when the trace-time of the trace search is earlier than the optimal arrival time of the shortest path (Lemma 3 in Appendix 4.4). In such cases, the algorithm terminates only when the destination node is closed by the forward search (similar to the CTAS algorithm, Section 3.3 in Chapter 3).

In order to integrate *impromptu rendezvous* termination into the BD-CTAS algorithm, we need to ensure that the trace-time is never an overestimate of the optimal arrival time at the destination (had the forward search been allowed to proceed until the destination). To this end, the algorithm employs an incremental strategy for determining the next times of the trace and forward search. Given the correctness of the trace-time of a trace search (i.e., it is not an overestimate), a pair of forward and trace searches explore the ST network to determine a single *sub-interval optimal lagrangian path* and determine the time instants for the next pair of searches. We refer to this unit of work as *one iteration* of BD-CTAS algorithm. Here, the algorithm simply ensures that the next trace-time for the trace search is not an overestimate of the optimal arrival time. This process starts at the first departure-time in $\lambda$ and continues until shortest paths for all the departure-times given in $\lambda$ are determined. To ensure the correctness for the first departure-time in $\lambda$, the algorithm uses the first time point in the range defined by $\lambda_{rev}$ (described earlier in the section) as the trace-time of the trace search. Recall that, by construction this trace-time is guaranteed not be an overestimate; in fact, it is the correct destination arrival time. This means that the algorithm does more work for the first departure time in $\lambda$. However, this extra cost is usually compensated by the savings generated by the impromptu rendezvous.

We now describe our approach for determining the next times after a pair of forward and trace searches. Assuming that the trace-time of the trace search in the previous instance was not an overestimate, one of the following two cases can be encountered during the execution. Case (a): the algorithm terminated because *impromptu rendezvous* condition was met. Which means both the trace and forward search closed a node with same label. Case (b): the algorithm terminated because the forward search closed the destination node.

*Case (a): Impromptu rendezvous was satisfied:* The *impromptu rendezvous* condition guarantees that whenever a node $v$ is closed by both forward and trace search with the same label, the combined path from source to $v$ and $v$ to destination is optimal for its respective departure-time (of the forward search) at source. However, for a more efficient solution for the ALSP problem, we need to forecast a minimum duration for which this path remains optimal. In the CTAS algorithm [34] this was done by choosing the earliest of the intersection points as the forecasted critical-time-poin (CTP), the next departure-time for re-computation. In other words, the path was guaranteed to be optimal for all departure-times between these two departure-times at the source. A natural extension of such an approach to a temporal bi-directional search would be to take the minimum of forward and trace critical time points to determine the next departure and trace times. Note that the trace critical time points would be in terms of arrival times at destination and would generally be higher than the forward CTPs. In order circumvent this, we need to take the minimum over the mutual distance (in time) between CTPs and their "reference time points" (departure-times of forward and trace-time of trace searches).

In order to guarantee the correctness of the above approach in a general case, we need to incorporate the notion of *lagrangian agreement duration* into the process of finding the minimum of the forward and trace CTPs. The *lagrangian agreement duration* is duration for which both the forward and trace path functions (ending at the common node) have same values. In order to compute the next departure and trace times, we take the minimum of the lagrangian agreement duration, and the forward and trace CTPs (after subtracting their respective departure and trace times). This minimum, referred to as $\gamma_{map}$, is added to the current departure-time of forward search and the trace-time of trace search to get the next times for the searches. Correctness of this case is presented in Lemma 5 (Section 4.4).

*Case (b): Forward search closed the destination node:* In this case, the algorithm ignores the data collected by the trace search and sets the next forward search departure-time to the earliest of observed intersection points (same as done by CTAS). The next trace-time of the trace search is set to one more than the current shortest path arrival time found by the forward search. Correctness of this case is argued in Lemma 6 (Appendix 4.4).

**Algorithm 2** Bi-Directional CTAS Algorithm

```
Input: a ST network $STN$, source $S$, destination $D$, a departure-time interval $\lambda = [t_{d_1} \cdots t_{d_k}]$
 1: Build a reverse ST network $STN_{rev}$ with each edge in $STN$ reversed.
 2: Set $t_{a_1}$ and $t_{a_m}$ to the arrival times (at $D$) of a shortest path between $S$ and $D$ for times $t_{d_1}$, and $t_{d_k}$
 3: Set the trace-time interval for the trace search $\lambda_{rev} = [t_{a_1} \cdots t_{a_m}]$
 4: Set the current departure-time of forward search $for_{st} = t_{d_1}$ and of trace search $tra_{st} = t_{a_1}$
 5: while a shortest path for each time $t \in \lambda$ waits to be determined do
 6:   Initialize priority queues for forward ($PQ_{for}$) and trace search ($PQ_{tra}$)
 7:   $FP^{min} \leftarrow$ min weight path function from $PQ_{for}$
 8:   $TP^{min} \leftarrow$ min weight path function from $PQ_{tra}$
 9:   Add the tail node of $FP^{min}$ and $TP^{min}$ to set of closed nodes
10:   Test the *impromptu* rendezvous condition
11:   while $D$ is not closed by forward search *or* impromptu rendezvous condition is not satisfied do
12:     Determine the earliest intersection point of $FP^{min}$ with other path functions in $PQ_{for}$ and save in $Pinter_{for}$
13:     Expand $FP^{min}$ and push the newly determined path functions into $PQ_{for}$ and delete paths ending on tail of $FP^{min}$
14:     Determine the earliest intersection point of $TP^{min}$ with other trace functions in $PQ_{tra}$ and save in $Pinter_{tra}$
15:     Expand $TP^{min}$ and push the newly determined trace functions into $PQ_{tra}$ and delete paths ending on tail of $TP^{min}$
16:     $FP^{min} \leftarrow$ min weight path function from $PQ_{for}$ and $TP^{min} \leftarrow$ min weight path function from $TQ_{for}$
17:     Add the tail node of $FP^{min}$ and $TP^{min}$ to set of closed nodes
18:     Test the impromptu rendezvous condition
19:   end while
20:   Compute $\gamma_{map}$
21:   if impromptu rendezvous condition was satisfied then
22:     $for_{st} = for_{st} + \gamma_{map} + 1$
23:     $tra_{st} = tra_{st} + \gamma_{map} + 1$
24:   else
25:     $for_{st} = \min\{Pinter_{for}\}$        {earliest intersection point in path intersection table.}
26:     $tra_{st} = 1+$ arrival time of shortest path found for time $t = (\min\{Pinter_{for}\} - 1)$
27:   end if
28: end while
```

**Pseudocode of the BD-CTAS algorithm** is given in Algorithm 2. The algorithm starts by computing a shortest path between the given source and destination for the first and the last departure-time in $\lambda$ (line 2). We use algorithms developed for single departure-time [16] for this purpose. As described earlier, the range defined by the arrival times of these shortest paths form the trace-time interval for the trace search (line 3). Initially, the departure-time of the forward and trace-time of the trace search are set to the first time points in $\lambda$ and $\lambda_{rev}$ respectively (line 4). The outer while loop (lines 5-28) ensures that a shortest path for each departure-time in $\lambda = [t_{d_1} \ldots t_{d_k}]$ is determined. The loop begins by initializing the priority queues for forward and trace search (line 6). The forward search priority queue, $PQ_{for}$, is initialized with the path functions of the source and its neighbors. The trace search priority queue, $PQ_{tra}$, is initialized with the trace functions of the destination and its neighbors. Using the inner while loop (11-19) the algorithm then runs a pair of forward and trace searches to compute a single sub-interval optimal Lagrangian path. Conditions described earlier in case (a) and case(b) are used to terminate the loop. Inside this loop the forward search executes on the input ST network, whereas the trace search executes on the reverse ST network, where all the edges of the original ST network are reversed. Finally, the next departure-time of the forward search and the trace-time of the trace search are computed in lines 20-27 for the next pair of searches.

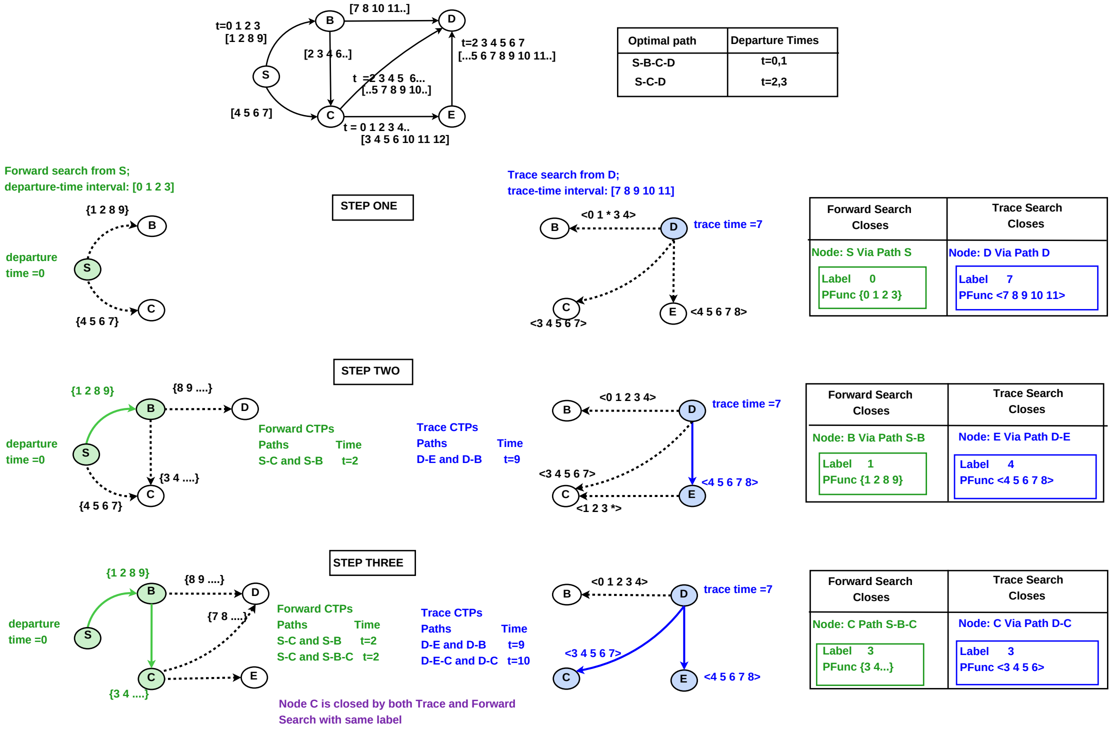

Figure 4.10: Execution trace of the BD-CTAS algorithm.

**Execution Trace of BD-CTAS algorithm:** Figure 4.10 illustrates an execution trace of the BD-CTAS algorithm on the ALSP instance shown in Figure 4.5. In the figure, forward search is shown in green and trace search is shown in blue. Nodes which are closed by either search have shaded background. In order to keep the figure clear and simple, we have not shown the inner details of the priority queue. As noted earlier, the priority queue of forward search is similar to that of CTAS. The trace search priority queue is ordered on the difference between the trace-time at the destination and the trace function values. We are only giving a high-level conceptual trace of BD-CTAS algorithm for the first iteration for the ALSP instance shown in Figure 4.5. Here, a pair of forward (from node $S$ with departure-time $t = 0$) and trace searches start (from $D$ with trace-time $t = 7$) to compute a single sub-interval optimal Lagrangian path.

In the first step (after closing $S$ and $D$) the forward and trace searches add the path functions to their corresponding neighbors to their respective priority queues. Path functions are indicated using $\{\}$ or ($< >$) next to the node. For instance, the forward path function of $S$-$B$ is $\{1\ 2\ 8\ 9\}$ and the trace path function of $D$-$B$ is $< 0\ 1\ *\ 3\ 4 >$.

In the second step, the forward search closes node $B$, and the trace search closes node $E$. The intersection points (among the path functions) encountered at this stage are shown in Figure 4.10. Figure 4.10 (on the right) also shows the optimal paths and their corresponding path functions for all the closed nodes in every step. Now, paths $S$-$B$ and $D$-$E$ are expanded to include the neighbors.

In the next step both searches close node $C$ with the same label 3. This is the impromptu termination condition. At this stage, the BD-CTAS algorithm would compare the forward and the trace path functions for node $C$, which are $\{3\ 4\ \ldots\}$ (forward) and $< 3\ 4\ 5\ 6\ 7 >$ (trace) to determine the lagrangian agreement duration to be 2. Combined with the forecasted forward and trace CTP information, the next departure-time of the forward search would be $t = 2$ $(0 + 2)$ and the next trace-time of the trace search would be $t = 7 + 2 = 9$. Thus, the algorithm has computed one sub-interval optimal Lagrangian path, $S$-$B$-$C$-$D$ with $\omega = 0, 1$. This process continues until shortest paths for all departure-times are found. A brief comparison with the execution trace of the CTAS algorithm (Figure A.6 in Appendix A.2) on the same input shows that BD-CTAS was able to skip the departure time of $t = 1$ (an irrelevant CTP forcasted by the CTAS algorithm).

## 4.4 Correctness and Completeness of BD-CTAS algorithm

Correctness claim of BD-CTAS algorithm has four key components key components. First, forward search is correct. This requires us to prove that the optimal path (or portion of optimal path) determined by the forward search is correct between the current departure-time and the forcasted forward CTP. This was previously established in Section 3.4 of Chapter 3. Second, trace search is correct. Correctness of trace search is established analogously and is given in Lemma 2. The third part involves establishing the correctness of the impromptu rendezvous termination condition. This requires us to prove that when the BD-CTAS algorithm terminates on the impromptu rendezvous condition, we have a path which is optimal for at least one departure time. This is established in Lemma 4 (using Lemma 3). And lastly, given the correctness of path for one departure time, we need to prove that BD-CTAS then forecasts the next departure time for the forward and trace-time for the trace search appropriately. Lemma 5 and Lemma 6 establish the correctness of this part. Using these four parts Theorem 2 establishes the correctness of BD-CTAS for any instance of the ALSP problem.

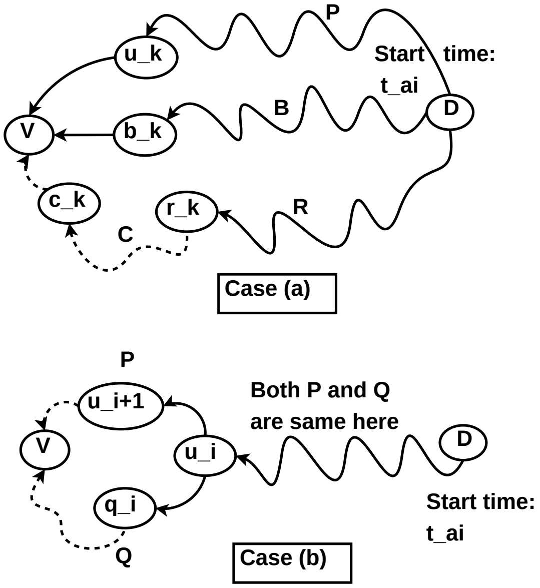

Figure 4.11: Sample cases for correctness.

**Lemma 2.** *Given an instance of trace search starting from the destination node $d$ at time $t_{a_i}$ in a reverse ST network. Let node $v$ be closed by this search and $t_\beta$ being the* *earliest trace critical time point observed so far. Let $P$: $d$-$u_1$-...-$u_k$-$v$ be path found by this search and $P'$ be the path with edges in $P$ reversed. We have the following*

- *$P'$ is the shortest path between $v$ to $d$ for all arrival times in $t' \in [t_{a_i} \quad (t_\beta + t_{a_i})]$ at $d$. By shortest we mean, $P'$ has latest departure among all paths for the same arrival time $t'$.*

*Proof.* The proof for this lemma consists of two parts. First part involves proving that $P$ (or $P'$) is optimal for time $t_{a_i}$. Whereas, the second parts concerns itself with proving the optimality for the entire time interval $[t_{a_i} \quad (t_\beta + t_{a_i})]$. We begin with the first part.

Given the greedy nature, similar concepts of expanding and closing a node in trace search, its basic correctness can be borrowed from Dijkstra‘s. Here, we would just prove that the trace search has gathered sufficient information when node $v$ is closed for arrival time $t_{a_i}$. Consider the case (a) in Figure 4.11 (top part), which shows that candidate paths to node $v$ through its neighbors $u_k$, $b_k$ and $c_k$. Clearly, one of these would be the predecessors of the optimal path. Also, optimal path leading to $v$ would be composed of optimal paths leading to one of these nodes followed by the edge to node $v$. Without loss of generality assume that when node $v$ was closed, the priority queue had trace functions $P$: <D,...,$u_k$,$v$ >, $B$:<D,...,$b_k$,$v$ > and $R$:<D,...,$r_{k-1}$,$r_k$ >. This means that nodes $u_k$, $b_k$, and $r_{k-1}$ were closed. According to the given case in Lemma, at this stage the algorithm would have picked $P$ and closed the node $v$. Now assume (for sake of argument) that there exists another path through $c_k$ ($D$–$r_k$ via path $R$–$v$ via path $C$) which was optimal for arrival time $t_{a_i}$. Given that all the travel times are positive, path $R$ which was not picked now, any positive additions (edges in path $C$) to it cannot make it smaller that path $P$. This proves the optimality of path $P$ for time $t_{a_i}$ at $d$.

The second part of the Lemma is proved using contradiction (case (b) in Figure 4.11). Assume that there exists a path $Q$ between $d$ and $v$ such that, path its edges reversed (i.e, edges in $Q$ are reversed) $Q'$ is shorter than $P'$ for a certain $t_\alpha$ ($t_{a_i} < t_\alpha \leq (t_\beta + t_{a_i})$) at $d$. The trace search would order the priority queue on the value of trace functions at time $t_{a_i}$. This is because $t_{a_i}$ is the starting time of trace search according to the given condition in Lemma. Without loss of generality assume that $u_i$ ($u_i \neq v$) be the node upto which both $Q$ and $P$ agree. This implies that path between $u_i$ and $d$ (in $P'$ and $Q'$) was optimal for $t_\alpha$. Therefore, the portion between $u_i$ and $v$ in $Q$ must be shorter than in $P$. After closing node $u_i$, the algorithm would include trace functions of its neighbors $q_i$ and $u_{i+1}$ and continue the process of closing the closest node in a greedy fashion. After closing a node, the algorithm always computes the earliest intersection point of its trace function with others. Now as portion between $u_i$ and $v$ in $Q$ is shorter than in $P$ for $t_\alpha$, this process will create a trace critical time point at $t_\alpha$. This contradicts the assumption that $t_\beta$ was the earliest trace critical time point ($t_\alpha \leq (t_\beta + t_{a_i})$). □

**Lemma 3.** *Given any instance of a temporal bi-directional search on a ST network with a forward search starting from source $S$ at time $t_d$, and trace search starting from destination $D$ at time $t_a$, the searches can close a node $v$ with the same distance label iff $t_a \geq a_{opt}$, where $a_{opt}$ is the optimal arrival time of the forward search.*

*Proof.* (By contradiction) Consider a case where the trace search starts at time $t_a < a_{opt}$. This means that the trace search starts earlier than the optimal arrival time $a_{opt}$. Further assume that, the trace search and forward search close a node $v$ with same distance label (for sake of contradiction). Now, consider the path resulting after combining: (a) the path determined by the forward search from $S$ to $v$; (b) path determined by trace search from $D$ to $v$ with its edges reversed. Now, this is a valid path in our ST network which departs from $S$ at time $t_d$ and arrives at $D$ at time $t_a$, which is a contradiction as the $a_{opt}$ ($> t_a$) was considered to the optimal arrival time of the forward search starting at $t_d$. □

**Lemma 4.** *Given any instance of a temporal bi-directional search on a ST network with a forward search starting from source $S$ at time $t_d$, and a trace search starting from destination $D$ at time $t_a$, it is sufficient to terminate as soon as both searches close a node $u$ with the same distance label, iff $t_a \leq a_{opt}$, where $a_{opt}$ is the optimal arrival time of the forward search.*

*Proof.* (By contradiction) Consider a case where the trace search (starting at $t_a$) and the forward search (starting at $t_d$) closes a node $u$ with the same distance label. Now, we have following three cases: (1) $t_a < a_{opt}$; (2) $t_a = a_{opt}$ or; (3) $t_a > a_{opt}$. Consider the first case. Using Lemma 3 we know that the trace and forward searches can close a node with same distance label, iff $t_a \geq a_{opt}$. This contradicts our original assumption that both trace and forward search have closed the node $u$ with the same distance label.

Now, we consider the second case when $t_a = a_{opt}$ (which is allowed as per Lemma 3). This implies that we have valid path between $S$ and $D$ which consists of path $S$ through $u$ followed by $u$ through $D$. Any other path which arrives at $D$ earlier than $t_a$ would contradict our original condition of $a_{opt}$ being optimal for $t_d$.

The third case $t_a > a_{opt}$ can be easily shown via examples to lead to sub-optimal paths. This proves the Lemma. □

**Lemma 5.** *Given an instance of the BD-CTAS algorithm with a forward search starting from source $S$ with a departure-time $t_{d_i}$; a trace search starting from destination $D$ at $t_{a_i}$, where $t_{a_i}$ is guaranteed not to be an overestimate; and termination on* impromptu rendezvous *condition with $\gamma_{map} = x$ $(x \geq 1)$,*

1. *BD-CTAS correctly determines the shortest path for departure-times $t_{d_i}$ through $t_{d_i} + x - 1$;*
2. *A trace-time of $t_{a_i} + x$ is not an overestimate of optimal arrival time for a forward search starting at time $t = t_{d_i} + x$.*

*Proof.* (By contradiction) We prove this Lemma using the properties of the strong FIFO networks, where an earlier departure strictly implies earlier arrival. We first prove item 1 followed by item 2. Using Lemma 3 and Lemma 4, we know that when BD-CTAS terminates with impromptu rendezvous condition, we have a shortest path between the source and the destination for the corresponding departure-time at source. Without loss of generality assume that both the searches closed node $v$ with the same label. This implies that, the path $P$ obtained by combining $S$ to $v$ of forward search and $D$ to $v$ of trace search is optimal for departure-time $t = t_{d_i}$. Given, $\gamma_{map} = x$ we know that path found by forward search from $S$ to $v$ is guaranteed not to change between times $t_{d_i}$ and $t_{d_i} + x - 1$ (by construction of $\gamma_{map}$ and correctness of CTAS). Similarly, path found by trace search between $D$ and $v$ is guaranteed not to change between times $t_{a_i}$ and $t_{a_i} + x - 1$ (by construction of $\gamma_{map}$ and correctness of trace search). Further, a $\gamma_{map} = x$ also implies that lagrangian agreement duration between forward and trace functions at $v$ was at least $x$ time units long. This proves the existence of the path $P$. The optimality of this path for departure-times (at $S$) $t \in [t_{d_i} \;\; t_{d_i} + x - 1]$ is now proved using contradiction. Note by nature of construction of path $P$ and strong FIFO networks, there would be a bijective mapping between the departure times $[t_{d_i} \;\; t_{d_i}+x-1]$ and the arrival times $[t_{a_i} \;\; t_{a_i}+x-1]$. Let this function be $DMap_P : [t_{d_i}+1 \;\; t_{d_i}+x-1] \rightarrow [t_{a_i}+1 \;\; t_{a_i}+x-1]$. For example, $DMap_P(t_{d_i}) = t_{a_i}$ and so on.

Now, Assume for sake of contradiction that there exists a path $Q$ between $S$ and $D$ which is shorter that $P$ for a departure-time $t_{d_\alpha} \in [t_{d_i} \;\; t_{d_i}+x-1]$. Wlg. assume that its corresponding arrival time at destination is $Q_\alpha$. This implies that $Q_\alpha < DMap_P(t_{d_\alpha})$ (by assumption). Given that our original ST network is strong FIFO, arrival time along $Q$ for the $t_{d_\alpha}-1$ would be $< Q_\alpha - 1$. However, $DMap_P(t_{d_\alpha}-1) = DMap_P(t_{d_\alpha})-1$ (By nature of construction of $\gamma_{map}$), thus making $Q$ shorter for $t_{d_\alpha}-1$ as well. Recursively proceeding this we would have the following: the arrival time along $Q$ for time $t_{d_i}$ would be *less* $t_{a_i}$. This contradicts the given condition that $t_{a_i}$ was not an overestimate of arrival time for departure-time $t_{d_i}$.

Proof for item 2 can also be given in similar fashion. Assume for sake of contradiction that $t_{a_i}+x$ is an overestimate of arrival time for a forward search starting at time $t = t_{d_i}+x$. This means that there exists a path $R$ whose arrival time at destination $Q_{d_i+x} < t_{a_i}+x$. As above, using the properties of strong FIFO, we can recursively construct a case where arrival time along $R$ for time $t_{d_i}$ would be *less* $t_{a_i}$ (a contradiction). □

**Lemma 6.** *Given an instance of BD-CTAS algorithm with a forward search starting from source $S$ with a departure-time $t_{d_i}$; a trace search starting from a destination $D$ at $t_{a_i}$, termination with destination node being closed and $t_{d_i}+x$ being the forecasted forward CTP,*

1. *BD-CTAS correctly determines the shortest path for departure-times $t_{d_i}$ through $t_{d_i}+x-1$;*
2. *A departure-time of $PFun_P(t_{d_i}+x-1)+1$ is not an overestimate of arrival time for a forward search starting at time $t = t_{d_i}+x$. Here, $PFun_P(t_{d_i}+x-1)$ is the arrival time at the destination along the current shortest path $P$ found by the forward search for time $t = t_{d_i}+x-1$*

*Proof.* Whenever BD-CTAS terminates with forward search closing the destination, information collected by the trace search (e.g. trace CTPs) is ignored. In this case, the next start-time of forward and trace search is determined solely on the basis of earliest forward CTP. Thus, the correctness of the first item in the Lemma can be ensured using the argument presented in the correctness proof of the CTAS algorithm (Lemma 7 in Section 3.4 of Chapter 3). On the other hand, the second item can be proved using the properties of the strong FIFO networks.

Assume for sake of contradiction that $PFun_P(t_{d_i} + x - 1) + 1$ is an overestimate. This implies that there exists another path $U$ between $S$ and $D$, whose arrival time for $t = t_{d_i} + x$, $U_{d_i+x}$ at destination is less than $PFun_P(t_{d_i} + x - 1) + 1$. This implies that the arrival time at destination along $U$ is at most $PFun_P(t_{d_i} + x - 1)$, which also happens to the arrival time along $P$ for time $t = t_{d_i} + x - 1$. Now, given the properties of the strong FIFO network, we know that the arrival time along the same path $U$ for time $t = t_{d_i} + x - 1$ would be at most $PFun_P(t_{d_i} + x - 1) - 1$. This is *contradiction as path P was optimal for start-times* $t_{d_i}$ *through* $t_{d_i} + x - 1$. Or in other words, $PFun_P(t_{d_i} + x - 1)$ was the optimal arrival time (or shortest distance) for departure-time $t = t_{d_i} + x - 1$. □

**Theorem 2.** *Given a source S; a destination D and; a discrete departure-time interval (at S)* $\lambda = [t_{d_1}\ t_{d_2}\ t_{d_3} \ldots t_{d_k}]$*, the BD-CTAS algorithm correctly computes a solution to the all-departure-time Lagrangian Shortest paths (ALSP) problem.*

*Proof.* The correctness of the BD-CTAS algorithm implies that it gives an optimal shortest path for each departure-time $t_{d_i} \in \lambda$. The algorithm starts by computing the shortest path between $S$ and $D$ for departure-times $t = t_{d_1}$ and $t = t_{d_k}$. Assume that the arrival times of these shortest paths at $D$ are $t_{a_1}$ and $t_{a_m}$. Using this information, the trace-time interval for the trace search from $D$ is now set to $\lambda_{rev} = [t_{a_1} \ldots t_{a_m}]$. We now prove the correctness of the BD-CTAS in an incremental fashion over all departure-times $t_{d_i} \in \lambda$.

Initial Step ($t_{d_i} = t_{d_1}$): We have used known algorithms [16] in this step to compute the arrival time $t_{a_1}$ and hence its correctness is trivially established. Following this, the algorithm starts a forward search from $S$ with departure-time $t_{d_1}$ and a trace search from $D$ with a trace-time $t_{a_1}$. This iteration can either terminate on impromptu termination condition or the forward search closing $D$. The correctness in case of impromptu rendezvous termination is established through the fact that $t_{a_1}$ was the actual arrival time at the destination (thus guaranteed not to be an overestimate). Correctness of the second case (forward search closing node $D$) is established through the correctness of

CTAS algorithm [34].

General case ($t_{d_i} \in [t_{d_2}\ t_{d_3} \dots t_{d_k}]$): Without loss of generality assume that the above initial step gave us a shortest path between $S$ and $D$ for times $t_{d_1}$ through $t_{d_i} - 1$. Let the next departure-time of forward and trace-time of trace search be $t_{d_i}$ and $t_{a_i}$ respectively. Using Lemma 5 and Lemma 6 we know that trace-time $t_{a_i}$ is not an overestimate. Thus, the correctness of the next iteration of the BD-CTAS algorithm is guaranteed. This process continues until all the $t_{d_i} \in \lambda$ are covered. This proves the correctness of the algorithm. □

## 4.5 Asymptotic complexity of Critical-Time-Point based approaches

In this section, we provide detailed asymptotic complexity analysis for CTP based approaches (both BD-CTAS and CTAS algorithms). We also compare the complexity of proposed algorithms with related work and provide an intuitive explanation of our dominance zone. Additionally, we also provide a formal argument (Theorem 3) for superior performance of BD-CTAS over CTAS algorithm [34] for the ALSP problem.

**Space Complexity:** The total space complexity of BD-CTAS (or CTAS) consists of two key components. First, space required for storing the ST network for the use of algorithms. In this work, we used time-aggregate graph [16] representation for storing the ST network. The space complexity of this data structure is $O(m+n)\mathcal{H}$ [16], where $n$ and $m$ are the number of nodes and edges in the underlying spatial network. $\mathcal{H}$ is number of distinct departure-times for which travel-time information (of each edge) is available in the dataset.

The second component in the total space complexity comes from space required for storing the priority queue. At any instant during the execution of the inner loop in BD-CTAS (lines 11–19 of Algorithm 2) or CTAS (lines 3–13 of Algorithm 1 in [34]), there can be at most $indegree(v)$ paths terminating at node $v$. Now, if path ending on $v$, $P^v$, is expanded, $v$ is closed for the current departure-time and $P^v$ is expanded (if it is not the destination node). Following this at most $indegree(v) - 1$ paths would be deleted from the priority queue. Thus, we can say at any instant during the execution, the total number of paths in the priority queue would at most be $\sum_{i=1}^{|V|} degree(v_i)$

$(degree(v_i) \leq indegree(v_i))$, which is $O(m)$. Now, each of these $O(m)$ paths would have a path function represented as a time series of length $\#departure - times$, which in worst case can have $O(\mathcal{H})$ items. Therefore, the total space of priority queue would be $O(m\mathcal{H})$. Combining with the space complexity of time-aggregate graph, the total space complexity would be $O(m + n)\mathcal{H}$.

**Time Complexity:** The total running time cost of CTAS and BD-CTAS algorithms can be presented in terms of the following: (a) $\#forecasted - CTPs$, i.e., the number of re-computations performed for a particular instance of the ALSP problem and; (b) *cost of one iteration*, i.e., the cost of determining a single sub-interval optimal lagrangian path. Both CTAS and BD-CTAS algorithms determine the solution of an ALSP problem instance by finding series of sub-interval optimal lagrangian paths (a dyad of a path $P_i$ and set of time instants $\omega_i$). The next departure-time outside $\omega_i$ being the forecasted critical time point. Thus, the overall cost incurred while solving a particular instance would be $\#forecasted - CTPs \times cost\ of\ one\ iteration$

Cost of computing one sub-interval optimal lagrangian path is of the same order in both CTAS and BD-CTAS algorithms. The difference in performance of the algorithms is due to $\#forecasted - CTPs$ during the run-time. The BD-CTAS algorithm encounters much less number of CTPs during run-time due to its bi-directional nature. The bi-directional nature of BD-CTAS algorithm allows it to explore much less (and potentially more relevant) search space, creating fewer irrelevant critical time points (as also seen in experimental analysis, Section 4.6). We now provide a detail description of cost of finding one sub-interval optimal lagrangian path.

The inner most loop in CTAS algorithm (lines 3–13 of Algorithm 1 in [34]) and BD-CTAS algorithm (lines 11–19 in of Algorithm 2) computes a single sub-interval optimal lagrangian path. In CTAS algorithm, this loop is characterized by the following: (1) extract path function ($Pf^{min}$) with the least value of arrival time (for the current departure-time) from the priority queue, assume this corresponds to a path $P^v$ with the terminal node $v$; (2) compute the earliest intersection of $Pf^{min}$ with other path functions present in the priority queue, (3) expand the path $P^v$ to create path functions to its open neighbors and, (d) delete paths ending on node $v$ from the priority queue. The inner most loop of the BD-CTAS algorithm also performs the same steps once for each of forward and the trace search respectively. we now describe the cost of each of these operations and number of times they are performed during computation of a single sub-interval optimal lagrangian path. These costs are for a binary heap-based implementation of the priority queues.

1. Extracting $Pf^{min}$ (path function in $P^v$: For a binary-heap implementation, this cost would be $O(\log m)$ (since there can be $O(m)$ paths in the queue). Since there can be at most $n$ extract mins (when destination is discovered last), the total cost of extracting all the $Pf^{min}$s would be $O(n \log m)$.

2. Compute earliest intersection of $Pf^{min}$: For a path function with $T$ values ($\#depature-times$ in ALSP instance ($\lambda$)=$T$), computing earliest intersection with any particular path function can take $O(T)$ in worst case. Total cost of computing earliest intersection of a single $Pf^{min}$ would be $O(T) \times sizeof-priority-queue \approx O(mT)$. Overall, for $n$ such operations the cost would be $O(nmT)$.

3. Expand $P^v$ to create path functions to $v$'s neighbors: This would correspond to at most $outdegree(v)$ inserts into the priority queue. In worst case, there can be $O(n)$ expands which would lead to $\sum_{i=1}^{|V|} outdegree(v_i)$ ($\approx O(m)$ as $outdegree(v_i) \leq degree(v_i)$) inserts into the priority queue. Thus, the total cost of expanding $P^v$s would be $O(m \log m)$ (with $O(\log m)$ as cost of single insert key).

4. Delete paths ending on $v$: When a path ending at node $v$ is extracted, at most $indegree(v)$ paths would be deleted from the priority queue. Thus, in worst case there would be $O(m)$ deletes from the priority queue with a total cost of $O(m \log m)$.

Thus, the cost of computing one sub-interval optimal lagrangian path for CTAS and BD-CTAS would be sum of all above cost, which is $O(n \log m + m \log m + nmT)$. Combined with the number of CTPs, the total cost of CTAS (and BD-CTAS) would be $\#forecasted - CTPs \times O(n \log m + m \log m + nmT)$. Now, in worst case both $\#forecasted - CTPs$ and $\#depature - times$ in ALSP instance could be $O(\mathcal{H})$. This could happen when the given ALSP instance required an re-computation for each of the $\mathcal{H}$ time instants available in the ST network dataset. This would make the total worst case time complexity to be $\mathcal{H} \times O(n \log m + m \log m + nm\mathcal{H})$.

### 4.5.1 Comparison with related work and dominance zone

Before we delve into the details of the actual comparison, it is important to note the difference in the worst case complexity of discrete and continuous versions of the ALSP problem. In the discrete version of the problem, the travel-times of edges are modeled as a discrete time series. And, between two distinct departure-times the travel-time is assumed to remain constant. On the other hand, in the continuous version, the travel-time is modeled using continuous functions e.g., piece-wise linear functions. Depending on the nature of problem (discrete vs continuous) the worst case complexity changes. In case of discrete version, the number of re-computations are bounded by $\#departure-times$ ($\lambda$) desired in the problem instance which, as mentioned before, in worst case can be $\mathcal{H}$. This means that in worst case, we just need to compute shortest path $\mathcal{H}$ times. Whereas, in case of continuous functions, the same worst case complexity becomes $n^{\Theta(\log n)}$ (where $n$ is the number nodes in the graph) [59]. In other words, we may have to re-compute the shortest path $n^{\Theta(\log n)}$ times, which is clearly prohibitive for real graphs of large sizes.

The worst case run-time complexity of 2S-LTT [3] is $O((n \log n + m)\alpha(\mathcal{H}))$, where $\alpha()$ is the cost of maintaining the piece-wise linear function over a time interval of length $\mathcal{H}$. For a discrete case, where edge costs are represented as time-series (this paper), this complexity becomes $O((n \log n + m)\mathcal{H})$. Time complexity of allFP was not mentioned in [51] and thus comparison with it is limited to experiments.

As can be seen critical time point (CTP) based approaches (CTAS and BD-CTAS) have higher worst case time complexity ($\mathcal{H} \times O(n \log m + m \log m + nm\mathcal{H})$). This is because both CTAS and BD-CTAS do more amount of additional work in terms of book-keeping and comparing entire times-series of arrival time information to eliminate all knowable redundant re-computation. The performance gained by reducing redundant work and its associated additional cost creates a trade off, making CTP based approaches more expensive when several of them are forecasted during the execution of the algorithms. Among CTAS and BD-CTAS algorithms, BD-CTAS can be shown (Theorem 3 in Section 4.5) to perform less re-computations than CTAS algorithm.

**Theorem 3.** *Given an ALSP instance on a ST network $G = (V, E)$, the number of critical-time points forcasted by the BD-CTAS algorithm does not exceed that of the*

*CTAS algorithm.*

*Proof.* For simplicity, we assume that the travel time function $\delta_e$ associated with every edge $e \in E$ maps each departure time to either 1 or $\infty$, i.e., $\delta_e) : t \rightarrow \{1, \infty\}$. For an equitable comparison between BD-CTAS and CTAS, we make two assumptions: First, $\delta_e$ exhibits a strong fifo property. This means each edge $e \in E$ has a travel time of 1 time unit up to a certain departure time and then changes to $\infty$ and remains that way. Second, the shortest path between any nodes in the ST network is unique for any given departure time.

Consider an ALSP instance with source $s$, destination $d$ and departure-time interval $\lambda = [t_{d_1}\ t_{d_2}\ t_{d_3} \ldots t_{d_k}]$. Without loss of generality assume that a shortest path between $s$ and $d$ exists and is of finite length for all departure times in $\lambda$.

Both BD-CTAS and CTAS would start from the departure-time $t_{d_1}$ and forecast the next critical time point, $t_{d_{nt}} \in \lambda$, for re-computation. Here, we argue that $t_{d_{nt}} - t_{d_1}$ for BD-CTAS would not be lower than that for CTAS algorithm. It would be exactly the same if the BD-CTAS terminates with the forward search closing the destination, in which case it behaves exactly like CTAS. Thus, wlg., we assume that the BD-CTAS algorithm terminated on the impromptu rendezvous condition. Let $v$ be the common node closed by both forward and trace searches with the same label. Let $d(s,d)_{for}$ denote the shortest travel time distance from $s$ as determined by forward search, and $d(v,d)_{tra}$ be the distance to $d$ from $v$ as determined by the trace search. Also, let $d(s,d)_{CTAS}$ be the distance computed by CTAS. Using the correctness of the BD-CTAS algorithm (Theorem 2) we have the following equation: $d(s,d)_{CTAS} = d(s,v)_{for} + d(v,d)_{tra}$.

Now given the construction of our ST network (edge costs can only be 1 or $\infty$), the number of nodes closed during the search would have a direct relation (e.g. monotonically increasing) to the shortest distance $d(s,d)_{CTAS}$ ($d(s,v)_{for}$ and $d(v,d)_{tra}$ in the case of forward and trace searches) computed by the CTAS algorithm. Let $\mathcal{F}$ be a function which maps this distance onto the number of nodes closed during the search before setting this optimal distance label. Note that $\mathcal{F}$ would be the same for the forward, trace and CTAS algorithm as they share the same candidate path enumeration style [2] . We assume that this function is super-linear ($n^x, x > 1$) in nature for our ST network. This assumption is intuitive since the search space of forward, trace and

[2] extract min from priority queue and expand the terminal node using $\delta$ of its neighbors

CTAS algorithm are likely to be "circular" around the origin as we do not use A* based heuristics. Also, the codomain of $\mathcal{F}$ would only consist of positive integers (trivially). On applying $\mathcal{F}$ to both sides of the above equation, we have:

$\mathcal{F}\big(d(s,d)_{CTAS}\big)$ ? $\mathcal{F}\big(d(s,v)_{for} + d(v,d)_{tra}\big)$

Given that $\mathcal{F}$ is a super-linear.

$\mathcal{F}\big(d(s,d)_{CTAS}\big) \;\geq\; \mathcal{F}\big(d(s,v)_{for}\big) + \mathcal{F}\big(d(v,d)_{tra}\big)$

Let $\mathcal{G}$ be a function which maps the number of nodes closed onto the difference between the current departure time and the forecasted CTP ($t_{d_{nt}} - t_{d_1}$ in this case). These entities are conceived to have an inverse relation (e.g. monotonically decreasing) between them, which means that as more nodes are closed, the more likely the search will forecast a CTP very close to current departure time. This is intuitive since a direct relation would not be feasible unless the edge weights were negative. We assume that $\mathcal{G}$ is not sub-linear, i.e., it is at least linear. Applying $\mathcal{G}$ to both sides of the previous equation, we have:

$$\mathcal{G}\Big(\mathcal{F}\big(d(s,d)_{CTAS}\big)\Big) \;\leq\; \mathcal{G}\Big(\mathcal{F}\big(d(s,v)_{for}\big) + \mathcal{F}\big(d(v,d)_{tra}\big)\Big)$$

Given that $\mathcal{G}$ is monotonically decreasing and the codomain of $\mathcal{F}$ consists only of positive integers (discrete nature of time),

$$\mathcal{G}\Big(\mathcal{F}\big(d(s,d)_{CTAS}\big)\Big) \;\leq\; \min\Bigg\{\mathcal{G}\Big(\mathcal{F}\big(d(s,v)_{for}\big)\Big), \mathcal{G}\Big(\mathcal{F}\big(d(v,d)_{tra}\big)\Big)\Bigg\}$$

Recall that BD-CTAS takes the minimum among, forward CTP, trace CTP and lagrangian agreement duration ($lag - dur$), for determining the next departure and trace time. This is done to determine the maximum length of time for which there is agreement between forward and trace search. So the above equation becomes:

$$\mathcal{G}\Big(\mathcal{F}\big(d(s,d)_{CTAS}\big)\Big) \text{ ? } \min\Bigg\{\mathcal{G}\Big(\mathcal{F}\big(d(s,v)_{for}\big)\Big), \mathcal{G}\Big(\mathcal{F}\big(d(v,d)_{tra}\big)\Big), lag - dur\Bigg\}$$

Given that shortest path is assumed to be unique, a min (in above equation) coming from $lag - dur$ would imply that shortest path does indeed change for departure time $lag - dur + 1$. Under the correctness claim of the CTAS algorithm this would mean that $\mathcal{G}\Big(\mathcal{F}\big(d(s,d)_{CTAS}\big)\Big) = lag - dur$. Thus,

$$\mathcal{G}\Big(\mathcal{F}\big(d(s,d)_{CTAS}\big)\Big) \;\leq\; \min\left\{\mathcal{G}\Big(\mathcal{F}\big(d(s,v)_{for}\big)\Big), \mathcal{G}\Big(\mathcal{F}\big(d(v,d)_{tra}\big)\Big), lag - dur\right\}$$

Applying this argument repeatedly over all of $\lambda$ would show that the number of CTPs forecasted by BD-CTAS algorithm would not exceed the number forecasted by CTAS. □

## 4.6 Experimental evaluation

**Experimental setup:** The overall goal of the experimental evaluation was to characterize the dominance zone of the proposed BD-CTAS algorithm. To this end, the following parameters were varied in the experiments: (a) length of the departure-time interval over which shortest paths were desired ($|\lambda|$), (b) length of the route in terms of its total travel time in minutes, and (c) time of day (rush hour vs non-rush hours). The experiments were carried on one real and two synthetic datasets over the road network of Hennepin county, Minnesota. The real dataset (provided by NAVTEQ [56]) contained 1481 nodes and 4510 edges. Travel-time information on all these edges was available at a time quanta of 15mins. For experimental purposes, travel-times were converted into time quanta of 1 min. This was done by replicating the data inside time interval. To maintain the correctness of the BD-CTAS algorithm, we extracted only those sets of departure-times where the edge followed the strong fifo property. One of the synthetic dataset contained 54593 nodes and 166970 edges, whereas the other had 102709 nodes and 302380 edges. Both of these datasets were created by first extracting the road network from open street map [60] and then adding a variation to the static travel-time of the edges to mimic its increase in the rush hour. This was done by increasing the travel-time after a randomly chosen departure-time during the rush hour.

In our experiments, we first randomly choose a set of different queries (each with different parameters) and then executed them on BD-CTAS, CTAS [34], Discrete version of 2S-LTT [3], Discrete version of allFP [51] and a naive approach of computing shortest path for each departure-time using SP-TAG [16]. Comparison against the A* versions of the related work algorithms is out scope of this paper. For each of these queries, we measured the total run-time in seconds. The total number of re-computations saved by

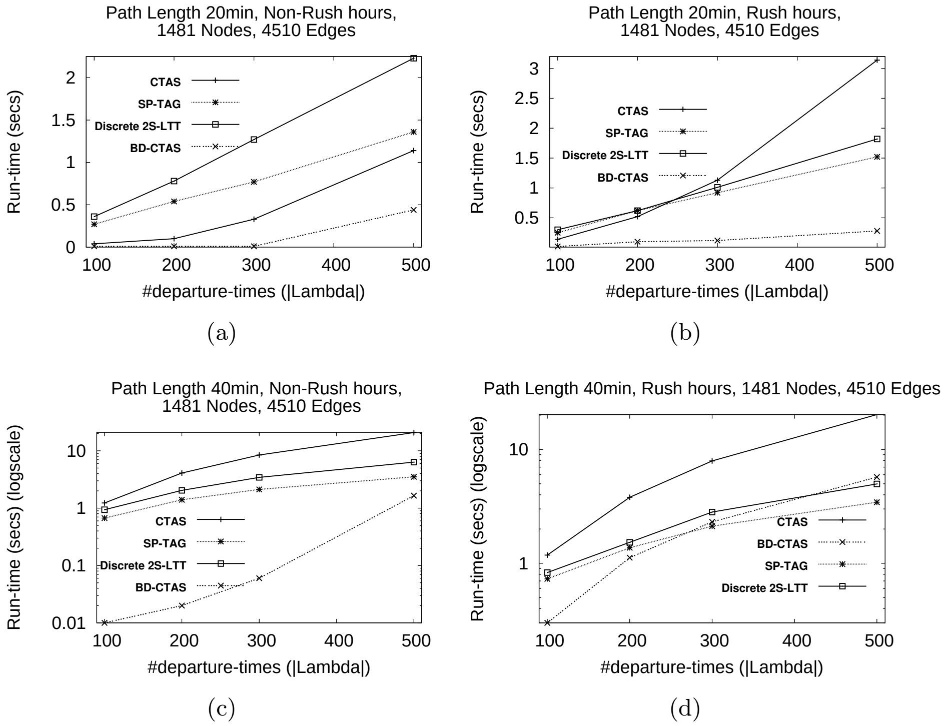

(a)

(b)

(c)

(d)

Figure 4.12: Effect of length of departure time interval ($|\lambda|$)

CTAS, BD-CTAS and Discrete 2S-LTT was also recorded for each run. The number of re-computations saved is defined as the difference between #departure-times and #forecasted-CTPs for the given ALSP problem instance. Experiments were conducted on an Intel Quad Core Linux workstation with a 3.40GHz CPU and 16GB RAM. We now discuss our results starting with our real dataset and followed by synthetic datasets. **Comparison with CTAS algorithm** *Effect of length of departure time interval ($|\lambda|$):* We evaluated the effect of length of departure-time interval ($|\lambda|$) over which the shortest path was desired. Figure 4.12(a) and Figure 4.12(b) show the run-times for a route of length (total travel time) of 20mins. Figure 4.12(c) and Figure 4.12(d) show the run-times for a route of length 40mins. Here, the length of the route refers to the time required to travel through these routes during non-rush hours (e.g. midnight). The experiments showed that run-times of both the algorithms increase with $|\lambda|$, but the run-time of BD-CTAS algorithm rises much more slowly than CTAS. This is because

BD-CTAS uses a bi-directional based search space, creating a much smaller number of irrelevant CTPs. Experiments also showed that more saving occurred during non-rush hours.

*Effect of total travel time of path:* We also evaluated the effect of length of the path (in terms of its total travel time) on the candidate algorithms. Figure 4.13 shows the execution time as the total travel time of the path was varied. As can be seen, the runtime of both the algorithms increased with increasing path length. However, the run-time of BD-CTAS rises much more slowly.

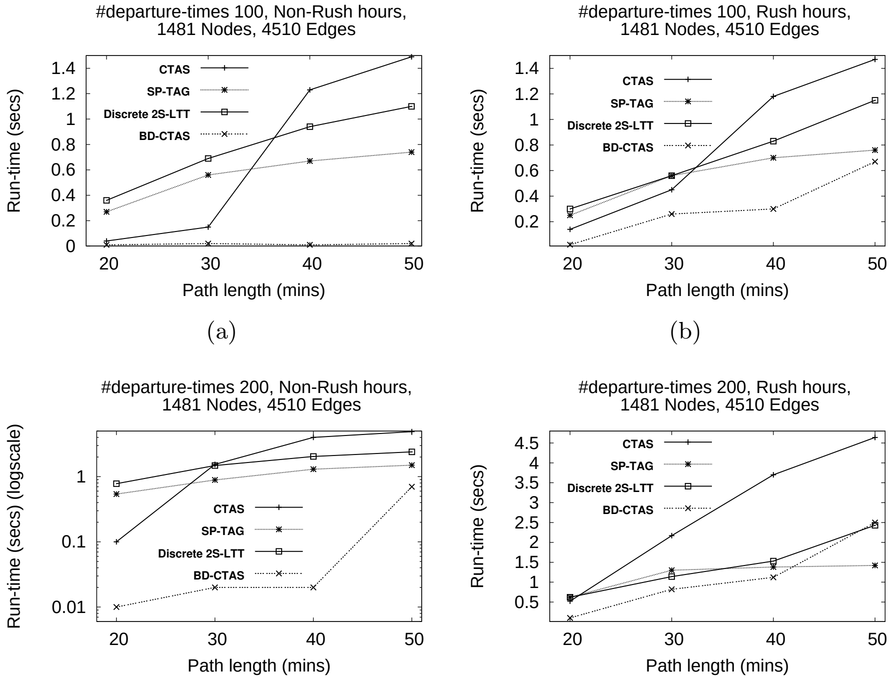

(a)

(b)

(c)

(d)

Figure 4.13: Effect of total travel time of path.

*Number of re-computations saved in BD-CTAS:* Figure 4.14 shows that BD-CTAS algorithm performed much less number of re-computations than CTAS.

*Effect of time of the day (rush hour vs non-rush hours)* Experiments showed that better performance was obtained for non-rush hours than rush hours (see Figure 4.13, Figure 4.12 and Figure 4.14). This is because there were fewer intersections among the path-functions.

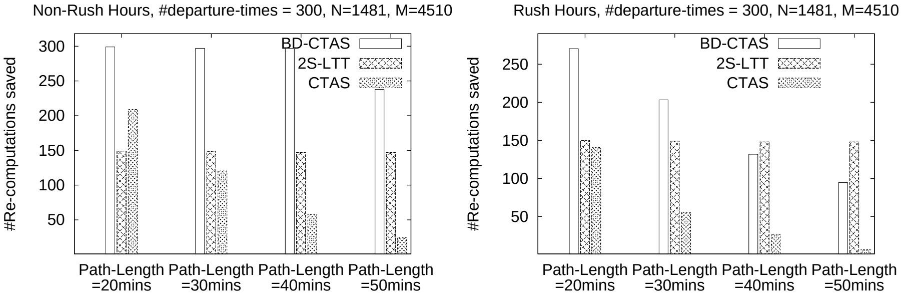

(a) During Non-Rush hours

(b) During Rush hours

Figure 4.14: Number of re-computations saved.

**Comparison with Naive algorithm:** In general, BD-CTAS performed better than the naive approach. However, for routes lengths greater than 40mins and $|\lambda| \geq 200$, SP-TAG started giving quicker response time during rush-hours (see Figure 4.12(d) and Figure 4.13(d)). A similar observation was made for non-rush hours as well, but for $|\lambda| > 500$. This is because, longer routes and departure-time intervals create a large number of forecasted CTPs and thus, it is much faster to simply instantiate the SP-TAG algorithm for all the departure-times. Recall that both BD-CTAS and CTAS achieve their performance benefits by making conservative estimates of the departure-times which can be skipped. This is achieved through additional book-keeping and processing over a common label setting algorithm like SP-TAG. Thus, it is conceivable that computational costs associated with additional book-keeping and processing may start to outweigh the gains obtained by skipping some departure-times when the number of critical time points is large.

**Comparison with the Discrete 2S-LTT algorithm** During rush hours, on longer paths (greater than 40mins), 2S-LTT was able to save more re-computations than BD-CTAS algorithm (Figure 4.14(b)) on ALSP instance with $|\lambda| \geq 300$ usually resulting in better run-time (Figure 4.12(d)). This is because, in our approach, when a path is expanded, we compute the intersection point with all the other paths (possible terminating on different nodes) present in the priority queue to ensure correctness. This sometimes forecasts CTPs which are irrelevant to the ALSP instance. Whereas, 2S-LTT compares the cost of current path against the earliest feasible cost to the same terminal node (as the current path) along other paths. This approach, though may not be able to close the node for longer times (as discussed earlier), but might forecast fewer irrelevant CTPs.

**Comparison with Discrete allFP algorithm:** Our experimental analysis shows that the run-time of the allFP algorithm rises sharply with length (i.e., total travel time) of the route (see Figure 4.15). In contrast, our approach was much less sensitive to length of the route. Due to this limitation allFP was not included in further experiments. Figure 4.15 shows that the BD-CTAS algorithm is faster than allFP algorithm by several orders of magnitude.

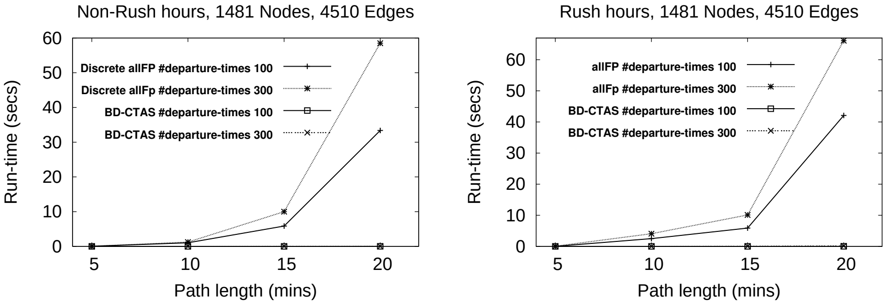

(a) (b)

Figure 4.15: Comparison with allFP algorithm.

**Experiments synthetic datasets:** Figure 4.16 illustrates the results on synthetic datasets. This experiment revealed trade-offs similar to the ones observed in the real datasets, i.e., both BD-CTAS and CTAS gain performance by skipping some departure-times. However, the additional cost of book-keeping and processing starts to out-weigh the benefits for cases with longer path-length and more $\#departure-times$ due to more CTPs. Further, our experiments also highlighted that the algorithms were in general slightly slower on larger datasets due to the larger size of TAG data-structure.

**Discussion:** A naive approach for solving the ALSP problem involves computing a shortest path for each departure time using a time-generalized version of Dijkstra's [15–22]. However, this leads to redundant re-computation of the shortest path across consecutive departure times sharing a common solution, creating an computational bottleneck for ALSP instances with long departure time intervals. For instance, in our

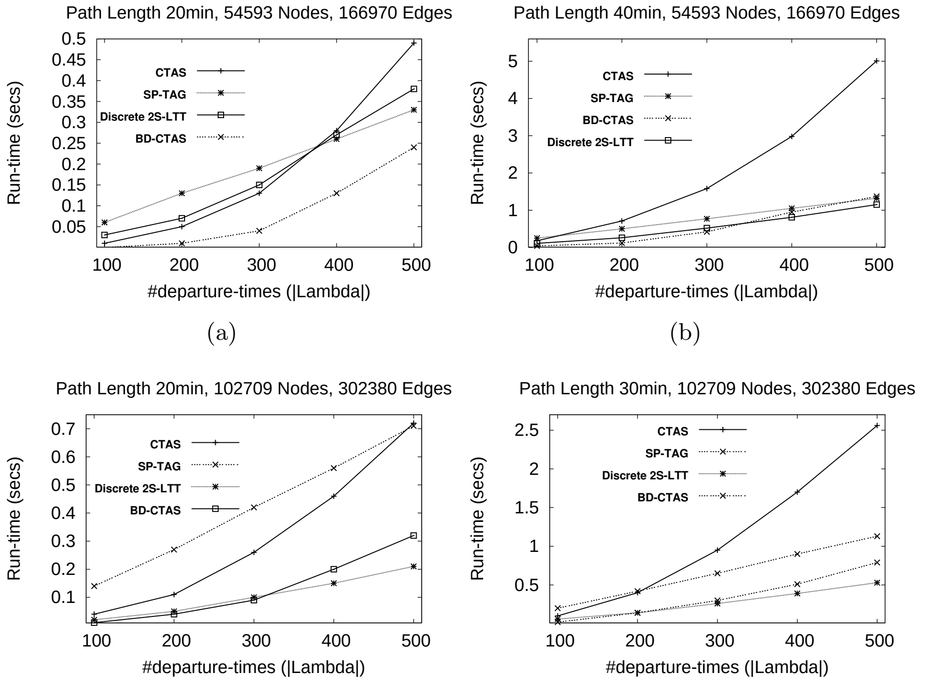

(a)

(b)

(c)

(d)

Figure 4.16: Experiments on synthetic datasets.

earlier University-Airport ALSP instance (Figure 3.1), it would have been computationally redundant to compute shortest path for departure-times 7:45, 8:00, 8:15 and 8:30 as the solution does not change.

## 4.7 Conclusions and Future work

The All-departure-time shortest Lagrangian shortest path problem (ALSP) is a key component of applications in transportation networks. ALSP is a challenging problem due to non-stationarity of the spatio-temporal network. A naive approach of re-computing the shortest path for each departure time incurs redundant computation across time instants sharing a common solution. The proposed critical-time-point based approaches (CTAS and BD-CTAS) reduces this redundancy by determining the departure times when the ranking among the alternate paths between the source and destination changes. Theoretical and experimental analysis show that this approach is more efficient particularly when the number of critical time points is small.

In the future we plan to extend the BD-CTAS algorithm by developing an A* based approach on continuous models [17]. We also plan to generalize the proposed algorithm to non-FIFO networks. Further, we plan to explore alternative approaches similar to [61] for solving ALSP. Performance of CTAS and BD-CTAS will also be evaluated on larger real datasets. We also plan to extend critical-time point based approaches to other problems on ST networks.

# Chapter 5

# Temporally Detailed Social Network Analytics

Given the ever-increasing proliferation of mobile and online social networking platforms, social interactions can increasingly be observed and studied at a fine temporal scale. Data from these platforms typically consists of time-stamped social events. These social events can represent several types of social interactions such as emails, phone calls, post-comment interactions, co-location pairs, etc. A time-stamped social event can be described as a relational tuple $<A_i,A_j,T>$, where $A_i$ and $A_j$ are the two individuals (or agents) who were interacting, and $T$ is the time-stamp when this was observed. Such an event creates a temporary link between $A_i$ and $A_j$, which can then be used in a time-aware analysis. A time-aware analysis can either consider the social events individually (e.g. change detection in streams) or could first create a set of frames containing interactions among members of a specific social system (e.g., employees of a university). Here, each frame would either contain events that occurred at a specific time point or comprise of all the events spread over a certain time duration (e.g., hour, day, week, etc.). A collection of all such frames (over a time window) recording interactions among the members of the same social system is referred to as a Temporally Detailed (TD) social network in this paper. Figure 5.1 illustrates a sample TD social network among W,X,A,C,D,U,U and Y. Here, an edge between two individuals denotes a social interaction.

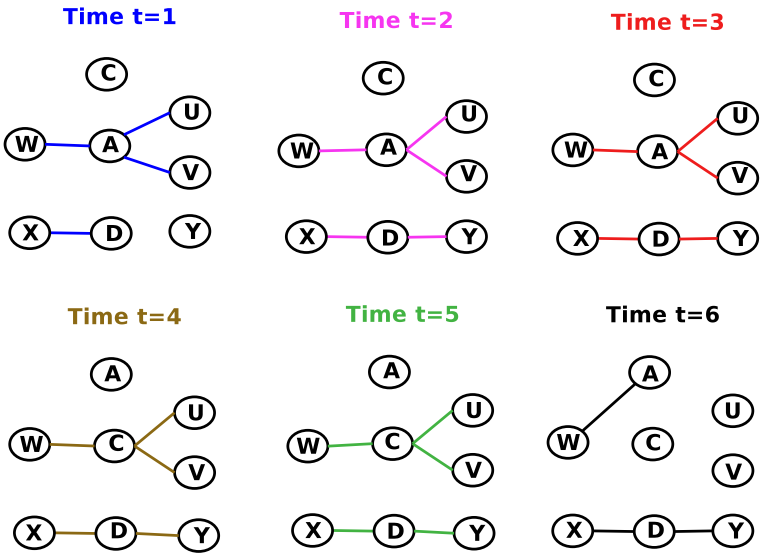

Figure 5.1: Sample Temporally-Detailed Social Network (best in color).

In this chapter, given a TD social network, we explore the computational challenges underlying a potential realization of what we refer to as temporally-detailed (TD) social network analytics. TD social network analytics can answer novel time-aware questions on the underlying social system. Examples include: "How did the betweenness centrality of an individual vary over past year?" "How is the closeness centrality of a person changing over time?" Etc. To this end, several pilot studies [13, 14, 29, 30, 62] have extended the traditional centrality metrics such as Betweenness and Closeness for TD social networks. These extended metrics capture the dynamics of the underlying social system and thus provide a better opportunity to understand its evolutionary behavior.

However, a TD social network still poses significant challenges for a computationally scalable realization of TD social network analytics. For instance, the shortest path between any two individuals in a TD social network–a key component in the extended versions of Betweenness and Closeness [13, 14, 29, 30]–is not stationary across time. As an example, in our previous TD social network shown in Figure 5.1, the shortest path between W and U passes through A for times $t = 1$,$t = 2$ and $t = 3$. Whereas, the same passes through C for times t=4 and t=5. Note that for sake of simplicity, we did not consider the temporal order of edges in this example, which is important while analyzing a TD social network as noted by other works as well [13,14,29,30]. It is important to note that non-stationarity can be seen when we consider temporal order of edges as well. If we consider the temporal order of the edges in Figure 5.1, then the shortest path between W and U passes through A only for times $t = 1$ and $t = 2$. This non-stationarity present in TD social networks violates the stationary ranking assumptions [63, 64] of classical dynamic programming (DP) based techniques (e.g. Dijkstras and its variants), and thus, makes it non-trivial to use them for computing the temporal extensions of shortest-path-based centrality metrics such as Betweenness and Closeness.

Current works [13, 14, 29, 30] intrinsically resort to re-computing the shortest paths (using a DP based technique) for all the times (for which the network is desired to be analyzed) while calculating the temporal extensions of Betweenness and Closeness. This approach yields a correct answer as given a particular time point, the ranking among paths is stationary. One could indeed use a DP based technique to re-compute the shortest paths (or the shortest path tree) and the centrality metric for each time point individually (as done in the related work). While such an approach provides a correct answer, it performs redundant work across times sharing a common solution. For instance, in our previous sample shown in Figure 5.1, the shortest path tree rooted at W does not change across $t = 1$,$t = 2$ and $t = 3$. Thus, it would be computationally redundant to re-compute the shortest path tree for $t = 2$ and $t = 3$ as the solution did not change. Such redundant work becomes a major computational bottleneck in case of large TD social networks observed for a long time-interval.

In this chapter, we propose to reduce this redundant re-computation through our novel approach of epoch-points. Epoch-points are the time points when the shortest path tree rooted a node changes. For example, in our previous sample shown in Figure 5.1, $t = 1$ (trivially), $t = 4$ and $t = 6$ form the epoch-points for the shortest path tree rooted at W. Epoch-points can be computed using one of the two strategies, pre-computing or lazy. In a pre-computing based method, all the candidate solutions (spanning trees) are enumerated and compared to determine the best tree for each time. This approach, however, would become a bottleneck in case of a large TD social network. To this end, we propose to use the lazy technique which computes epoch-points on-the-fly. The key insight in a lazy approach is that immediately after the computation of the shortest path tree for the earliest ($n^{th}$) time, one has adequate information to forecast the first ($n^{th}$) epoch-point. Epoch-point based algorithms for computing the temporal extensions of shortest-path-based centrality metrics such as Betweenness [13, 14, 29, 30] show better scalability by reducing the work across time-points sharing a common solution.

**Contributions:** This chapter makes following contributions:

1. We introduce epoch-point based approaches as a computational technique for temporally detailed analytics on TD social networks.
2. We propose a novel data structure called temporally-detailed priority queue helps in computing epoch-points on the fly (the lazy approach of computing epoch-points).
3. We propose an *epoch-point based algorithm called EBETS* for computing temporal extensions of Betweenness centrality. Note that EBETS can be easily modified to compute temporal extensions of closeness centrality as well. For purposes of brevity, we chose not to include that extension in the paper.
4. We prove the correctness and completeness of our proposed approach.
5. We evaluate EBETS experimentally via real datasets.
6. We provide an empirical comparison of temporal extension of betweenness centrality and traditional betweenness centrality on a real dataset.

The rest of the paper is organized as follows. Section 5.1 describes the basic concepts (e.g., representation models for TD social networks) and defines the problem of temporally-detailed social network analytics. In Section 5.2, we propose the concept of epoch-points for the problem of temporally-detailed social network analytics and describe our temporally-detailed priority queue to compute them on-the-fly. We propose an epoch-point based algorithm called EBETS for computing the temporal extension of betweenness centrality in Section 5.3. In Section 5.4, we prove the correctness and completeness our epoch-point based algorithm. The experimental evaluation of our algorithm is given in Section 5.5. Empirical comparison of temporal extension of betweenness centrality and traditional betweenness centrality in given in Section 5.6. We conclude this chapter in Section 5.7.

## 5.1 Basic Concepts and Problem Definition

### 5.1.1 Background on Representational models

A temporally-detailed (TD) social network can be conceptually represented in multiple. Current representational models used for TD social networks can be broadly classified into following two: (a) Snapshot based or (b) Explicit flow-path based models. It is important to note that choice of model depends on the 'social phenomena' being studied. We now briefly describe both these kind of models and give an intuition on when they are preferred.

**Snapshot model:** This model represents the temporally-detailed social network as a series of snapshots taken at different time instants. Here, each snapshot can either comprise of all the social events that happened at a specific time instant or can be an aggregation of all the events which happened over a certain time window (e.g., hour, day etc.). Figure 5.1 uses this model to represent a sample temporally-detailed social network. This kind of models are most suitable for studying temporally evolving patterns of activity of individuals [65], creation of temporally linked structures [66], addition of social links [67] etc.

**Explicit flow-path models:** These models are based on the idea of representing the temporal relationship among events upfront. For example, a sample temporal relationship could be based on the idea of "which temporally ordered events could imply a potential flow of information in the network?" Importance of these kind of models was highlighted by many works [29, 68–71] which focused on studying information flow in a social network. The basic idea proposed by these works being that "Information flows along the network in time." To this end, representational models [13, 14] were proposed in literature which show the temporal relationship of social event upfront. We refer to them as 'explicit flow-path models.' Figure 5.2 illustrates one such approach with the social event data shown in Figure 5.1. Here, the node corresponding to every agent is replicated across the time instants and directed edges, representing a potential information flow, are added in a "temporally-ordered" sense. For instance, consider a potential flow path $W \rightarrow A \rightarrow U$ which starts at $W$ at $t = 1$ and reaches $U$ at $t = 3$ via $A$ (assuming that it takes one time unit for the information to flow on an edge). This flow path is implied through following two directed edges (shown in bold in Figure 5.2) in

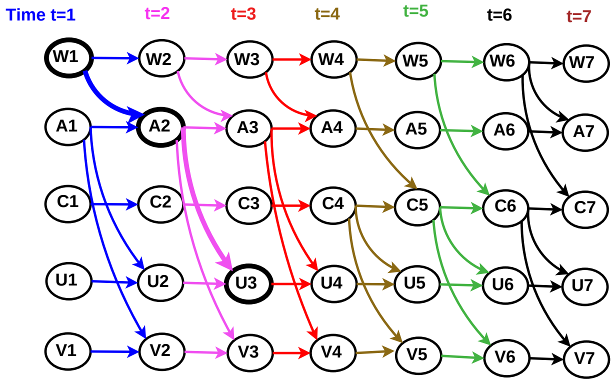

Figure 5.2: Explicit flow-path models (best in color).

the graph: (a) an edge between the copy of node $W$ at $t = 1$ and $A$ at $t = 2$, and (b) an edge between the copy of node $A$ at $t = 2$ and $U$ at $t = 3$.

**Snapshot models vs Explicit flow-path models:** Both snapshot and explicit flow-path models represent the same social event data but in two different ways. Further, one representation can be easily converted into another, i.e, snapshot based models can also be used to study flow based questions (by considering events across snapshots). And similarly, explicit flow-path based models can be used to study temporally evolving patterns, potentially seen upfront in a snapshot based model.

In this paper, we will use a *compressed* version of snapshot based models to describe our work. These are called as *Time aggregated graphs* [37]. In this model, we assign a time series, called an *interaction time series*, to each edge. This time series captures the time instants at which interactions have occurred. Figure 5.3 illustrates this model with the TD social network shown in Figure 5.1. Here, edge $(W, A)$ is associated with an interaction time series $[1\ 1\ 1\ X\ X\ X\ X]$. This implies that $W$ interacted with $A$ at times $t = 1, 2, 3$. Using this model, the information flow paths can also be easily retrieved by following the edges in a temporally-ordered fashion. Figure 5.3 also illustrates our previous information flow path $W \to A \to U$ which starts at $W$ at $t = 1$ and reaches $U$ at $t = 3$ via $A$.

**Problem Definition:** The problem of temporally-detailed social network analytics

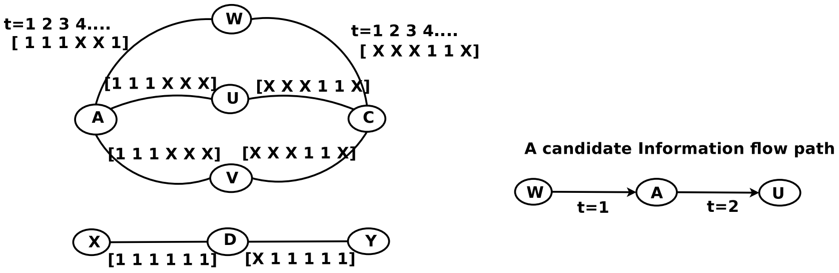

Figure 5.3: Time aggregated graph

(TDSNA) is defined as follows:

**Input:** (a) Temporally-detailed social network; (b) Shortest path based centrality metrics (e.g., betweenness and closeness)

**Output:** An algorithm design paradigm for computing these metrics over an discrete interval of time.

**Objective:** Computational scalability.

**Constraints:** Correctness and completeness of the solution.

## 5.2 Computational Structure of TD social network analytics

A nave approach for the TDSNA problem could be to repeatedly re-compute the shortest path tree using a DP based algorithm for each time. However, this would incur redundant re-computation across times sharing a common solution, leading to a severe computational bottleneck in case of long time-intervals for large TD social networks. To reduce this computational cost, we propose the notion of epoch-points which divide the given time-interval into a set of disjoint sub-intervals in which the ranking among alternative candidate paths is stationary. Within these intervals, the shortest path tree can now be computed using a single run of a dynamic programming (DP) based algorithm. The advantage of such an approach is that we would not compute the shortest path tree for many times in the given interval. We would re-compute only at the epoch-points without missing any time instant in the given time-interval where the shortest path tree can change. Note that the shortest path tree rooted at any node is not unique. It just

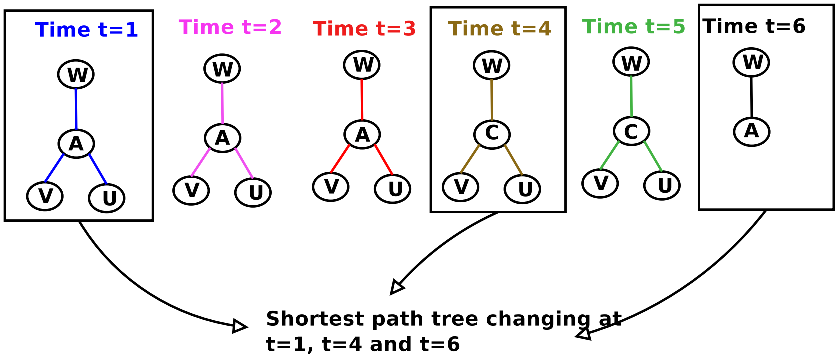

Figure 5.4: Shortest path tree rooted at node W for different times.

represents ‘a’ shortest path to the internal and leaf nodes of the tree from its root. To this end, we define epoch-points in terms of the maximum duration of ‘optimality’ of the current shortest path tree. Epoch-points are formally defined in Definition 1.

**Definition 1.** *Epoch-Points Given a shortest path tree $STree(v)$ for a time $t = t_{cur}$ which is rooted at node $v$ and contains nodes $U = \{u_1, u_2, \ldots, u_k\}$. The earliest time instant $t_{epoch} > t_{cur}$ is a epoch-point with respect to $STree(v)$ if one of the following holds:*

1. *There is a path $P$ (at $t = t_{epoch}$) from $v$ to some $u_i \in U$ which is shorter than the current path in $STree(v)$.*

2. *The current path to some $u_i \in U$ in $STree(v)$ no longer exists at $t = t_{epoch}$.*

3. *There is a node $w \notin U$ which is reachable from $v$ at time $t = t_{epoch}$.*

Figure 5.4 illustrates the proposed idea of epoch-points for the shortest path tree rooted at $W$ for the TD social network shown in Figure 5.1. The figure shows that the shortest path tree rooted at node W changes at $t = 1$ (trivially), $t = 4$, and $t = 6$ making them the epoch-points in this case. Note that the trees represented in Figure 5.1 are constructed based on the snapshot model where the temporal order of edges was not considered. Basically, each shortest path tree in Figure 5.4 corresponds to an instance of Dijsktra’s (from node W) on each of the 6 snapshots in Figure 5.1. These trees would be slightly different if we consider temporal order of edges (for modeling flows). We did not consider them in this example for ease of communication. Note, that the concept of Epoch-Points is valid for both snapshot and flow-path based studies. Just "what constitutes a shortest path?" changes across snapshot and flow-path based studies. In a flow-path based study, the edges must be considered in a temporally-ordered fashion.

A key challenge in designing an epoch-point based algorithm for the TDSNA problem is to minimize the amount of time needed to compute the epoch-points while ensuring correctness and completeness. Epoch-points can be computed in two ways, pre-computing strategy or a lazy strategy. In a pre-computing based method, all the candidate solutions (spanning trees) are enumerated and compared to determine the best tree for each time. This approach, however, may become a computational bottleneck in the case of a temporally-detailed social network, as there can be large number of candidate spanning trees. In this paper, we investigate the lazy technique, which computes epoch-points on-the-fly while exploring candidate paths. The key insight in a lazy approach is that immediately after the computation of the shortest path tree for the first ($n^{th}$) time, one has adequate information to forecast the first ($n^{th}$) epoch-point. In our previous example of shortest path tree of node W, this would mean that, after computing the shortest path at $t = 1$ we could forecast $t = 4$ as the next epoch-point for the re-computation to start. In other words, a single logical work-unit of the proposed algorithm would be: "compute the shortest path tree for one time and forecast the next epoch-point for re-computation."

An epoch-point is forecasted through the use of a modified priority queue, which we call as a ***temporally-detailed (TD) priority queue***. Table 5.1 illustrates its properties in contrast the regular priority queues. Unlike a regular priority queue, whose elements are scalar values, a TD priority queue is composed of time-series of values. For our shortest path tree problem, a time-series in this queue would contain the cost along a path to a node in the open list for the times under consideration. The queue is ordered on the current time ($t_{ord}$ in Table 5.1) under consideration. For instance, in our previous example of shortest path tree of node W over the time interval [1 6], we would order the queue based on costs for $t = 1$ for the first logical work-unit and then for the forecasted epoch-point for the second work unit, and so on. Apart from the standard priority queue operations such as insert, extract-min, update-key, we have a new operation called "forecast-epoch-point." This new operation is called

| Properties/operations | Priority Queue | Temporally-Detailed Priority Queue |
|---|---|---|
| Keys | Scalar values | Time-series of values |
| Ordering | Ascending or Descending | Ascending or Descending on a time index $t_{ord}$ |
| Insert operation | Inserts scalar value | Inserts a time-series |
| Update-Key operation | Updates a scalar value | Updates an entire time-series |
| Extract-Min | Returns a scalar with lowest cost | Returns a time-series with least value of $t_{ord}$ |
| Forecast-Epoch-Point | --Not Available-- | Maximum time $t_{ept}(> \quad t_{ord})$ for which the previous extract-min has least value among all keys in the queue |

Table 5.1: Priority Queue vs Temporally-Detailed Priority Queue.

at the end of each extract-min, at that stage it compares the time-series corresponding to the extract-min with the other time-series in the queue to determine the maximum time duration (beyond $t_{ord}$) for which the chosen time-series has the lowest value. This value is stored in an auxiliary data-structure as a "potential epoch-point." At any stage during the execution, we have the following loop invariant:

**Proposition 1.** *The choices (i.e., extract-mins from the TD priority queue) made during execution hold their validity for all the times between the time for which the queue is ordered (trivially) and the* min{*potential epoch-points observed so far*}.

Using this loop invariant and exploring the paths in a greedy fashion (similar to Dijkstra's enumeration style), when we expand (extract-min + forecast-epoch-point) a node $v$, we have a shortest path between the root of the tree to $v$ which is optimal for all the times between $t_{ord}$ (on which the queue was ordered) and the min{potential epoch-points observed so far}. This min{potential epoch-points} then becomes the forecasted epoch-point when the re-computation starts.

## 5.3 Epoch based Betweenness Centrality

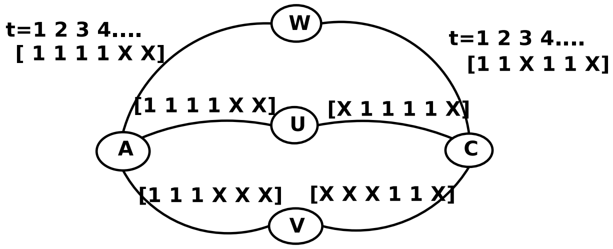

Figure 5.5: Sample temporally-detailed social network.

This section describes a general epoch-point based algorithm for computing temporal extension of betweenness centrality on a temporally-detailed social network. A key component of this computation would be to determine shortest paths between all pairs of nodes for either all the times or for a given range of time instants. As mentioned previously, these shortest paths could change with time. As soon as the optimal shortest path to a node in the tree changes, we deem the shortest path tree to has changed (ref Definition 1). The time points where these changes happen are termed as the epoch-points (ref Definition 1). These epoch-points need to be determined in order to efficiently compute a temporal extension of betweenness centrality [13, 14, 29, 30] for several time points in a TD social network. Note that, even if the shortest path tree changes according to Definition 1, the overall betweenness centrality value may not change. However, in order to ensure correctness, we re-compute the shortest path tree (and the betweenness centrality) for all the epoch-points as defined in Definition 1.

In order to determine the epoch-points using a temporally-detailed (TD) priority queue, we need to model the total cost of a path for different time instants which would be inserted in the TD priority queue as keys. We propose to do this via–what we refer to–as a *path-function.* A formal definition of the path-function is given below.

**Definition 2.** ***Path-function:*** *A path function is a time series that represents the total cost of the path from the root of the tree to the end node of path as a function of time. A path function is determined by combining the interaction time series of its component edges in a suitable fashion, e.g., in a time-ordered way for modeling information flow.*

For instance, consider the path $<W$,$A$,$U>$ in the TD social network shown in Figure

5.5. This path contains two edges, (W,A) and (A,U). The interaction time series of edge (W,A) is [1 1 1 1 X X], while that of (A,U) is [1 1 1 1 X X]. Depending on the nature of the 'social phenomena' being studied, these interaction time-series can be combined in multiple ways. If the 'social phenomena' of interest is preferable via a snapshot model, then these can be simply added (interpreting 'X' as $+\infty$) to create the path function of $<W,A,U>$ over time instants [1 6] as [2 2 2 2 X X]. This means that length of the path $<W,A,U>$ for times $t = 1, 2, 3, 4 \ldots$ is two edges, and the path is undefined for times $t = 5, 6$.

On other hand, if the 'social phenomena' being studied requires modeling information flows then we need to consider the temporal order of interaction events on the edges [29, 68–71]. Further, the cost of the path is noted in terms of the arrival time at the end node of the path [14]. In other words, cost of a path, e.g. S-X-Y, for time $t = \alpha$ is interpreted as "If I start at S at time $t = \alpha$ and traverse S-X-Y, then when (a time $t > \alpha$) can I take an outgoing edge from Y?" This boils down to considering following two aspects: (a) How much time does it take for the information to flow on an edge? and (b) Is information allowed to wait at a node? Depending on our choices for item (a) and item (b), the resulting path-function may be different. We now illustrate the procedure for constructing path-function for modeling flows under following design decisions: For item (a), we assume it takes 1 time unit for the information to travel on an edge. And for item (b), we assume that the information is not allowed to wait. Note that these assumptions are only for illustration purposes, and are not constraints on our epoch-point based approaches. Usually, these design decisions would depend on nature of the 'social phenomena' being studied.

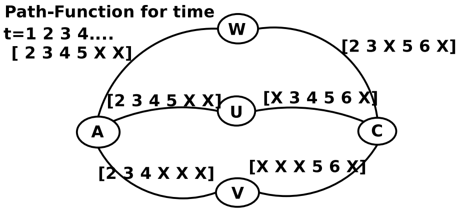

Figure 5.6: Path functions for all the singleton edges.

Consider the interaction time series of edge (W,A): [1 1 1 1 X X] which denotes that W and A interacted at times $t = 1, 2, 3$ and 4. Following our previous assumptions for item (a) and item (b), we interpret this interaction time series in following way: If we start at W at time $t = 1, 2, 3, 4$, we can take the next outgoing edge from A at times $t = 2, 3, 4, 5$. Note that 'X' is interpreted as "cannot follow this edge" (implemented as $+\infty$). This gives the path-function [2 3

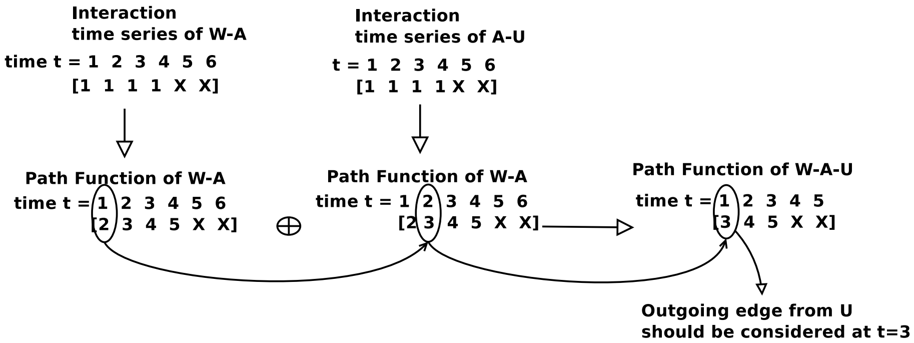

Figure 5.7: Path function computation for modeling information flows.

4 5 X X] for the edge (W,A). Similarly, we would get the path-function [2 3 4 5 X X] for the edge (A,U). Figure 5.6 shows the path-functions computed in this way for all the singleton edges ((W,A), (W,C), (A,U), etc.) in the TD social network illustrated in Figure 5.5. Now consider the case of determining the path function of <W,A,U>. Figure 5.7 illustrates this process. If we take the edge W-A at time $t = 1$, we would be able to edge (A-U) at time $t = 2$ and then take the next outgoing edge from node U at time $t = 3$. Thus, the value of path-function of <W,A,U> for $t = 1$ would be 3. Following this process, the complete path-function of <W,A,U> for $t = 1, 2, 3, 4, 5$ (under the previous assumptions for item (a) and item (b)) would be [3 4 5 X X]. Note that a path function for <W,A,U> modeling flows cannot be defined for $t = 6$ for the network shown in Figure 5.5 because the network was not 'observed' for $t = 7$ which is needed if a flow has to modeled for $t = 6$.

As mentioned previously, different path-functions would be obtained if waiting is allowed or it takes more than 1 time unit for the information to travel on a edge. For instance, consider the case when waiting is allowed. Waiting is a natural consequence when the goal is to model the notion of "lifetime" of an information unit [72–74] flowing through the network. Waiting can be implemented by incorporating the notion of ***maximum wait allowed*** into the path-function construction. For example, consider the interaction time series of (C,V) [X X X 1 1 X]. Under the no waiting scheme, this translated to the path-function: [X X X 5 6 X] (see Figure 5.6). Now, consider the case when an information unit is allowed to wait for a maximum of 2 time units at any node. This means if the information has to flow through the edge (C,V) it must arrive at node C (or V as this is an undirected edge) by times $t = 2, 3, 4$ or 5. Case of $t = 4$ and $t = 5$ is trivial as C and V interacted at these times. However, $t = 2$ and $t = 3$ imply that the information waits at C (or V) for two and one time units respectively. In this case, we would get the following path-function for (C,V): [X 5 5 5 6 X]. Note the value 5 for times $t = 2$ and $t = 3$ in this path-function, these capture the notion of maximum wait allowed to be 2 time units. It is important to note that our proposed epoch-based approaches are transparent to the way the path-functions are constructed. It retains correctness across both snapshot style and information flow style paths. However, waiting does play a role on the computational performance of the proposed algorithm. To this end, we vary this parameter in our experiments (Section 5.5).

Given path-functions of candidate paths, epoch-points are determined by computing the earliest intersection point between the path functions and 'X' is interpreted as $+\infty$.

### 5.3.1 Basic Concepts of Temporal Betweenness Centrality Metrics

Several works [13, 14, 29, 30] have defined temporal extensions of betweenness centrality. Although they slightly vary in their formal definition, they share the common underlying structure given in Equation 5.1. Here, $C_B(v)[t]$ denotes the betweenness centrality of a node $v$ at time $t$. In the equation, $\sigma_{sd}[t]$ refers to the number of shortest paths between node $s$ and node $d$ at time $t$, and $\sigma_{sd}(v)[t]$ refers to the number of shortest paths between node $s$ and node $d$ that pass through node $v$ at time $t$. Here, the concept of *"shortest path between node $s$ and node $d$ at time $t$"* was interpreted according to Definition 3. This interpretation is close to what we refer as "modeling information flows" in this paper.

$$C_B(v)[t] \;=\; \sum_{\forall s \neq v \neq d \in V} \frac{\sigma_{sd}(v)[t]}{\sigma_{sd}[t]} \tag{5.1}$$

**Definition 3.** ***Temporal Shortest Path:*** *A path $P_{sd} = s, x_1, x_2, x_3 \ldots, x_k, d$ between $s$ and $d$, where $s$ and $x_1$ interacted at time $t$, is considered to be a shortest path for time $t$ if it has following two properties.*

- *All the nodes in $P_{sd}$ should be visited in a* temporally ordered *sense. This means that if $(x_i, x_j)$ and $(x_j, x_k)$ are two consecutive edges in $P_{sd}$ corresponding to the* *interactions at times* $t_{x_ix_j}$ *and* $t_{x_jx_k}$*, then* $t_{x_ix_j} < t_{x_jx_k}$.

- *If there is another path* $Q_{sd} = s, y_1, y_2, y_3 \ldots, d$ *between s and d, where s and* $x_1$ *interacted at time t, then the interaction time of the edge (*$y_k$*,d) is not less than that of (*$x_k$*,d), i.e,* $t_{y_kd} \geq t_{x_kd}$.

In order to study the betweenness centrality of an individual over an time interval, Equation 5.1 was computed repeatedly for all the times in the time-interval of interest [13, 14, 29, 30]. Internally they used a temporal generalization of path counting technique proposed in [75]. More specifically, the notion of *pair-dependencies* in [75] was generalized to a temporal case. Equation 5.2 shows this generalization for the metric given in Equation 5.1. Here, $\delta_{sd}(v)[t]$ denotes the *temporal pair-dependencies* on node $v$ at time $t$.

$$\begin{aligned} C_B(v)[t] &= \sum_{\forall s \neq v \neq d \in V} \frac{\sigma_{sd}(v)[t]}{\sigma_{sd}[t]} \\ &= \sum_{s \neq v \neq d \in V} \delta_{sd}(v)[t] \quad where\ \delta_{sd}(v)[t] = \frac{\sigma_{sd}(v)[t]}{\sigma_{sd}} \\ &= \sum_{\forall s \in V} \delta_{s\cdot}(v)[t] \quad where\ \delta_{s\cdot}(v)[t] = \sum_{\forall d \in V} \delta_{sd}(v)[t] \end{aligned} \tag{5.2}$$

Here, a single $\delta_{s\cdot}(v)[t]$ is computed using Equation 5.3. This is a temporal generalization of Theorem 6 in [75]. This equation is computed using recursive fashion (using stacks), starting with the last node in a shortest path whose $\delta_{s\cdot}()$ is initialized to zero.

$$\begin{aligned} \delta_{s\cdot}(v)[t] &= \sum_{w: v \in P_s(w)[t]} \frac{\sigma_{sv}(v)[t]}{\sigma_{sw}[t]} \cdot (1 + \delta_{s\cdot}(w)[t]) \\ where\ P_s(w) &= \{u \in V : u\ is\ predecessor\ to\ w\ in\ a\ shortest\ path \\ &(According\ to\ Definition\ 3)\ from\ s\ for\ time\ t\} \end{aligned} \tag{5.3}$$

### 5.3.2 Epoch-point based BETweenness centrality Solver

Our proposed Epoch-point based BETweenness centrality Solver (EBETS) efficiently computes the epoch points *on the fly* without enumerating all the possible candidate paths. We do this by using a search and prune strategy (similar to Dijkstra's algorithm) coupled with our temporally-detailed priority queues. This ensures bounded exploration of the space of possible candidate paths while ensuring correctness at the same time. EBETS employs the previously mentioned temporal generalization of the path counting technique proposed in [75] to count the number paths passing through any particular node. The input and output of EBETS are formally defined next.

**Input:** The input EBETS consists of (a) temporally-detailed social network dataset over $V$ individuals observed for $\mathcal{H}$ time steps and; (b) a time interval $\lambda \subset \mathcal{H}$ represented as discrete time instants

**Output:** Temporal betweenness centrality (as defined in Equation 5.1) of all individuals $v \in V$ for all the time instants $t \in \lambda$.

Note that the proposed EBETS algorithm can be easily adapted to other variations of temporal betweenness centrality (apart from Equation 5.1) and temporal shortest paths (apart from Definition 3).

As mentioned previously, the spirit of an epoch based approach is to efficiently determine the time points (i.e, the epoch points) when the shortest path changes (according to Defnition 1). Epoch-points would partition the given time interval $\lambda$ into a set of disjoint sub-intervals, over which the shortest path tree does not change. The *sub-interval SPtree* denotes this shortest path tree.

**Definition 4.** ***sub-interval SPtree** ($SPT_v$)**:*** *A pair of a tree rooted at $v$ and a set of time instants $\omega_v$ such that the path from $v$ to any of the nodes in $SPT_v$ is the temporal shortest path (according to Definition 3) for all the time instants in $\omega_v$. In other words, the shortest path tree $SP_v$ is guaranteed not to change during $\omega_v$.*

The key idea of EBETS is compute successive sub-interval SPtree's for each node $v \in V$ until all the time instants in the input time-interval $\lambda$ are covered. For each sub-interval SPtree, the temporal generalization of pair-dependency (Equation 5.3) is computed to for the times $\omega_v$. These are also summed up during the execution to obtain the centrality given by Equation 5.1. While computing a sub-interval SPtree, EBETS maintains following two tables:

**Path Intersection Table:** Stores the potential epoch points returned from Forecast-Epoch-Point operation of the temporally-detailed priority queue. This table is referred while determining the next epoch-point for re-computation.

**Predecessor Table:** Stores all the possible predecessor(s) of a node across possible temporal shortest paths from the root of tree. This is used to compute Equation 5.3.

**Algorithm 3** Epoch-point based BETweenness centrality Solver (EBETS) Algorithm

```
for all nodes $s \in V$ do
  cur-time ← first time instant in $\lambda$
  upper-time ← last time instant in $\lambda$
  while cur-time $\leq upper - time$ do
    Initialize a temporally-detailed priority queue $TDPQ$
    Insert path functions corresponding to neighbors of $s$ into $TDPQ$
    while $TDPQ$ is not empty do
      $pf_{min}$ ← Extract-Min operation on $TDPQ$
      $min_{tail}$ ← Tail node of path corresponding to $pf_{min}$
      $t_{min}$ ← Forecast-Epoch-Point operation on $TDPQ$
      Save $t_{min}$ in the path intersection table
      if multiple paths in $TDPQ$ end on $min_{tail}$ then
        for all time instants $t$ in interval $cur - time$ through $t_{min} - 1$ do
          Set the second last node of all the paths (including $pf_{min}$) which have the same cost
            $pf_{min}$ for time $t$ as predecessor $min_{tail}$
        end for
      else
        Set the second last node in $pf_{min}$ as the predecessor of $min_{tail}$ for all times cur-time
          through $t_{min}$
      end if
      Delete all the paths ending on $pf_{tail}$ from $TDPQ$
      Determine the path functions resulting from expansion of the chosen path
      Insert the newly determined path functions into $TDPQ$
    end while
    cur-time ← min{$t_{min}$ in path intersection table}
    Clear path intersection table
    Re-initialize the predecessor table for times greater than cur-time
    Compute the dependency of $s$ on each vertex for times between the previous and the cur-time
  end while
end for
```

We now provide a detailed description of the EBETS algorithm and illustrative execution trace on the temporally-detailed social network shown in Figure 5.5. A pseudocode of EBETS is shown in Algorithm 3. The outermost for-loop (line 1–28 in Algorithm 3) ensures that the shortest path tree from all the nodes is determined. Within this for loop, the algorithm computes the shortest path tree of a single node $v$ for all the time instants in $\lambda$ by determining successive sub-interval SPtrees rooted at $v$. This is done in the while-loop on line 4. Before this, we initialize two variables, *cur-time* and *upper-time* to the first and last time in $\lambda$ respectively. The while-loop on line 4 executes until the value of *cur-time* is less than *upper-time.* The inner most while-loop on line 7 determines a single *sub-interval SPtree* for node $v$. Here, we first initialize a temporally-detailed priority queue, $TDPQ$, with path functions corresponding to immediate neighbors of source node. The queue is ordered based on the values of the path-functions for time *cur-time.* The while loop on line 7 runs until $TDPQ$ is not empty. In each iteration of this while loop, the path function having the least cost for *cur-time* ($pf_{min}$) is extracted its corresponding epoch-point is determined using forecast-epoch-point operation on $TDPQ$. The forecast-epoch-point operation does this by computing the earliest (in terms of time) of intersection point of $pf_{min}$ with the other path functions in the $TDPQ$. This intersection point $t_{min}$, a potential epoch-point, is stored in the *path intersection table.* Note that in the absence of intersection points, the value of $t_{min}$ is set to one more than the last time in $\lambda$.

Following this, the algorithm determines all the possible predecessors of the tail node ($min_{tail}$) of the path corresponding to $pf_{min}$. This is accomplished as follows: We first choose all the paths in the $TDPQ$ whose tail node is same the as $min_{tail}$. Now, the second to last nodes of all these paths are potential predecessors of $min_{tail}$. Among these candidates the ones who have the same cost as that of $pf_{min}$ are stored as predecessors of $min_{tail}$ (at their corresponding time instants). For example, consider a path <s,x,y> whose corresponding path function [2 3 4 5 X] was chosen as $pf_{min}$. Further, consider another path function [2 3 4 X X], corresponding to path <s,z,y>, present in the queue. For convenience, assume that the *cur-time* was $t = 1$ (corresponding to the first value in the path function), $t_{min}$ would be 5. Here, the node $z$ would be included in predecessors of node $y$ for times $t = 1, 2, 3$. Whereas, node $x$ would be included for times $t = 1, 2, 3, 4$. This process is accomplished in lines 12–18 of the Algorithm 3. After the predecessors are determined, other paths ending on $min_{tail}$ are deleted from $TDPQ$ (line 19) and $pf_{min}$ is expanded to include each of its neighbors.

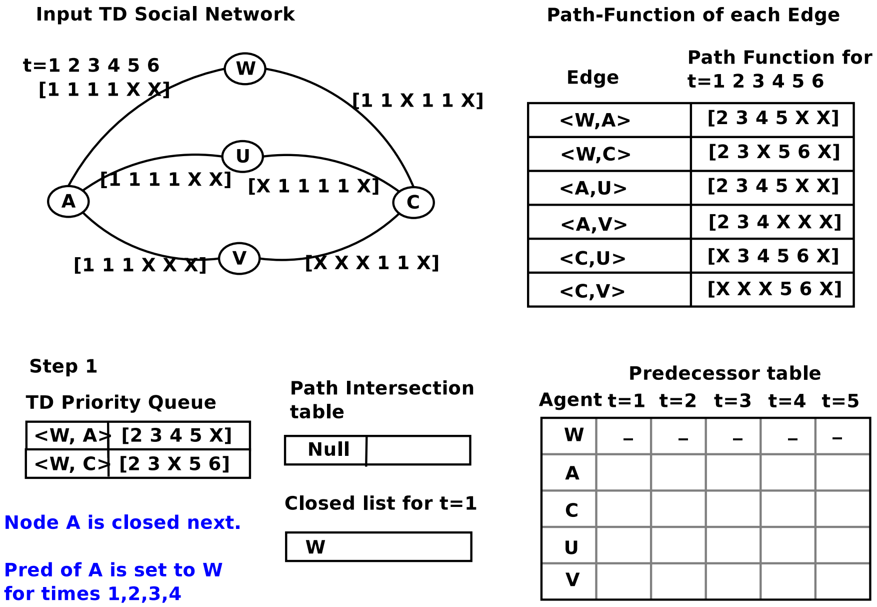

Path-Function of each Edge

| Edge | Path Function for<br>t=1 2 3 4 5 6 |
|---|---|
| <W,A> | [2 3 4 5 X X] |
| <W,C> | [2 3 X 5 6 X] |
| <A,U> | [2 3 4 5 X X] |
| <A,V> | [2 3 4 X X X] |
| <C,U> | [X 3 4 5 6 X] |
| <C,V> | [X X X 5 6 X] |

Step 1

TD Priority Queue

| | |
|---|---|
| <W, A> | [2 3 4 5 X] |
| <W, C> | [2 3 X 5 6] |

Path Intersection table

| | |
|---|---|
| Null | |

Closed list for t=1

| |
|---|
| W |

Node A is closed next.

Pred of A is set to W for times 1,2,3,4

Predecessor table

| Agent | t=1 | t=2 | t=3 | t=4 | t=5 |
|---|---|---|---|---|---|
| W | _ | _ | _ | _ | _ |
| A | | | | | |
| C | | | | | |
| U | | | | | |
| V | | | | | |

Figure 5.8: EBETS Execution trace: Start of Step 1

The newly determined path functions (line 21) are inserted into $TDPQ$. This process continues until $TDPQ$ is empty. Note that when $pf_{min}$ is expanded, $min_{tail}$ is closed for *cur-time*. This means that there cannot be any other path leading to $min_{tail}$ from the root with a shorter length. After exiting from the inner while loop on line 7, we have a sub-interval SPtree rooted at node $s$ (as per Line 1) whose optimality is guaranteed for all times between *cur-time* and the minimum of $t_{min}s$ stored in the path intersection table. Following this EBETS performs following three tasks. First, *cur-time* (next time for re-computation) is set to the minimum of $t_{min}s$ stored in the path intersection table (line 23 in Algorithm 3). In a worst case scenario, this value could just be the next time instant in $\lambda$. In such a case, the sub-interval SPtree determined by the inner most while loop would be valid for only one time in $\lambda$. Second, the predecessor table is reinitialized for times greater than the new *cur-time*. Third, the dependency (given by Equation 5.3) of each of the nodes in the sub-interval SPtree is computed for times between the previous and the new *cur-time*.

### 5.3.3 Execution trace

We now provide an execution trace of the EBETS on the temporally-detailed social network shown in Figure 5.5. Here, the set $\lambda = 1, 2, 3, 4, 5$. For brevity, we only show the computation of a single sub-interval temporally-ordered SPtree with source $W$. For this execution trace, we have the following: (a) Our path-functions are modeling information flows, (b) It takes 1 time unit for the information to flow on an edge, (c) Waiting is not allowed.

In the first iteration of the while-loop on line 4 the value of *cur-time* would be 1 (first time instant in $\lambda$). The inner while-loop on line 7 begins with a temporally-detailed priority queue initialized with the path functions corresponding to immediate neighbors of $W$ (see Figure 5.8). Now, the path function having the lowest cost at $t = 1$ would be chosen as $pf_{min}$ on line 8. In this case, the path <W,A> has the lowest cost for $t = 1$. The path-function of <W,A> intersects with that of <W,C> at time $t = 5$ which be the value of $t_{min}$. In other words, forecast-epoch-point would return $t = 5$, which is stored in the path intersection table. Now, since there are no other paths ending on node $A$ in queue, $W$ would be set as the predecessor of $A$ for times $1, 2, 3, 4$ (all times between *cur-time* and $t_{min} - 1$). Lines 20-21 would expand the path <W,A> to insert the path-function corresponding to <W,A,U> and <W,A,V> (see Figure 5.9) into the queue.

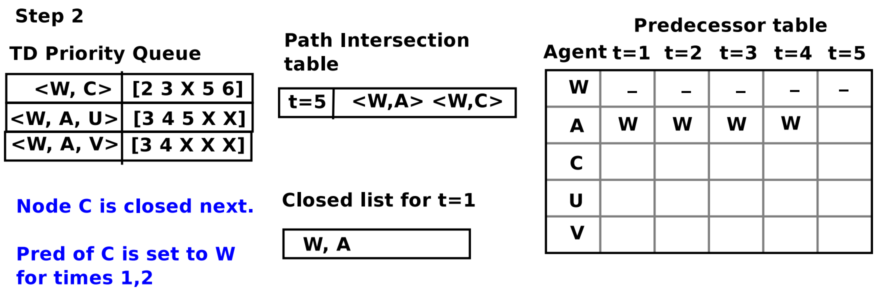

**Step 2**

**TD Priority Queue**

| | |
|---|---|
| <W, C> | [2 3 X 5 6] |
| <W, A, U> | [3 4 5 X X] |
| <W, A, V> | [3 4 X X X] |

Node C is closed next.

Pred of C is set to W for times 1,2

**Path Intersection table**

| | |
|---|---|
| t=5 | <W,A> <W,C> |

**Closed list for t=1**

W, A

**Predecessor table**

| Agent | t=1 | t=2 | t=3 | t=4 | t=5 |
|---|---|---|---|---|---|
| W | – | – | – | – | – |
| A | W | W | W | W | |
| C | | | | | |
| U | | | | | |
| V | | | | | |

Figure 5.9: EBETS Execution trace: Start of Step 2

For the second iteration of the while loop on line 7, the algorithm would select the path <W,C> as $pf_{min}$ and node $C$ would be closed for time $t = 1$. Forecast-epoch-point would consider the intersection of the path function of <W,C> with <W,A,U> at $t = 3$

(see Figure 5.9). This intersection point would be stored in the path intersection table. Now, since there are no paths ending with node $C$ in the queue (see Figure 5.9), $W$ would be set as the predecessor of $C$ for times $t = 1, 2$. The algorithm then expands the path <W,C> and the path-functions corresponding to <W,C,U> and <W,C,V> are inserted into the queue.

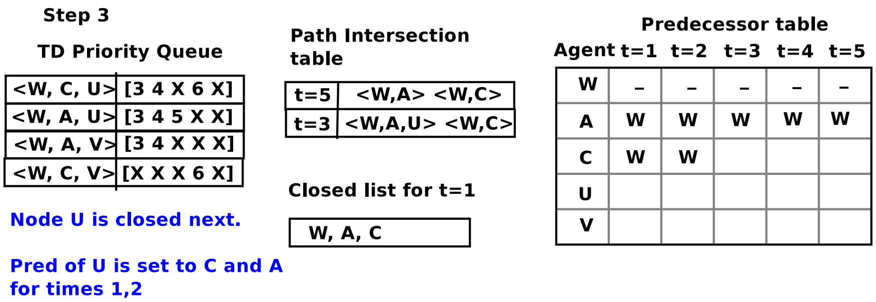

Step 3

TD Priority Queue

| | |
|---|---|
| <W, C, U> | [3 4 X 6 X] |
| <W, A, U> | [3 4 5 X X] |
| <W, A, V> | [3 4 X X X] |
| <W, C, V> | [X X X 6 X] |

Node U is closed next.

Pred of U is set to C and A for times 1,2

Path Intersection table

| | |
|---|---|
| t=5 | <W,A> <W,C> |
| t=3 | <W,A,U> <W,C> |

Closed list for t=1

W, A, C

Predecessor table

| Agent | t=1 | t=2 | t=3 | t=4 | t=5 |
|---|---|---|---|---|---|
| W | – | – | – | – | – |
| A | W | W | W | W | W |
| C | W | W | | | |
| U | | | | | |
| V | | | | | |

Figure 5.10: EBETS Execution trace: Start of Step 3

In the third iteration of the while loop on line 7, the algorithm would select the path <W,C,U> as $pf_{min}$ (ties broken arbitrarily) and node $U$ would be closed for time $t = 1$. Forecast-epoch-point would return $t = 3$ as there is an intersection of the path function of <W,C,U> with <W,A,U> at $t = 3$ (see Figure 5.10). This intersection point is stored in the path intersection table. Now, there are two paths, <W,C,U> and <W,A,U>, in the queue which end on node $U$ and have the same cost of $t = 1$ and $t = 2$. Thus, both $A$ and $U$ would be set as predecessors of $U$ for times $t = 1$ and $t = 2$. <W,C,U> is not expanded further as it does not have any unclosed neighbors. At line 19, the algorithm deletes both <W,C,U> and <W,A,U> from the queue.

In the fourth iteration of the while loop on line 7, the algorithm would select the path <W,A,V> as $pf_{min}$ and node $V$ would be closed for time $t = 1$. Forecast-epoch-point would return $t = 3$ as <W,A,V> ceased to exist at $t = 3$ (see Figure 5.11). This intersection point is stored in the path intersection table. Now, there are no other two paths ending on $V$ for times $t = 1$ and $t = 2$. Thus, only $A$ is set as a predecessor of $V$ for times $t = 1$ and $t = 2$. <W,A,V> is not expanded further as it does not have any unclosed neighbors. At line 19, the algorithm deletes both <W,C,V> and <W,A,V> from the queue.

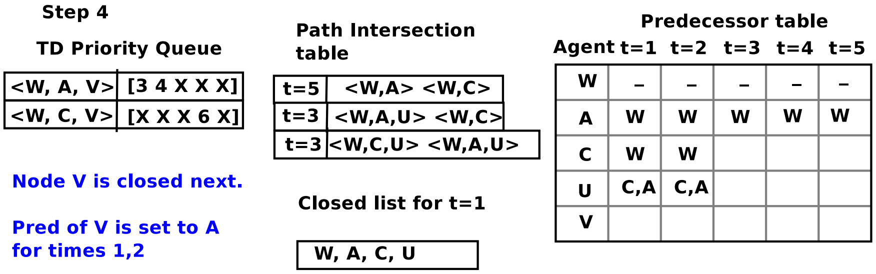

Step 4

TD Priority Queue

| | |
|---|---|
| <W, A, V> | [3 4 X X X] |
| <W, C, V> | [X X X 6 X] |

Node V is closed next.

Pred of V is set to A for times 1,2

Path Intersection table

| | |
|---|---|
| t=5 | <W,A> <W,C> |
| t=3 | <W,A,U> <W,C> |
| t=3 | <W,C,U> <W,A,U> |

Closed list for t=1

W, A, C, U

Predecessor table

| Agent | t=1 | t=2 | t=3 | t=4 | t=5 |
|---|---|---|---|---|---|
| W | – | – | – | – | – |
| A | W | W | W | W | W |
| C | W | W | | | |
| U | C,A | C,A | | | |
| V | | | | | |

Figure 5.11: EBETS Execution trace: Start of Step 4

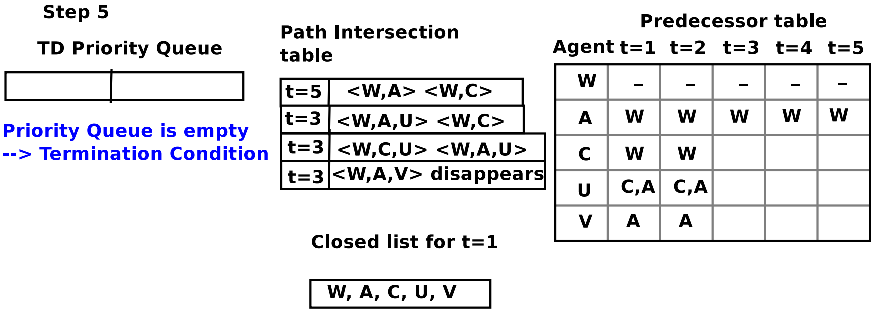

Step 5

TD Priority Queue

Priority Queue is empty
--> Termination Condition

Path Intersection table

| | |
|---|---|
| t=5 | <W,A> <W,C> |
| t=3 | <W,A,U> <W,C> |
| t=3 | <W,C,U> <W,A,U> |
| t=3 | <W,A,V> disappears |

Closed list for t=1

W, A, C, U, V

Predecessor table

| Agent | t=1 | t=2 | t=3 | t=4 | t=5 |
|---|---|---|---|---|---|
| W | – | – | – | – | – |
| A | W | W | W | W | W |
| C | W | W | | | |
| U | C,A | C,A | | | |
| V | A | A | | | |

Figure 5.12: EBETS Execution trace: Start of Step 5

For the fifth iteration of the while loop on line 7, the priority queue would be empty. This is the termination condition of the while-loop on line 7. After the the termination of this loop, the next *cur-time* is determined by selecting the earliest of the $t_{min}s$ stored in the path intersection table. This happens to be $t = 3$ for this example (see Figure 5.12). Thus effectively, the algorithm has now determined a sub-interval SPtree with source $W$ valid for times $t = 1$ and $t = 2$. Note that we did not compute the shortest path tree for $t = 2$ separately. The above process of computing a sub-interval SPtree will now repeat for $t = 3$. Before proceeding to the next iteration of the while-loop on line 4, the algorithm re-initializes the predecessor table for times $t = 3$ and greater. After that partial dependencies of all the nodes in this sub-interval SPtree are computed for times $t = 1$ and $t = 2$ using Equation 5.3.

## 5.4 Analytical Evaluation

The EBETS algorithm divides a given interval (over which shortest path trees have to be determined) into a set of disjoint sub-intervals. Within these intervals, the tree does not change. The correctness of EBETS algorithm requires that the set of predecessors determined for any particular node (lines 12-18 of Algorithm 3) be comprehensive. On the other hand, the completeness of the algorithm guarantees that none of the epoch-points are missed. Lemma 8 and Corollary 3 are used to show that the set of predecessors determined by EBETS is comprehensive, i.e., the algorithm records all the potential predecessors of a node while building an sub-interval SPtree. On the other hand, Lemma 7 shows that the EBETS algorithm does not miss any epoch-point. These lemmas are used to prove the correctness and completeness of the EBETS algorithm.

**Lemma 7.** *The EBETS algorithm re-computes the shortest path tree (for any particular node $s \in V$) for all those times $t_i \in \lambda$, where the tree for previous time $t_{i-1}$ can be different from that of $t_i$.*

*Proof.* The shortest path tree of a node $s \in V$ is considered to have changed if the shortest path to any node $t$ (from $s$) in the tree is different across times $t_i$ and $t_{i-1}$ or there is node $w$ outside of tree which is now reachable. For the sake of brevity, we only give the proof for case when the shortest path to a single node $t$ in the tree has changed. This can be easily generalized for case of $w$ and the whole tree.

Consider the network shown in Figure 5.13(a) where a shortest path tree of the node s is to be determined for each time instant in $\lambda = [1, 2 \ldots T]$. In this proof we focus on the shortest path to node $d$ instead of the whole tree. First, the source node is expanded for the time instant $t = 1$. As a result, path functions for all the neighbors <s,u>, <s,$x_1$>, <s,$x_2$>, ... <s,$x_i$> are added to the priority queue. Without loss of generality, assume that the path <s,u> is chosen in the next iteration of the innermost loop. Also assume that the earliest intersection point between <s,u> and the path functions in the priority queue is at $t = \alpha$ (between <s,u> and <s,$x_1$>). After expanding <s,u> the queue would contain paths <s,u,d>, <s,$x_1$>, ..., <s,$x_i$>. Here we can have two cases. First, path <s,u,d> has lower cost for time $t = 1$. Second, path <s,$x_1$> has lower cost for time $t = 1$.

Consider the first case, again without loss of generality assume that the earliest intersection point between the path functions <s,u,d> and <s,$x_1$> is at $t = \beta$. Note that both $t = \alpha$ and $t = \beta$ denote the times at the source node. Now, $\beta \leq \alpha$ (note that $\beta$ cannot be greater than $\alpha$ as all the edges have positive weights). In such a case the shortest path is recomputed for time $t = \beta$ and the path <s,u,d> is closed for all times $1 \leq t < \beta$. Assume for the sake of argument, that there is a shortest path $P_x =< s, x_2, \ldots, d >$ from $s$ to $d$ that is different from path <s,u,d> and is optimal for a time $t_x \in [1, \beta)$. This means that path $< s, x_2 >$ should have had least cost for time $t = t_x$. In other words, the earliest intersection point between functions in the priority queue and $< s, u, d >$ should have been at $t = t_x$ rather than at $t = \beta$ (a contradiction). Moreover, as all the edge costs are positive, if sub path <s,$x_2$> was not shorter than <s,u,d> for times $t \in [1, \beta)$. Any positive weight addition to the path-function (through other edges) cannot make $P_x$ shorter than <s,u,d> for $t \in [1, \beta)$

Now we consider the second case when <s,$x_1$> had lower cost for time $t = 1$. Now, path <s,$x_1$> would be expanded and path function <s,$x_1$,d> would be added to priority queue. A similar argument as above can be given for this case as well. □

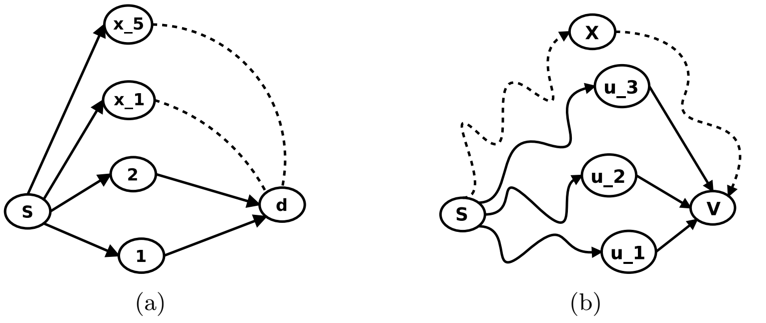

(a)

(b)

Figure 5.13: Sample network for Lemma 7 and Lemma 8

**Corollary 2.** *The EBETS algorithm correctly computes the shortest path tree (for any particular node $s \in V$) for any particular time instant $t \in \lambda$.*

**Lemma 8.** *The set of predecessors determined for a node $v$ for a time $t \in \lambda$ is complete.*

*Proof.* Let $P(v) = P_{u_1}(v), P_{u_2}(v), P_{u_2}(v), \ldots, P_{u_k}(v)$ denote the set of paths currently in the priority queue whose tail node is $v$. Here, $P_{u_i}$, where $i \in [1, k]$, denotes the path whose second-to-last node is $u_i$ (and last node being $v$) and $cost(P_{u_i}(v))$ denotes the cost of path $P_{u_i}(v)$ for time $t = \alpha$. Without loss of generality assume that the node $v$ is being closed for time $t = \alpha$ (see Figure 5.13(b)) through the path $P_{u_1}$, i.e., $P_{u_1}$ is found to be a shortest path for node $v$. Now, the EBETS algorithm assigns a node $u_x$ as a predecessor of node $v$ based on the following cases;

**Case 1:** $u_x$ is the second-to-last node in the shortest path found, i.e., $u_x = u_1$.
**Case 2:** $u_x \in U$, where $U = \{u_i | cost(P_{u_i}(v)) = cost(P_{u_1}(v)) \& i \neq 1\}$.

In order to prove the lemma, we show that the above two cases are correct and complete. We first show the correctness followed by completeness. Using Corollary 2 we know that when a node $v$ is closed by the EBETS algorithm for any particular time $t$, it has correctly determined the shortest path for $v$. Therefore, the node preceding $v$ in this path is clearly a predecessor of time $t$. This proves the correctness of Case 1. Correctness of Case 2 can be also guaranteed in similar fashion as we include the second-to-last nodes of only those paths whose cost is same as that of the shortest path found by EBETS.

In order to show the completeness, we need to prove that there cannot be any other path $Q$, not currently in the priority queue, with $cost(Q) = cost(P_{u_1})$. For sake of argument assume that there exists a path $Q =< s, \ldots, x, v >$, not currently in $TDPQ$, and $x$ is valid predecessor of $v$ for time $t = \alpha$. By definition the distance of $x$ from $s$ should be less than that of $v$ (as we have only positive weights). This means that node $x$ should be closed before $v$. Now, whenever a node is closed by the algorithm, path functions corresponding to its neighbors are added to the priority queue. This contradicts our original assumption that path $Q$ was not present in the priority queue. □

**Corollary 3.** *The set of predecessors determined for a node $v$ for all times $t \in \lambda$ is complete.*

*Proof.* Using Lemma 7, we know that EBETS does not miss any epoch point. Now, during the time interval between two consecutive epoch-points, Lemma 8 can be used to conclude that the predecessors are correctly determined for all time time instants within the interval. Using these two arguments we can conclude that EBETS correctly determines the predecessors of a node $v$ for all times $t \in \lambda$. □

**Theorem 4.** *EBETS algorithm is correct and complete.*

*Proof.* For any particular node $v$, there can be several sub-interval SPtrees, $SPT_v = \{SPT_v^1, SPT_v^2, \ldots, SPT_v^k\}$, over the $\lambda$, where each $SPT_v^i$ is associated with a set of time instants $\omega_v^i$ and $\bigcup_{\forall i \in |SPT_v|} \omega_v^i \;=\; \lambda$. The correctness of the algorithm is shown by Lemma 8 and Corollary 3. The completeness proof is presented in three parts. First, using Lemma 7 we can conclude that the EBETS algorithm does not miss any epoch point. Secondly, the loop on line 4 of the algorithm ensures that all time instants in $\lambda$ are considered. Finally, the outer most loop on line 1 ensures that all the nodes $v \in V$ are processed. This proves the completeness of the algorithm.

□

**Discussion:** The EBETS algorithm would perform less computation than a naive approach which determines the shortest path tree of a node for each time in the user specified time interval $\lambda$. However, this happens only when the ratio of the number of epoch-points to that of time instants in $\lambda$ is low. This ratio can be denoted as the change probability shown by Equation 5.4.

$$change\_probability = \frac{\#epoch\ points}{\#time\ instants\ in\ \lambda} \tag{5.4}$$

When the change probability is nearly 1, there would be a different shortest path tree (of a node) for each time in the interval $\lambda$. In this worst case scenario, the EBETS approach would also have to recompute the shortest path tree for each time.

## 5.5 Experimental Evaluation

The overall goal of experimental evaluation was to characterize the performance of epoch-point based betweenness centrality algorithms. To this end, the performance of EBETS algorithm was compared against a baseline algorithm which involved computing the shortest path tree for each time in the given time interval of interest (input parameter $\lambda$). For comparison, both algorithms computed the temporal extension of

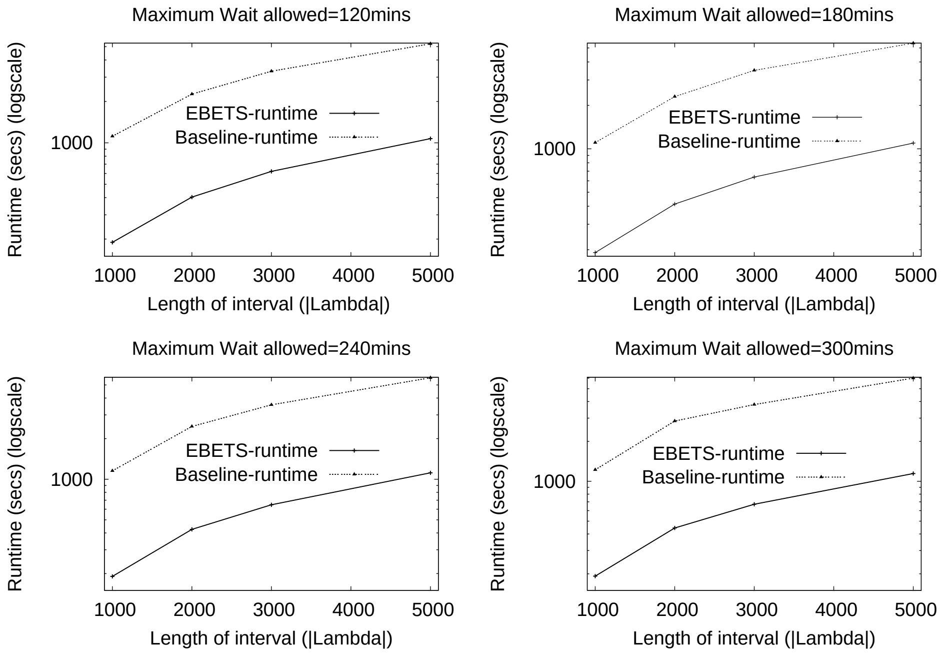

Figure 5.14: Effect of length of time interval ($|\lambda|$).

betweenness centrality given in Equation 5.1 and followed the temporal shortest path definition given in Definition 3. Both EBETS and the baseline algorithms were implemented in C++ language. The experiments were carried out on a real dataset containing email communications spread over 83 days in early 2004 from a large European university. This dataset recorded about 161227 email communications among approximately 2000 individuals. Events in this dataset (email communications) were recorded in the following format: $<A,B,t>$, where $A$ and $B$ are two individuals in the University and $t$ denotes the time-stamp (in minutes) of the interaction. Experiments were carried out on a Linux workstation with Intel Xeon Processor and 8GB RAM.

The first step of the experimental evaluation involved creating a time aggregated graph out of the social event data. Since the dataset contained emails communications, these translated into directed edges in the time aggregated graph. Then, a set of different queries (each with a different set of parameters) was run on the EBETS and the baseline algorithm. The following parameters were varied in the experiments: (a) $|\lambda|$: Length of the time interval over which the centrality metric was computed, (b) Network size, and (a) Maximum wait allowed. In each of the experiments the total execution time of both the algorithms was recorded.

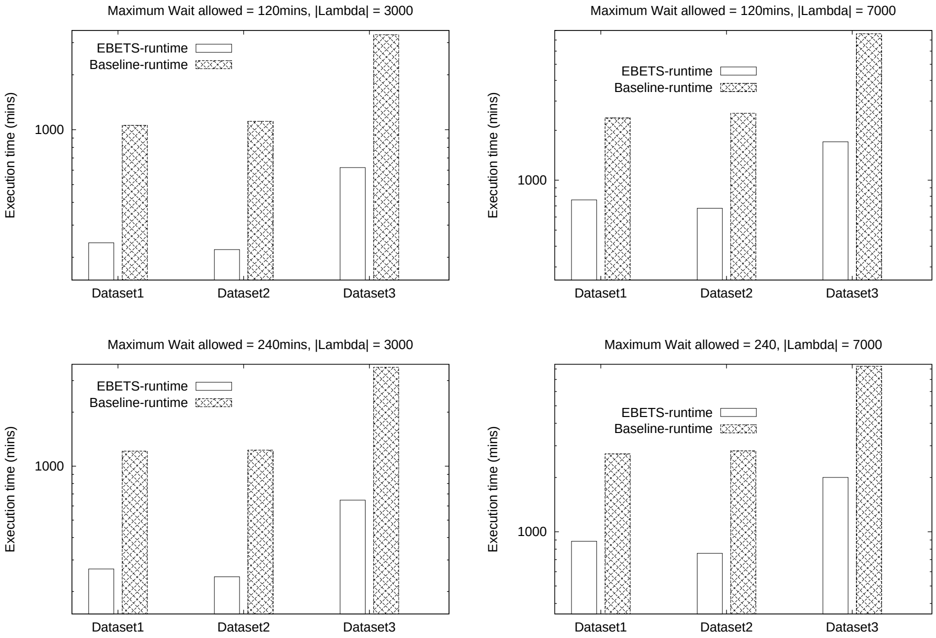

Figure 5.15: Effect of Network size.

**Effect of Length of time interval ($|\lambda|$):** This experiment evaluated the effect of length of time interval ($\lambda$) on the candidate algorithms. The results, shown in Figure 5.14, indicate that execution time of both the algorithms increased linearly with increase in $|\lambda|$. However, for any particular value of $|\lambda|$ and maximum allowed wait, EBETS was faster than the baseline by an order of magnitude.

**Effect of Network size:** We tested the algorithms on three different size networks. To create the networks, we removed some nodes and their edges from our original dataset (referred to as Dataset3) to created two smaller datasets called Dataset1 and Dataset2. Dataset1 had 1095 nodes and 18000 edges, whereas Dataset2 had 1300 nodes and 21000 edges. In both the smaller datasets the length of the time series was approximately

100,000. The algorithms were tested on all the three datasets. We also varied the maximum wait allowed and length of lambda. Figure 5.15 shows the effect of the Network size on the performance of the algorithms. As can be seen the execution of time of both the algorithms increased with the increase in network size, but EBETS still outperforms the baseline.

**Effect of Maximum Wait allowed:** We also tested the effect of increasing the *maximum wait allowed* parameter on the candidate algorithms. As shown in Figure 5.16, run-time for both the algorithms increased with a longer waits. However, run-time of EBETS increased at a slower rate than that of baseline algorithm. Moreover, for any particular value of maximum allowed wait parameter, the EBETS algorithm was faster than the baseline algorithm by several orders of magnitude.

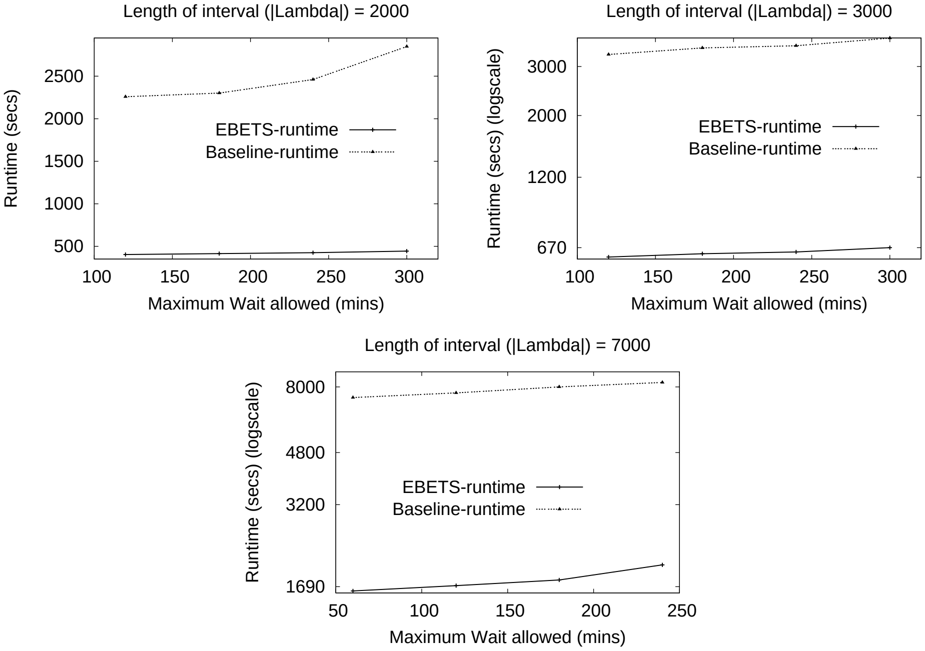

Figure 5.16: Effect Maximum Wait allowed for $|\lambda| = \{2000, 3000, 7000\}$.

## 5.6 Temporal Betweenness Centrality vs Traditional Betweennness Centrality

In this section, we present an empirical comparison of temporal betweenness centrality (Equation 5.1) based on temporal shortest paths (Definition 3) against the traditional betweenness centrality computed on aggregated snapshots. The data we use in this study is a set of email communications spread over eighty three days in early 2004 from a large European university. The dataset has been used in several previous studies [76–79], with a focus on both the prevalence of dynamic triads [76] and on characterizing the inter event dynamics of users (i.e. the time between two consecutive email sends) [77–79]. Though we will utilize findings from these works extensively, it is important to note that this dataset does contain several nodes which appear to be mail servers as well as several people who do not communicate often enough (as also noted in [76–78]). We choose to remove such nodes from the study.

**How does temporal betweenness centrality compare with the traditional betweenness centrality calculated on aggregated panels?**

[76] notes, when studying the data utilized in this case study, that “temporal dynamics create coherent space-time structures that...will in general be very different from the fixed ones that appear in the static network”. However, [76] is in this quote referring to the network created by aggregating all the events into a single panel, i.e., the network comprised of all eighty three days of interaction data. In contrast, our interest here is in comparing the results of temporal betweenness centrality (based on temporal shortest paths) to the traditional betweenness centrality computed over panels obtained by aggregating over shorter time intervals.

One disadvantage to our approach is that, while it is straightforward to determine which agent is the most central at any given time instant (a minute, in this case study), it is not immediately obvious how one should determine which agent is the most central over an entire time interval. This is because at each time instant, all agents may be on some number of temporal shortest paths, and thus have some non-zero betweenness centrality score. Therefore, if we wish to determine which agent was the most central on a given day, we must somehow aggregate over all temporal betweenness values, for all agents, for each minute in that day. Though our approach was not geared towards such an cumulative notion of centrality, a quantitative comparison between our method and the aggregated panel is necessary and thus some calculation of the ranks of different agents for betweenness over a given aggregation must be computed.

The manner in which we choose to do this is used for its simplicity and explainability, though others no doubt exist which may be more powerful along one or both of these dimensions. In order to determine which agent is most central over a given period of interval, we first determine the most central agent (i.e. the one with the highest temporal betweenness score) at each time instant (minute), and then aggregate over the desired time period (e.g. a day) to produce a count, for each agent, of the number of time instants he/she was most central for. The rank of a node (e.g. most central, second most central, etc.) for the given time interval is then determined by his or her rank in this list of counts.

Before we can compare to some betweenness metric on aggregated panels of the network, we must also determine what representation of the network each panel will have. [80] considers different meanings of an edge in an email network, including removing mass emails to get a more social view of the network. Here, because we consider betweenness as an information flow metric, we choose to keep mass emails in the data. On a different note, [77] sees that most users receive more emails than they send, suggesting further that, of course, agents thus receive far more emails than they respond to. This finding suggests email communication may be particularly susceptible to differences in directed versus undirected measures of betweenness, and hence we use a directed approach in order to compare best with our algorithm.

Having operationalized the notion of an agent being “most central” over any given time interval across both methods, we now may compare the results of our metric with the traditional betweenness centrality on aggregated panel. We compare across five different levels of aggregation: one hour, two hours, ten hours, one day and three days. In full, the process for comparing the metric at a single level of aggregation (e.g. a day) can be described in three steps. We first aggregate the interaction data into panels and then compute the traditional *weighted, directed* betweenness centrality [81,82] for agents in each using the igraph package in R [83]. Note of this step, the traditional betweenness centrality would ignore the the temporal order of interactions on the edges. We then use the method described in Section 5.3 to compute the centrality of each agent within the time-aggregated graph representation of each of the panels for the temporal betweenness centrality metric (we consider the temporal order here). Finally, we utilize one of three comparison metrics, first introduced by [84] and later used by [85], to compare agreement between the two approaches for each set of aggregated interactions.

The three comparison metrics we use are “Top 1”, “Top 3” and “Top 10%” (the original names provided by [84]. “Top 1” refers to the percentage of panels over which the most central node is the same across both techniques. “Top 3” refers to the percentage of panels that the top node using the traditional approach on aggregated panel is one of the top three nodes utilizing our metric. “Top 10%” refers, similarly, to the percentage of panels in which the top node in the traditional approach on aggregated panel approach is one of those in the top ten percent using our metric. We choose these metrics over other similar metrics [86] because they are straightforward to understand while still providing depth for intuition. In collecting results, we only consider as input those panels where at least one node was central using both approaches and where there were no ties as to the most central node in the aggregated panel network. It is also important to note that at lower maximum allowed wait values and aggregations, because often less than 30 nodes have some non-zero centrality value, our results suggest the counter-intuitive finding that in some cases, “Top 3” shows a higher percentage of agreement across the two algorithms than “Top 10%”. Also, because larger aggregation levels naturally have fewer data points, the reader will notice that confidence intervals surrounding the point estimates for these metrics naturally increase with aggregation.

Figure 5.17 shows the results for each of the three comparison metrics, where points represent the point estimate and error bars give the 95% confidence intervals using Wilson’s formula [87]. The figure plots of the percentage of aggregation sets (on Y axis) where the most central agent according to traditional betweenness centrality is in the top one (top set of plots), top three (middle set) or top 10% (bottom set) of most central agents using temporal betweenness centrality. The values on the X-axis represent different maximum allowed wait values our algorithm was run with, while the values in the grey bars above each graph represent the level of aggregation, in minutes, over which the interactions were split. In considering the “Top 1” and “Top 3” metrics (the

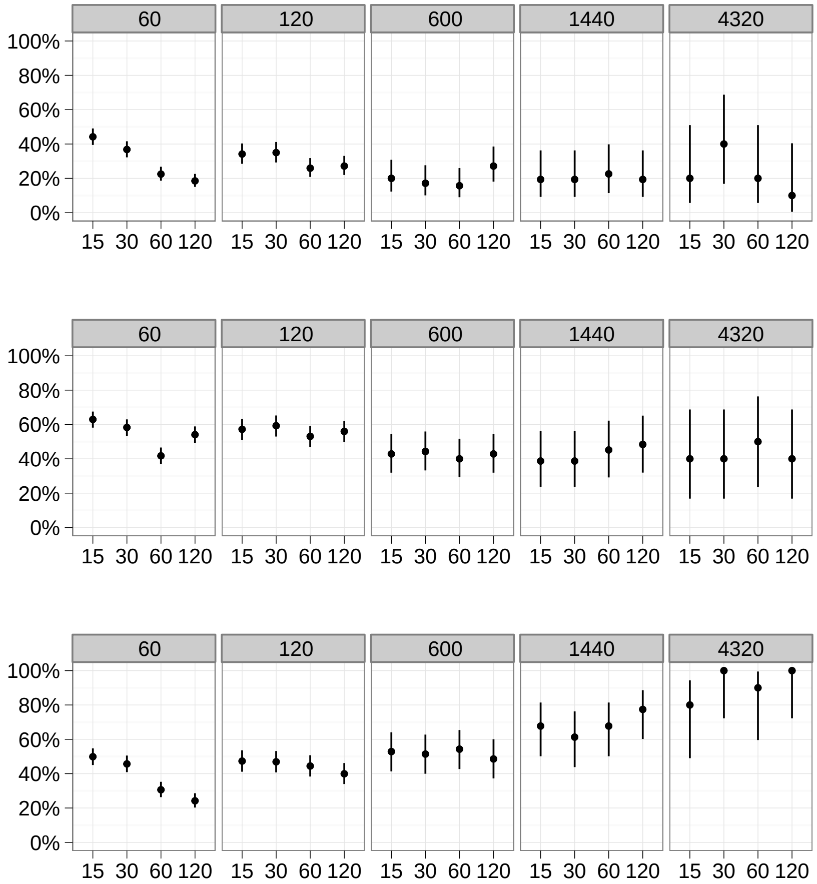

Figure 5.17: Traditional betweenness centrality vs Temporal betweenness centrality.

top two plots), we see that although there is reasonably high variance across individual combinations of maximum allowed wait and aggregation level, there are several general patterns. First, agreement between the two methods is slightly higher at lower levels of aggregation. This finding is not particularly surprising; at lower levels of aggregation, there are fewer emails and less time to be aggregated over; resulting in fewer invalid temporal paths and fewer unrealistic durations for which information is held at a given node. However, at these levels, we do see that higher maximum allowed wait values have much lower levels of agreement. This, also, has a fairly obvious explanation in that these values consider data far outside the boundaries of the aggregation, and thus will likely present different pictures of the network. This explanation is further supported by the fact that this difference appears to slow at higher levels of aggregation.

Figure 5.17 thus suggests following conclusions. First, the agreement between the two metrics on the most central nodes (Top 1 comparison metric) is not more than 60%. Second, there is very high agreement between the two metrics in case of Top 10% over long periods of aggregation. This shows that temporal betweenness centrality does measure something which does not entirely agree with what is being measured by the traditional betweenness centrality. In other words, these results do show an inclination towards the fact time agnostic based techniques may consider paths which are not feasible for information flow.

## 5.7 Conclusion

Temporally-detailed Social network Analytics (TDSNA) has value addition potential due to its potential to answer time-aware questions about the underlying social system, e.g., “How is the betweenness centrality of an individual changing over time?” However, designing scalable algorithms for TDSNA is challenging because of the non-stationary ranking of shortest path between any two nodes in a TD social network. This non-stationary ranking violates the assumptions of dynamic programming underlying the common shortest path algorithms such as Dijkstra’s used by current techniques. To this end, we proposed the concept of epoch-point based approaches which divide the given time interval–over which observe non-stationarity–into a set of disjoint time intervals which show stationary ranking. Based on the concept of epoch-points, we developed a novel algorithm, called EBETS, for computing the temporal extension of betweenness centrality. EBETS saves computation over the baseline algorithm which re-computes the solution for every time instant. Experimental evaluation showed that EBETS out performs the baseline algorithm. In future, we plan to extend our concept of epoch-based algorithms to adapt floyd warshall’s algorithm for all-pair shortest paths. This would be useful in developing more scalable algorithms for temporal extensions of closeness centrality. We also plan to extend our approach to centrality metrics in multiplex networks and networks where interaction among a group of people are recorded through hyperedges.

# Chapter 6

# Conclusions and Future Directions

This chapter presents a summary of results obtained in this thesis followed by a brief discussion on potential future directions.

## 6.1 Summary of results

Big Temporally-Detailed Graph (Big-TDG) data is an emerging trend. Sample Big-TDG data such as temporally-detailed (TD) roadmaps have value-adding potential is societal use-cases such as eco-routing. Likewise, TD social networks could help in answering time-aware questions on the underlying social system (e.g, "How is the betweenness centrality of an individual changing over time?"). However, both TD roadmaps and TD social networks pose challenges to the state of the art in computer science. TD roadmaps capture several properties of n-ary relations which cannot be completely decomposed into properties of binary relations without losing its semantic value. This challenge was formulated as follows:

- Given emerging diverse spatio temporal network (STN) datasets, e.g., GPS tracks, temporally detailed roadmaps and traffic signal data, the aim was to develop a data-model which achieves a seamless integration of these datasets for routing related use-cases (queries) and supports efficient algorithms. This problem is important for travel itinerary comparison and navigation applications. However, this was challenging due to the conflicting requirements of expressive power and computational efficiency as well as the need to support ever more diverse STN datasets, which now record non-decomposable properties of n-ary relations. Examples include travel-time and fuel-use during a journey on a route with a sequence of coordinated traffic signals and turn delays. Current data models for STN datasets are limited to representing properties only of binary relations, e.g., distance on individual road segments. In contrast, Chapter 2 proposed a novel data-model, called Lagrangian Xgraphs, which can express properties of both binary and n-ary relations. Initial study shows that Lagrangian Xgraphs are more convenient for representing diverse STN datasets and comparing candidate travel itineraries.

Both TD roadmaps and TD social networks show non-stationary ranking of alternate candidate paths across different time points. In other words, the shortest path between any two nodes in a TD roadmap or a TD social network changes with time. In a TD roadmap this variation is due to changing traffic congestion across rush and non-rush hours; in a TD social network it is caused due to variation in activity levels of individuals. This non-stationary ranking of alternate candidate paths violates the assumptions of dynamic programming shortest path algorithms such as Dijkstra's algorithm. This challenge was formulated through the following:

- Given a spatio-temporal network, a source, a destination, and a desired departure time interval, the All-departure-time Lagrangian Shortest Paths (ALSP) problem determines a set which includes the shortest path for every departure time in the given interval. ALSP is important for critical societal applications such as eco-routing. However, ALSP is computationally challenging due to the non-stationary ranking of the candidate paths across distinct departure-times. Current related work for reducing redundant computation across consecutive departure-times sharing a common solution exploits only partial information e.g., the earliest feasible arrival time of a path. In contrast, our approach uses all available information, e.g., the entire time series of arrival times for all departure-times. This allows elimination of all knowable redundant computation based on complete information available at hand. This idea was operationalized through the concept of critical-time-points (CTP), i.e., departure-times before which ranking among candidate paths cannot change. Chapter 3 proposed a CTP based forward search strategy, and Chapter 4 proposed a CTP based temporal bi-directional search for the ALSP problem via a novel impromptu rendezvous termination condition. Theoretical and experimental analysis showed that the proposed approach outperforms the related work approaches particularly when there are few critical-time-points.

- The increasing proliferation of mobile and online social networking platforms has given us unprecedented opportunity to observe and study social interactions at a fine temporal scale. A collection of all such social interactions among a group of individuals (or agents) observed over an interval of time is referred to as a temporally-detailed (TD) social network. TD social networks open up the opportunity to explore temporally-detailed questions on the underlying social system, e.g., "How is the betweenness centrality of an individual changing with time?" To this end, related work has proposed temporal extensions of centrality metrics (e.g., betweenness and closeness). However, scalable computation of these metrics for long time-intervals is challenging. This is due to the non-stationary ranking of shortest paths (the underlying structure of betweenness and closeness) between a pair of nodes which violates the assumptions of classical dynamic programming based techniques. To this end, Chapter 5 proposed a novel computational paradigm called epoch-point based techniques for addressing the non-stationarity challenge in a TD social network. Using the concept of epoch-points, this chapter proposed a novel algorithm for computing shortest path based centrality metric such as betweenness on a TD social network. Correctness and completeness of the proposed algorithm were established. Experimental analysis showed that the proposed algorithm outperforms the alternative by a wide margin.

## 6.2 Potential future research directions

Table 6.1 lists the current literature for shortest path and betweenness centrality algorithms in the area of temporal-detailed graphs (second column), contributions made by this thesis (third column) and a few potential future directions (last column) which are

| | Current Literature | Thesis Contributions | Future Reserach Directions |
|---|---|---|---|
| Conceptual | Time aggregated graphs [9--14] and Time expanded graphs [13,15] | Lagrangian Xgraphs | Data-models for engine measurements. |
| | Frame of reference: Eulerian | Frame of reference: Lagrangian | |
| Logical | | | Logical model for querying Big-TDG data |
| Physical | Algorithms for single start time Shortest path [15--28] on a TD roadmap | Algorithms for all start-time shortest paths on a TD roadmap | Generalize CTP based approaches to other DP problems |
| | Algorithms for a single time-point betweenness centrality [13, 14, 29, 30]) on a TD social network | Betweenness centrality over a time-interval in a TD social network | |

Table 6.1: Potential future directions of this thesis.

briefly described next.

*Conceptual models for vehicular engine measurements:* Sensors on vehicular engines are making it possible to collect data on their performance as they move through a real-world transportation network. These datasets consist of a sequence of space-time locations on a route (via map-matched GPS points) annotated with multiple engine sub-system measurements like engine speed in revolutions per minute, fueling rate, vehicle speed, throttle position, intake air temperature, etc [88]. As a first step towards developing algorithms for analytics on this data, we need to construct a conceptual representation model of this data which expresses the required features (e.g. engine science concepts) upfront for engine related use-case queries. The goal here would be to explore the trade-off between representational convenience (e.g. brevity) and computational scalability in defining a data-model. One could investigate research questions like: How many physical dimensions (e.g. geographic locations, speed, and acceleration) should be modeled explicitly in the model? Should we allow the edge properties to be discrete-value or a continuous function? etc.

*Logical model for querying on Big-TDG data:* The goal would be to design a minimal set of datatypes and operations to concisely represent common Big-TDG data queries and support traversal of the graph. This task is challenging due to the conflicting goals of concise representation and support for computationally efficient algorithms. Table 2.1 in Chapter 2 presented a set of preliminary operations, but several research questions remain unanswered. For instance, is the set of proposed Lagrangian Xgraph data-types and operations (Table 2.1 in Chapter 2) closed, i.e., can operation results be represented within the set? Is this set expressive enough to represent spatio-temporal routing queries about a traveler's experience relevant to eco-routing? Does it facilitate in design of computationally efficient algorithms? How should the set be refined to address the conflicting needs of expressive power and support for efficient algorithms?

*Generalize critical-time-points to a broader set of DP problems:* Critical-time-points (CTPs) could be investigated for their generalizability in a larger set of computational problems. For illustration, consider the All-pair All start-time Lagrangian Shortest path Problem (AALSP). Given a temporally-detailed roadmap and a departure-time interval, the AALSP problem determines a route collection which includes the shortest path, for every departure-time in the given interval, for every possible (start, destination) pair. CTP may adapt the traditional All-pair Shortest Path (ASP) algorithms (e.g., Floyd Warshall's, Johnson's) to reduce redundant computation across departure-times sharing a common solution. However, this task is much harder than adapting Dijkstra's algorithm for ALSP, since we do not know the departure-times for the sub-paths being combined in the recurrence step. This issue invalidates even a naive approach of invoking the ASP algorithm for all distinct departure-times. The applicability of CTP based approaches could be further investigated for other dynamic programming use-cases such as maximum likelihood decoding techniques (e.g. Viterbi algorithm) for hidden Markov models, optimal policy determination techniques for Markov decision processes (e.g. Value iteration algorithm for finite horizon problems), and Selinger's algorithm for query optimization and other discrete-time optimization problems.

# References

[1] Peter Koonce and et al. Traffic signal timing manual. Technical Report FHWA-HOP-08-024, US Dept of Trans. Federal Higway Admin., June 2008.

[2] Bing maps. http://www.bing.com/maps/.

[3] Bolin Ding, Jeffrey Xu Yu, and Lu Qin. Finding time-dependent shortest paths over large graphs. In *Proc. of the Intl. Conf. on Extending database technology (EDBT)*, pages 205–216, 2008.

[4] J. Manyika et al. Big data: The next frontier for innovation, competition and productivity. McKinsey Global Institute `http://goo.gl/AA8DS`, May 2011.

[5] Shashi Shekhar, Viswanath Gunturi, Michael R. Evans, and KwangSoo Yang. Spatial big-data challenges intersecting mobility and cloud computing. In *MobiDE*, pages 1–6. ACM, 2012.

[6] A Community Whitepaper resulting from the 2012 Spatial Computing 2020 Workshop funded by the Computing Community Consortium. From gps and virtual globes to spatial computing - 2020: The next transformative technology. `www.cra.org/ccc/visioning/visioning-activities/spatial-computing`.

[7] J. Lovell. Left-hand-turn elimination. NY Times, December 9th, 2007.

[8] Us energy information administration. http://www.eia.gov/totalenergy/data/monthly/.

[9] Betsy George and Shashi Shekhar. Time-aggregated graphs for modeling spatio-temporal networks. *J. Data Semantics*, 11:191–212, 2006.

[10] Erik G. Hoel, Wee-Liang Heng, and Dale Honeycutt. High performance multimodal networks. In *Advances in Spatial and Temporal Databases*, volume 3633 of *LNCS*, 2005.

[11] Ralf Hartmut Güting. Graphdb: Modeling and querying graphs in databases. In *Proc. of the 20th International Conference on Very Large Data Bases*, pages 297–308, 1994.

[12] Betsy George and Shashi Shekhar. Modeling spatio-temporal network computations: A summary of results. In *GeoSpatial Semantics, Second International Conference, GeoS 2007, Mexico City, Mexico, November 29-30, 2007, Proceedings*, pages 177–194. Springer. LNCS 4605.

[13] Hyoungshick Kim and Ross Anderson. Temporal node centrality in complex networks. *Physcial Review E*, 85(2), 2012.

[14] Habiba, Chayant Tantipathananandh, and Tanya Y. Berger-Wolf. Betweenness centrality measure in dynamic networks. Technical Report 2007-19, Center for Discrete Mathematics and Theoretical Computer Science, 2007.

[15] Ekkehard Khler, Katharina Langkau, and Martin Skutella. Time-expanded graphs for flow-dependent transit times. In *Algorithms  ESA 2002*, volume 2461, pages 49–56. 2002.

[16] Betsy George, Sangho Kim, and Shashi Shekhar. Spatio-temporal network databases and routing algorithms: A summary of results. In *Symposium on Spatial and Temporal Databases (SSTD)*, pages 460–477, 2007.

[17] Ugur Demiryurek, Farnoush Banaei-Kashani, Cyrus Shahabi, and Anand Ranganathan. Online computation of fastest path in time-dependent spatial networks. In *Proc. of the 12th intl. conf. on Advances in spatial and temporal databases*, SSTD'11, pages 92–111. Springer-Verlag, 2011.

[18] Daniel Delling and Dorothea Wagner. Landmark-based routing in dynamic graphs. In *Experimental Algorithms*, pages 52–65. Springer Berlin Heidelberg, 2007.

[19] Daniel Delling. Time-dependent sharc-routing. In *Proc. of the 16th annual European symposium on Algorithms*, pages 332–343, 2008.

[20] Daniel Delling and Dorothea Wagner. Time-dependent route planning. In *Robust and Online Large-Scale Optimization*, volume 5868 of *Lecture Notes in Computer Science*, pages 207–230. Springer Berlin Heidelberg, 2009.

[21] Ismail Chabini and Shan Lan. Adaptations of the a* algorithm for the computation of fastest paths in deterministic discrete-time dynamic networks. *IEEE Trans. on Intel. Trans. Systems*, 3(1):60–74, 2002.

[22] Ariel Orda and Raphael Rom. Shortest-path and minimum-delay algorithms in networks with time-dependent edge-length. *J. ACM*, 37(3):607–625, July 1990.

[23] Giacomo Nannicini, Daniel Delling, Dominik Schultes, and Leo Liberti. Bidirectional a* search on time-dependent road networks. *Networks*, 59(2):240–251, 2012.

[24] Giacomo Nannicini, Daniel Delling, Leo Liberti, and Dominik Schultes. Bidirectional a* search for time-dependent fast paths. In *Experimental Algorithms*, pages 334–346. Springer Berlin Heidelberg, 2008.

[25] Daniel Delling and Giacomo Nannicini. Bidirectional core-based routing in dynamic time-dependent road networks. In *Algorithms and Computation*, pages 812–823, 2008.

[26] Giacomo Nannicini. Point-to-point shortest paths on dynamic time-dependent road networks. *4OR*, 8(3):327–330, 2010.

[27] Ugur Demiryurek, Farnoush Kashani, and Cyrus Shahabi. A case for time-dependent shortest path computation in spatial networks. In *Proc. of the SIGSPATIAL Intl. Conf. on Advances in GIS*, GIS '10, pages 474–477, 2010.

[28] Jing Yuan and et. al. T-drive: driving directions based on taxi trajectories. In *Proc. of the ACM SIGSPATIAL*, pages 99–108, 2010.

[29] John Tang, Mirco Musolesi, Cecilia Mascolo, Vito Latora, and Vincenzo Nicosia. Analysing information flows and key mediators through temporal centrality metrics. In *Proceedings of the 3rd Workshop on Social Network Systems*, SNS '10, pages 3:1–3:6, 2010.

[30] John Tang, Mirco Musolesi, Cecilia Mascolo, and Vito Latora. Temporal distance metrics for social network analysis. In *Proceedings of the 2Nd ACM Workshop on Online Social Networks*, WOSN '09, pages 31–36, New York, NY, USA, 2009. ACM.

[31] KwangSoo Yang, M.R. Evans, V.M.V. Gunturi, J.M. Kang, and S. Shekhar. Lagrangian approaches to storage of spatio-temporal network datasets. *Knowledge and Data Engineering, IEEE Transactions on*, 26(9):2222–2236, 2014.

[32] Dan Sha and C. K. Wong. *Time-Varying Network Optimization*. International Series in Operations Research and Management Science, Vol. 103, Springer, 2007.

[33] VenkataM.V. Gunturi and Shashi Shekhar. Lagrangian xgraphs: A logical data-model for spatio-temporal network data: A summary. In Marta Indulska and Sandeep Purao, editors, *Advances in Conceptual Modeling*, volume 8823 of *Lecture Notes in Computer Science*, pages 201–211. Springer International Publishing, 2014.

[34] Venkata M. V. Gunturi, Ernesto Nunes, KwangSoo Yang, and Shashi Shekhar. A critical-time-point approach to all-start-time lagrangian shortest paths: a summary of results. In *Proc. of 12th intl. conf. on Adv. in spatial and temporal databases*, pages 74–91, 2011.

[35] Venkata M. V. Gunturi and et. al. A critical-time-point approach to all-start-time lagrangian shortest paths. *Accepted in IEEE Transactions on Knowledge and Data Engineering*, 2015.

[36] Henry Liu and Heng Hu. Smart-signal phase ii: Arterial offset optimization using archived high-resolution traffic signal data. Technical Report CTS 13-19, Intel. Trans. Sys. Inst., Center for Transportation Studies, Univ. of Minnesota, Apr-2013.

[37] B. George and S. Shekhar. Time-aggregated graphs for modelling spatio-temporal networks. *J. Semantics of Data*, XI:191, 2007.

[38] Yu Zheng and Xiaofang (Eds.) Zhou, editors. *Computing with Spatial Trajectories.* Springer, 2011.

[39] Shashi Shekhar and et al. Spatial pictogram enhanced conceptual data models and their translation to logical data models. In *Intl. Works. on Integrated Spatial Databases, Digital Inages and GIS*, pages 77–104. Springer-Verlag, 1999.

[40] Yvan Bedard. Visual modeling of spatial databases: Towards spatial PVL and UML. *Geoinformatica*, 53(2), 1999.

[41] Shashi Shekhar and et al. Data models in geographic information systems. *Commun. ACM*, 40(4), April 1997.

[42] G.K. Batchelor. *An introduction to fluid dynamics.* Cambridge Univ. Press, 1973.

[43] Christine Parent and et al. Spatio-temporal conceptual models: Data structures + space + time. In *Proc. of the Intl. Symp. on Adv. in GIS*, pages 26–33. ACM, 1999.

[44] Erlend Tssebro and Mads Nygrd. Representing topological relationships for spatiotemporal objects. *GeoInformatica Springer US*, 15(4):633–661, 2011.

[45] Renato Fileto and et al. Baquara: A holistic ontological framework for movement analysis using linked data. In *Conceptual Modeling*, pages 342–355. Springer, 2013.

[46] G. Gallo, G. Longo, S. Pallottino, and S. Nguyen. Directed hypergraphs and applications. *Elsevier, Discrete applied mathematics*, 42(2):177–201, 1993.

[47] C. Berge. *Graphs and Hypergraphs.* Elsevier Science Ltd, 1985.

[48] Michael R. Evans and et. al. A lagrangian approach for storage of spatio-temporal network datasets: a summary of results. In *Proc. of the ACM SIGSPATIAL*, pages 212–221, 2010.

[49] Delta airlines. http://www.delta.com/.

[50] C.H. Deutsch. Ups embraces high-tech delivery methods. NY Times, July 12, 2007.

[51] Evangelos Kanoulas, Yang Du, Tian Xia, and Donghui Zhang. Finding fastest paths on a road network with speed patterns. In *Proc. of the 22nd Intl. Conf. on Data Engineering (ICDE)*, page 10, 2006.

[52] Jon Kleinberg and Eva Tardos. *Algorithm Design*. Pearson Education, 2009.

[53] David E. Kaufman and Robert L. Smith. Fastest paths in time-dependent networks for intelligent vehicle-highway systems application. *I V H S Journal*, 1(1):1–11, 1993.

[54] B. George, S. Shekhar, and S. Kim. Spatio-temporal network databases and routing algorithms. Technical Report 08-039, Univ. of Minnesota - Comp. Sci. and Engg., 2008.

[55] Viswanath Gunturi, Shashi Shekhar, and Arnab Bhattacharya. Minimum spanning tree on spatio-temporal networks. In *Proc. of the 21st Intl. Conf. on Database and expert systems applications: Part II*, DEXA'10, pages 149–158, 2010.

[56] Navteq. http://www.navteq.com/.

[57] Lívia A. Cruz, Mario A. Nascimento, and José Antônio Fernandes de Macêdo. k-nearest neighbors queries in time-dependent road networks. *JIDM*, 3(3):211–226, 2012.

[58] Ugur Demiryurek, Farnoush Banaei-Kashani, and Cyrus Shahabi. Efficient k-nearest neighbor search in time-dependent spatial networks. In *Proc. 21st Intl. Conf. on Database and Expert Systems Applications: Part I*, pages 432–449, 2010.

[59] Luca Foschini, John Hershberger, and Subhash Suri. On the complexity of time-dependent shortest paths. In *SODA*, pages 327–341, 2011.

[60] Openstreetmap. http://www.openstreetmap.org/.

[61] Daniel Delling and et. al. Phast: Hardware-accelerated shortest path trees. *Journal of Parallel and Distributed Computing*, 73(7):940 – 952, 2013.

[62] Hyoungshick Kim, John Tang, Ross Anderson, and Cecilia Mascolo. Centrality prediction in dynamic human contact networks. *Computer Networks*, 56(3):983 – 996, 2012.

[63] S. Russel and P. Norwig. *Artificial Intelligence: A Morden Approach*. Prentice-Hall, Upper Saddle River, NJ, 1995.

[64] Dimitri P. Bertsekas. *Dynamic Programming: Deterministic and Stochastic Models*. Prentice-Hall, Englewood Cliffs, NJ, 1987.

[65] Dan Braha and Yaneer Bar-Yam. From centrality to temporary fame: Dynamic centrality in complex networks. *Complexity*, 12(2):59–63, 2006.

[66] Jean-Pierre Eckmann, Elisha Moses, and Danilo Sergi. Entropy of dialogues creates coherent structures in e-mail traffic. *Proceedings of National Academy of Sciences (2004)*, 101(40), 143330–14337.

[67] Gueorgi Kossinets and Duncan J. Watts. Empirical analysis of an evolving social network. *Science*, 311(5757), 2006.

[68] R. Nia, C. Bird, P. Devanbu, and V. Filkov. Validity of network analyses in open source projects. In *2010 7th IEEE Working Conference on Mining Software Repositories (MSR)*, pages 201–209, May 2010.

[69] James Howison, Andrea Wiggins, and Kevin Crowston. Validity issues in the use of social network analysis with digital trace data. *Journal of the Association for Information Systems*, 12(12), December 2011.

[70] Gueorgi Kossinets, Jon Kleinberg, and Duncan Watts. The structure of information pathways in a social communication network. In *Proceeding of the 14th ACM SIGKDD international conference on Knowledge discovery and data mining*, KDD '08, pages 435–443, 2008.

[71] Kristina Lerman, Rumi Ghosh, and Jeon-hyung Kang. Centrality metric for dynamic network analysis. In *Proceedings of KDD workshop on Mining and Learning with Graphs (MLG)*, July 2010.

[72] L. Weng, A. Flammini, A. Vespignani, and F. Menczer. Competition among memes in a world with limited attention. *Scientific Reports*, 2, 2012.

[73] Dashun Wang, Zhen Wen, Hanghang Tong, Ching-Yung Lin, Chaoming Song, and Albert-Lszl Barabsi. Information spreading in context. In *Proceedings of the 20th international conference on World wide web*, WWW '11, page 735?744. ACM, 2011.

[74] F. Wu and B. A. Huberman. Novelty and collective attention. *Proc. Natl. Acad. Sci. USA*, 104(45):17599–17601, 2007.

[75] Ulrik Brandes. A faster algorithm for betweenness centrality. *Journal of Mathematical Sociology*, 25(2):163–177, 2001.

[76] Jean-Pierre Eckmann, Elisha Moses, and Danilo Sergi. Entropy of dialogues creates coherent structures in e-mail traffic. *Proceedings of the National Academy of Sciences of the United States of America*, 101(40):14333–14337, October 2004.

[77] Albert-Lászlo Barabási. The origin of bursts and heavy tails in human dynamics. *Nature*, 435(7039):207–211, May 2005.

[78] R. Dean Malmgren, Jake M. Hofman, Luis A.N. Amaral, and Duncan J. Watts. Characterizing individual communication patterns. In *Proceedings of the 15th ACM SIGKDD international conference on Knowledge discovery and data mining*, KDD '09, pages 607–616, New York, NY, USA, 2009. ACM.

[79] R. Dean Malmgren, Daniel B. Stouffer, Adilson E. Motter, and Lus A. N. Amaral. A poissonian explanation for heavy tails in e-mail communication. *Proceedings of the National Academy of Sciences*, November 2008.

[80] Rebeka Johnson, Balzs Kovcs, and Andrs Vicsek. A comparison of email networks and off-line social networks: A study of a medium-sized bank. *Social Networks*, pages –, 2012.

[81] L.C. Freeman. Centrality in social networks conceptual clarification. *Social networks*, 1(3):215–239, 1979.

[82] J. M. Anthonisse. The rush in a directed graph. CWI Technical Report Stichting Mathematisch Centrum. Mathematische Besliskunde-BN 9/71, Stichting Mathematisch Centrum, 1971.

[83] Gabor Csardi and Tamas Nepusz. The igraph software package for complex network research. *InterJournal*, Complex Systems:1695, 2006.

[84] Stephen P. Borgatti, Kathleen M. Carley, and David Krackhardt. On the robustness of centrality measures under conditions of imperfect data. *Social Networks*, 28(2):124–136, May 2006.

[85] Terrill L. Frantz, Marcelo Cataldo, and Kathleen M. Carley. Robustness of centrality measures under uncertainty: Examining the role of network topology. *Comput. Math. Organ. Theory*, 15(4):303–328, December 2009.

[86] P.-J. Kim and H. Jeong. Reliability of rank order in sampled networks. *The European Physical Journal B - Condensed Matter and Complex Systems*, 55(1):109–114, 2007.

[87] Alan Agresti and Brent A. Coull. Approximate is better than "Exact" for interval estimation of binomial proportions. *The American Statistician*, 52(2), May 1998.

[88] V. Gunturi, S. Shekhar, W. Northrop, and A. Kotz. Big spatio-temporal network data analytics for smart cities: Research needs. Proceedings of the NSF workshop on Big Data and Urban Informatics Workshop 2014 (http://urbanbigdata.uic.edu/proceedings/).

# Appendix A

# Appendix

## A.1 Illustration of different algorithms on the University-Airport ALSP instance

This section provides a detailed trace of the related work and our proposed critical time point approaches on our previous University-Airport ALSP instance for the 8 departure times listed in Figure 4.1 of Chapter 4 (replicated as Figure A.1 in this Chapter). Specifically, we provide details on the number of re-computations performed by the related and our proposed work on this ALSP instance.

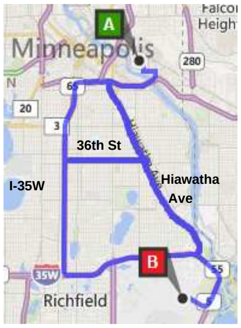

| ID | Departure Time | Preferred Route |
|---|---|---|
| 1 | 7:30am | via Hiawatha |
| 2 | 7:45am | via Hiawatha |
| 3 | 8:00am | via Hiawatha |
| 4 | 8:15am | via Hiawatha |
| 5 | 8:30am | via Hiawatha |
| 6 | 8:45am | via I35W |
| 7 | 9:00am | via I35W |
| 8 | 9:15am | via I35W |

Figure A.1: Preferred routes between the University and the Airport [2].

Figure A.2 illustrates the UMN-MSP airport ALSP problem instance (Figure A.1) using a simplified graph to represent the underlying road network (Figure A.2(a)). The nodes A, D, H and, I in the Figure represent University, Airport and, an intermediate transit node on Hiawatha and I-35 route. The Hiawatha Ave. route to the airport is represented by the pair of edges (A,H) and (H,D), and the I-35 route is represented by the pair (A-I) and (I,D). The edge (I,H) in the Figure A.2(a) represents the 36th St. section of a third route to the airport via I35W-36th St-Hiawatha.

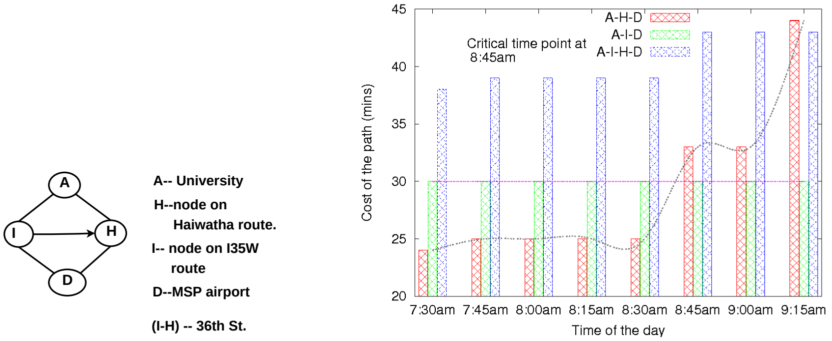

(a) Graph representation of network

(b) Total cost of candidate paths (best in color)

Figure A.2: Illustration of non-stationary ranking of candidate paths.

Figure A.2(b) represents the total cost of the 3 candidate paths to Airport. Here, A-H-D, A-I-D and, A-I-H-D represent the Hiawatha, I35W and, the 35W-36th ST-Hiawatha routes respectively. A schedule along these three routes and cost of edge D-I is given in Figure A.3 for different departure-times [1] . In the Figure, the time written inside the circle represents the arrival time at that node. For instance, the Hiawatha route between UMN and airport for a departure time of 7:30am is shown as $A$7:30→$H$7:42→$D$7:54. This means that a journey starting at UMN (node $A$) at 7:30 would reach an intermediate node on Hiawatha (node $H$) at 7:42 and, finally arrive at airport (node $D$) by 7:55. The cost of the edge between two consecutive departure-times is assumed to remain constant. For example, cost of the edge A-H is assumed to remain 13 mins between 7:45am and 8:00am. Thus, a journey departing from A at 7:47am would arrive at H by 8:00am.

For purpose of comparison, we define and use the work-unit *alsp-iteration*. An alsp-iteration is characterized by enumerating and pruning of candidate paths starting from

[1] Due to space constraints we illustrate the cost only those routes which are most relevant to the algorithms

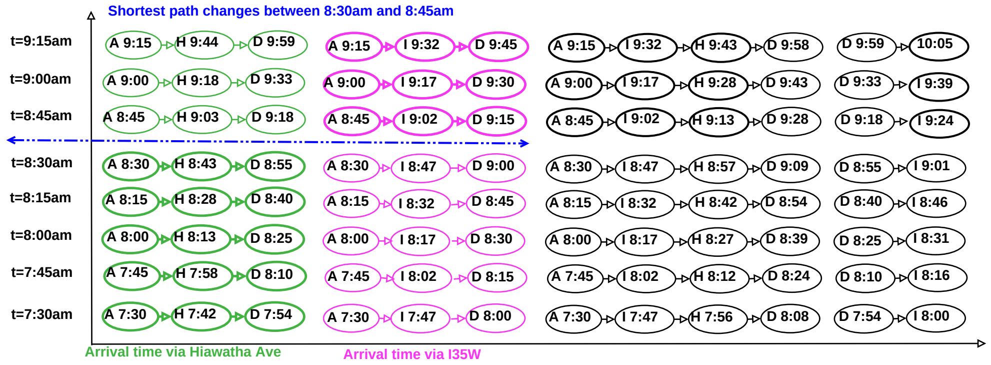

Figure A.3: Schedule on candidate paths for different departure times

the source node (for a particular departure-time) or from both source and destination (in case of BD-CTAS) until a termination condition is met. In each alsp-iteration nodes are closed for either one (naive approach) or multiple time instants ( [3] and our approach) to reduce redundant re-computation across departure times sharing a common solution. Clearly, if more nodes are closed in a single *alsp-iteration*, fewer would be the number of re-computations. Figure A.4(a) illustrates the nodes closed by a naive approach which re-computes shortest path for each departure time. Here, each row represents nodes with their corresponding optimal distance labels for a particular departure-time. A solution to our University-Airport ALSP instance would require all of these to be computed by the naive algorithm. As the Figure shows, in any particular alsp-iteration the naive approach can only compute labels of nodes belonging to a single row. Thus, it would take 8 re-computations for the entire University-Airport ALSP instance. We use this as a baseline for comparing partial information based approaches (e.g. Discrete version of 2S-LTT in [3]) and our complete information based approaches (CTAS and BD-CTAS) proposed in this paper.

Figure A.4(b) illustrates the labels computed by 2S-LTT [3] in different alsp-iterations. As as can be seen, 2S-LTT uses only partial information to close nodes and thus requires a more number (6) of re-computations (as shown in Figure 4.2(b) in Chapter 4). For instance, in the first alsp-iteration (departure-time: 7:30am) time series of arrival times at node H, [7:42 8:00 . . .] is compared against 7:56 (arrival along A-I-H for a departure of 7:30am). Consequently, label of node H is computed only for 7:42am.

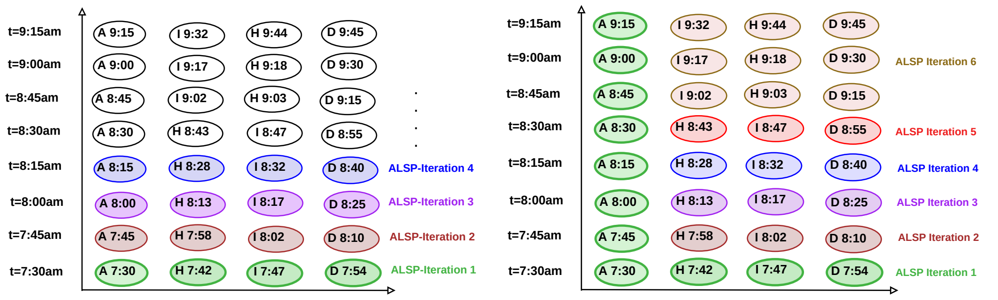
t=9:15am A 9:15 I 9:32 H 9:44 D 9:45
t=9:00am A 9:00 I 9:17 H 9:18 D 9:30
t=8:45am A 8:45 I 9:02 H 9:03 D 9:15
t=8:30am A 8:30 H 8:43 I 8:47 D 8:55
t=8:15am A 8:15 H 8:28 I 8:32 D 8:40
t=8:00am A 8:00 H 8:13 I 8:17 D 8:25
t=7:45am A 7:45 H 7:58 I 8:02 D 8:10
t=7:30am A 7:30 H 7:42 I 7:47 D 7:54
ALSP-Iteration 4
ALSP-Iteration 3
ALSP-Iteration 2
ALSP-Iteration 1
ALSP Iteration 6
ALSP Iteration 5
ALSP Iteration 4
ALSP Iteration 3
ALSP Iteration 2
ALSP Iteration 1

(a) Nodes closed (shaded) by Naive approach (b) Nodes closed (shaded) by Discrete 2S-LTT approach

Figure A.4: Illustration of Naive approach and 2S-LTT [3]

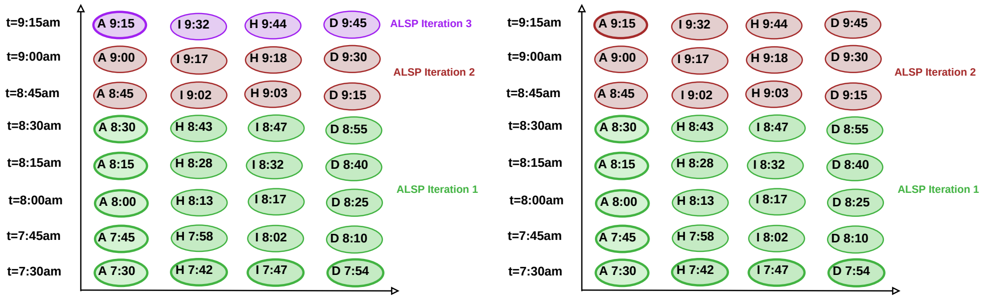
t=9:15am A 9:15 I 9:32 H 9:44 D 9:45
t=9:00am A 9:00 I 9:17 H 9:18 D 9:30
t=8:45am A 8:45 I 9:02 H 9:03 D 9:15
t=8:30am A 8:30 H 8:43 I 8:47 D 8:55
t=8:15am A 8:15 H 8:28 I 8:32 D 8:40
t=8:00am A 8:00 H 8:13 I 8:17 D 8:25
t=7:45am A 7:45 H 7:58 I 8:02 D 8:10
t=7:30am A 7:30 H 7:42 I 7:47 D 7:54
ALSP Iteration 3
ALSP Iteration 2
ALSP Iteration 1
ALSP Iteration 2
ALSP Iteration 1

(a) Nodes closed (shaded) by CTAS (b) Nodes closed (shaded) by BD-CTAS

Figure A.5: Illustration of CTAS and BD-CTAS on UMN-MSP ALSP instance

In contrast, the proposed critical time point based approaches (CTAS and BD-CTAS) use complete information available at hand to compute labels. Figure A.5(a) illustrates the labels computed by CTAS algorithm in different alsp-iterations. The Figure highlights the benefit of using complete information, as CTAS performed only 3 re-computations. Our temporal bi-directional approach, BD-CTAS performs even fewer re-computations (only 2 as shown in Figure A.5(b)) as it avoids irrelevant CTPs. The iteration 3 of CTAS (Figure A.5(a)) was due to a irrelevant CTP created by intersection of path functions of A-H and A-I-H. Here, though the optimal path to node H changes (from A-H to A-I-H) at 9:15am, it does not effect the optimal path to destination which is A-I-D.

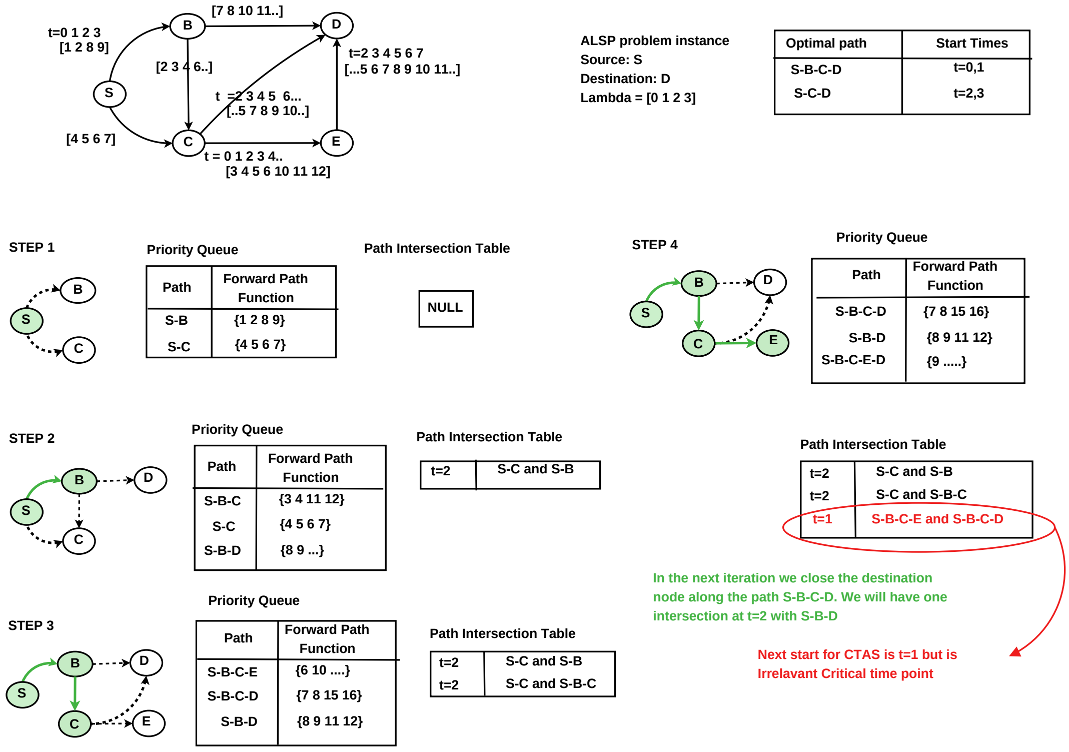

Figure A.6: Execution trace of CTAS algorithm on ST network shown in Figure 4.5(a).

## A.2 Execution trace of CTAS algorithm

An execution trace of the CTAS algorithm on sample ST network shown in Figure 4.5(a) (Section 4.1 in Chapter 4) is given in Figure A.6. The Figure shows that CTAS algorithm forecasts a irrelevant CTP at $t = 1$, which was avoided by the bi-directional approach as shown in Figure 4.10 (Section 4.3 in Chapter 4.